MycoKeys 36: 1–19 (2018)
doi: 10.3897/mycokeys.36.22548
http://mycokeys.pensoft.net

RESEARCH ARTICLE

A peer-reviewed open-access journal
MycoKeys
Launched to accelerate biodiversity research

Different diversification histories in tropical and temperate lineages in the ascomycete subfamily Protoparmelioideae (Parmeliaceae)

Garima Singh[1], Francesco Dal Grande[1], Jan Schnitzler[2], Markus Pfenninger[1], Imke Schmitt[1,3]

1 *Senckenberg Biodiversity and Climate Research Centre (SBiK-F), Frankfurt am Main, Germany* **2** *Department of Molecular Evolution and Plant Systematics, Institute of Biology, Leipzig University, Germany* **3** *Department of Biological Sciences, Institute of Ecology, Evolution and Diversity, Goethe Universität Frankfurt am Main, Germany*

Corresponding author: *Garima Singh* (garima.singh@senckenberg.de)

Academic editor: *P. Divakar* | Received 27 November 2018 | Accepted 19 June 2018 | Published 2 July 2018

Citation: Singh G, Grande FD, Schnitzler J, Pfenninger M, Schmitt I (2018) Different diversification histories in tropical and temperate lineages in the ascomycete subfamily Protoparmelioideae (Parmeliaceae). MycoKeys 36: 1–19. https://doi.org/10.3897/mycokeys.36.22548

Abstract

Background: Environment and geographic processes affect species' distributions as well as evolutionary processes, such as clade diversification. Estimating the time of origin and diversification of organisms helps us understand how climate fluctuations in the past might have influenced the diversification and present distribution of species. Complementing divergence dating with character evolution could indicate how key innovations have facilitated the diversification of species.

Methods: We estimated the divergence times within the newly recognised subfamily Protoparmelioideae (Ascomycota) using a multilocus dataset to assess the temporal context of diversification events. We reconstructed ancestral habitats and substrate using a species tree generated in *Beast.

Results: We found that the diversification in Protoparmelioideae occurred during the Miocene and that the diversification events in the tropical clade *Maronina* predate those of the extratropical *Protoparmelia*. Character reconstructions suggest that the ancestor of Protoparmelioideae was most probably a rock-dwelling lichen inhabiting temperate environments.

Conclusions: Major diversification within the subtropical/tropical genus *Maronina* occurred between the Paleocene and Miocene whereas the diversifications within the montane, arctic/temperate genus *Protoparmelia* occurred much more recently, i.e. in the Miocene.

Keywords
Diversification pattern, dating, extra-tropical, mountain uplifts, ancestral state reconstruction, substrate, habitat, parallel evolution, lichenised fungi

Introduction

Tropical taxa are generally older than their extra-tropical relatives (Gaston and Blackburn 1996, Cattin et al. 2016). Age differences between tropical and extra-tropical species have been attributed to different climatic histories, environment and geography of the two regions (Dobzhansky 1950, Fischer 1960, Dubey and Shine 2011, Cattin et al. 2016, Richardson and Pennington 2016). Past glaciation events have mainly influenced extra-tropical regions, causing several waves of extinction (Weir and Schluter 2007, Rolland et al. 2014). Tropical regions did not experience the same climatic extremes faced by extra-tropical regions (Wallace 1878). Due to the stable climatic conditions and lower extinction rates, species have persisted longer in the tropical regions than the extra-tropical regions (Richardson and Pennington 2016). The ages of extant tropical and extra-tropical species have been well studied and compared for plants and animals (Moreau and Bell 2013, Kerkhoff et al. 2014, Cattin et al. 2016). However, there are only a few studies on the timing of diversification of closely related extant tropical and extra-tropical lichen-forming fungi (Kraichak et al. 2015, Lumbsch et al. 2008, Lumbsch 2016). Understanding the origins and diversification of tropical and extra-tropical taxa may be useful for explaining present patterns of species diversity and for identifying the mechanisms behind diversification.

Most lichenised fungi belong to the Lecanoromycetes within the Ascomycota. Within Lecanoromycetes, Parmeliaceae is the largest family of lichenised fungi consisting of approximately 2,500–3,000 species. This family has recently been divided into two subfamilies, Protoparmelioideae and Parmelioideae (Divakar et al. 2017, Kraichak et al. 2017). Although the diversification patterns of Parmelioideae and various clades within Parmelioideae are well-studied (Amo de Paz et al. 2011, Leavitt et al. 2012, Divakar et al. 2015), the diversification patterns of Protoparmelioideae remain unexplored. Interestingly, although closely related, the species diversity in the two subfamilies is drastically different, with Protoparmelioideae consisting of only about 25–30 species (Singh et al., 2015, Singh et al. 2017), in contrast to the species-rich Parmelioideae (Crespo et al. 2010, Thell et al. 2012). Unravelling the timing of the major diversification events of Protoparmelioideae may help understand the historical events that have led to the disparity in species richness of these two subfamilies. Furthermore, Protoparmelioideae consists of two genera inhabiting different climatic zones: the genus *Protoparmelia* consists predominantly of taxa inhabiting arctic and temperate regions, while the genus *Maronina* comprises mainly taxa inhabiting tropical and subtropical regions (Suppl. material 1; Kantvilas et al. 2010, Papong et al. 2011, Divakar et al. 2017). Protoparmelioideae therefore presents an opportunity to compare the divergence between closely-related species inhabiting tropical and extra-tropical regions.

Inferring the ancestral states of the characters, along with the diversification time, may help us understand how traits have evolved with respect to major geological events. For instance, the diversification of certain lineages in Parmelioideae may have been caused by key innovations that provided adaptive advantages, e.g. melanin production in *Melanohalea* (Divakar et al. 2013). Species richness of Parmelioideae has been linked to past climatic and geological events that provided new habitat and substrate opportunities (Amo de Paz et al. 2011, Leavitt et al. 2012, Kraichak et al. 2015). Inferring the ancestral habitat and substrate may provide useful insights into the diversity differences between the two sister clades.

The goals of this study were 1) to investigate whether tropical taxa have a different diversification history from extra-tropical taxa in Protoparmelioideae (Parmeliaceae) and 2) to infer the ancestral habitat and substrate in Protoparmelioideae to understand how these characters evolved within the subfamily.

Materials and methods

Dataset

We used the dataset from Singh et al. (2015) for estimating the divergence times in Protoparmelioideae (Suppl. material 2). This dataset is referred to as dataset 1 and it consists of 99 samples of *Protoparmelia* s. str. (11 species), 37 samples of the newly resurrected genus *Maronina* (12 species) and 73 taxa from close relatives of Protoparmelioideae, i.e. from Parmelioideae (40 taxa), Lecanoraceae (4 taxa), Gypsoplacaceae (2 taxa), Ramboldiaceae (10 taxa), *Protoparmelia* s. l. (24 taxa) and *Miriquidica* (12 taxa). This dataset comprises six loci: *RBP1* (696 bp), *TSR1* (756 bp), *MCM7* (655 bp), nuLSU (1064 bp), mtSSU (834 bp) and ITS (807 bp). Species concepts used in the current study are based on Singh et al. (2015). In short, this study inferred the independent evolutionary lineages in *Protoparmelia* and *Maronina* based on molecular data. Previously accepted taxa were considered putative species (12 described species). In addition, well-supported monophyletic clades in the six-locus concatenated ML and Bayesian phylogenetic trees (BS > 70%, PP > 0.95) were also considered as putative species, resulting in a 25-species-scenario. The marginal posterior probability of the 25-species-scenario was estimated using the programme BP&P v3, which utilises a reversible-jump Bayesian Markov chain Monte Carlo (MCMC) algorithm to infer the posterior probability of each delimited species and the posterior probability for the overall number of delimited species. The species tree from *BEAST was used to infer the speciation probabilities by BP&P (Yang and Rannala 2014). Further details of this analysis are mentioned in Singh et al. (2015).

Molecular dating can be done by using fossil records, substitution rates of genetic markers or by using the already estimated divergence date for a node in a phylogeny as the calibration point. The split of Protoparmelioideae from Parmelioideae has been shown to have occurred ~108 Ma (Amo de Paz et al. 2011) and 102 Ma (Kaasalainen

et al. 2015, Divakar et al. 2017). We included the most recent estimate, i.e. by Divakar et al. (2017), to estimate the diversification times within Protoparmelioideae. We used a normal distribution (instead of a uniform prior), with the mean of 102.0 Ma and sdev = 9 Ma (Divakar et al. 2017) and truncated the upper and lower estimates of the split between Parmelioideae and Protoparmelioideae to 130 and 80 Ma, respectively. For each marker, we implemented the most appropriate model of DNA sequence evolution which was inferred using JModelTest (Darriba et al. 2012). We estimated divergence times in Protoparmelioideae by implementing a Birth-Death prior using an uncorrelated Bayesian relaxed molecular clock model (uncorrelated lognormal) and unlinked substitutions models across the loci as implemented in the programme BEAST v1.8.1 (Drummond et al. 2006, Drummond and Rambaut 2007). We performed the analysis with two independent Markov chain Monte Carlo (MCMC) runs of 50 million generations (10% burn-in), sampling one tree every 5000 generations (9000 trees obtained). We used the programme Tracer v1.6 to evaluate each chain and obtain the effective sample sizes for each parameter (Rambaut et al. 2014). Using TreeAnnotator version 1.8.0, the chains were combined to obtain the maximum clade credibility tree with mean node heights posterior distributions of estimated divergence dates (Drummond and Rambaut 2007).

Identifying climatic zones of the clades

We extracted the climatic data for the *Protoparmelia* and *Maronina* species based on the coordinate information of the sampling sites. We used the global environmental stratification (GEnS) software, which is based on statistical clustering of bioclimatic data (Metzger et al. 2013). This is a high-resolution quantitative stratification of climatic data, which classifies the geographic regions of the world into 18 global environmental zones, based on a broad set of climate-related variables extracted from WorldClim (Hijmans et al. 2005, Metzger et al. 2013). The 18 global environmental zones are- A: arctic 1, B: arctic 2, C: extremely cold and wet 1, D: extremely cold and wet 2, E: cold and wet, F: extremely cold and mesic, G: cold and mesic, H: cool temperate and dry, I: cool temperate and xeric, J: cool temperate and moist, K: warm temperate and mesic, L: warm temperate and xeric, M: hot and mesic, N: hot and dry, O: hot and arid, P: extremely hot and arid, Q: extremely hot and xeric and R: extremely hot and moist. The 18 environmental zones are further grouped into seven broad biomes, namely arctic/alpine (environmental zones A, B, C & D), boreal/alpine (environmental zones E, F & G), cool temperate (environmental zones H, I & J), warm temperate (environmental zones K & L), subtropical (environmental zone M), dry lands (environmental zones N, O, P & Q) and tropical (environmental zone R; Metzger et al. 2013).

We performed linear discrimination analysis (LDA) using the package MASS in R (Venables and Ripley 2002) to infer if there is significant differentiation in the climatic variables between the *Protoparmelia* and *Maronina* inhabiting warm temperate regions. Linear discrimination analysis provides the linear combinations of the variables (here

the 19 bioclimatic variables) that give the best possible separation between the groups i.e. in our study, taxa inhabiting warm temperate regions in *Protoparmelia* and *Maronina*. *Protoparmelia badia* B2 and *Maronina isidiata* E were excluded from this analysis as these species are represented by only two samples. We inferred the separation achieved by the discriminant function using the least correlated bioclim variables (first 4 bioclim variables) and calculated the mean values of the discriminant functions for each group.

Ancestral state reconstruction

We reconstructed the ancestral habitat and substrate of Protoparmelioideae. We obtained information on habitat and substrate from literature (Aptroot et al. 1997, Nash et al. 2004, Lendemer and Lumbsch 2008, Coppins and Chambers 2009, Kantvilas et al. 2010, Papong et al. 2011). For the new species sensu Singh et al. (2015), information on habitat was inferred from the spatial framework analysis based on Metzger et al. (2013), which groups the global environment into seven "broad biomes" namely, arctic/alpine, boreal alpine, cool temperate, warm temperate, subtropical, dry lands and tropical. To infer the ancestral habitat of Protoparmelioideae, we grouped the "broad biomes" into cold (arctic/alpine, boreal alpine, cool temperate) and warm regions (warm temperate, subtropical, dry lands and tropical).

We used the 6-locus dataset from Singh et al. (2017), dataset 2, to infer the species tree using *BEAST as implemented in BEAST v2.2 (Drummond and Rambaut 2007). We used a Birth-Death process and gamma-distributed population sizes for the species tree prior and a pairwise linear population size model with a constant root. The closest model to the best-suggested model from jModelTest under the AICc criterion was selected as the substitution model for each locus (Suppl. material 3). Two independent Markov Chain Monte Carlo (MCMC) analyses were performed for a total of 50,000,000 generations, sampling every 1,000 steps. Convergence of the runs to the same posterior distribution and the adequacy of sampling (using the Effective Sample Size [ESS] diagnostic) were assessed with Tracer v1.6. The first 10% of the samples were removed as burn-in, resulting in 45,000 trees. 5,000 trees were then randomly sampled from these trees using the package ape in R, for inferring ancestral habitat and substrate and using BayesMultiState (Pagel and Meade 2006).

We reconstructed the ancestral habitat and substrate with binary character state coding using BayesMultiState implemented in BayesTraits version 3.0 (Pagel and Meade 2006). We employed the reversible-jump MCMC, where models are visited in proportion to their posterior probability. We traced the evolution of these characters on the molecular phylogeny using maximum likelihood (ML) and Bayesian inferences (BI) approaches. To account for phylogenetic mapping uncertainty, we evaluated probabilities of ancestral states calculated from the 5000 BI trees using the MCMC method in BayesMultiState, implemented in the BayesTraits v3.0. Ancestral states were then reconstructed for selected nodes for each character, which were selected based on their posterior probability support values of the BI analysis. We used a reversible-jump hy-

perprior with a gamma prior (exponential prior seeded from a uniform distribution on the interval 0 to 30) to reduce uncertainty of choosing priors in the MCMC analysis. Based on the preliminary analyses, we set the ratedev value to 8, to achieve an acceptance rate of proposed changes between 20 and 40% to ensure adequate mixing. The option "AddNode" was used to find the proportion of the likelihood associated with each of the possible states at each node. Three independent MCMC runs were performed with 2,000,000 iterations. Chains were sampled every 500th iteration after a burn-in of 20,000 iterations (40 trees).

Network analysis

Phylogenetically distant but geographically co-existing species may experience interspecies gene flow (Lumaret and Jabbour-Zahab 2009, Martin et al. 2013, Kol-Maimon et al. 2014). This might lead to the transfer of genes and the presence of similar characters in phylogenetically unrelated species (Makarenkov and Legendre 2004, Bapteste et al. 2013). Gene flow and homoplasy of characters can both be used to explain gain and loss of characters on a phylogenetic tree. We performed a network analysis to check if genetically distant species with similar characters are affected by interspecies gene flow.

We used PhyloNet to detect hybridisation events in the data while accounting for incomplete lineage sorting (Than et al. 2008). We applied the ML approach implemented in PhyloNet to infer the possibility of reticulation events in Protoparmelioideae, allowing up to two reticulations in 50 runs. The outgroup was excluded from the network analysis. We also ran multiple independent analyses on randomly selected subsets of 10 species, represented by one sample each due to the inability of PhyloNet to deal with the large dataset. The MCMC chain was run for 250,000 iterations and burn-in of 10,000 iterations (25 trees).

Results

Identifying climatic zones of the clades

We identified the habitat of different Protoparmelioideae taxa using GEnS (Suppl. material 4; Metzger et al. 2013). We found that, of the 11 *Protoparmelia* species, seven inhabit extremely cold to cold and cool temperate regions and four inhabit cool and warm temperate to warm temperate regions (Suppl. material 4). As for *Maronina*, eight species inhabit extremely hot to hot regions (zones M, N, Q and R according to Metzger et al. 2013) and four species inhabit warm temperate to warm temperate and hot regions (zones K, L, M, N and Q, Suppl. material 4). Linear discrimination analysis (LDA) showed that the mean values of the discriminant functions for each clade based on the most uncorrelated bioclim variables (first 4 bioclim variables, based on the scree

plot; Suppl. material 5) was -3.517 and 1.034, respectively, for group 1 and group 2 and the misclassification rate was 4.54 (Suppl. material 6). The low rate of misclassification strongly supports the climatic difference between *Protoparmelia* and *Maronina* taxa inhabiting warm temperate regions. The stacked histogram clearly shows differentiation between the two groups (Suppl. material 5). Our results show that *Protoparmelia* and *Maronina* species inhabiting the broad "warm temperate biome" (Metzger et al. 2013) are well differentiated by more fine-scaled climate data.

Divergence dating

The split between Parmelioideae and Protoparmelioideae occurred around 87 Ma during the Cretaceous. The tropical lowland genus *Maronina* split from the extra-tropical, arctic/temperate genus *Protoparmelia* around 67 Ma (Fig. 1, Table 1). Diversification within Protoparmelioideae occurred from the Oligocene to the early Pliocene. Most of the speciation events in both *Protoparmelia* and *Maronina* occurred during the Miocene (Table 1).

Ancestral state reconstruction

We reconstructed the ancestral habitat and substrate of Protoparmelioideae using ML and Bayesian approaches. We did not find any conflict between the two approaches and both approaches supported a similar character at the investigated nodes. The Bayesian analysis was run three times for each character at each node and we did not find any conflict amongst the three runs (Table 2). We found that the ancestor of Protoparmelioideae was a rock-dwelling and cold environment inhabiting lichen-forming fungus (Fig. 2).

Network analysis

Network analysis was performed to infer events such as hybridisation and gene flow in Protoparmelioideae. Our analysis indicates that reticulation events are unlikely amongst species in Protoparmelioideae. We did not find any cases of hybridisation amongst taxa in Protoparmelioideae.

Discussion

In this study, we investigated the diversification timing in Protoparmelioideae. The sister-relation between Protoparmelioideae and Parmelioideae was supported in our analysis as in previous studies (Arup et al. 2007, Singh et al. 2013, Divakar et al. 2015,

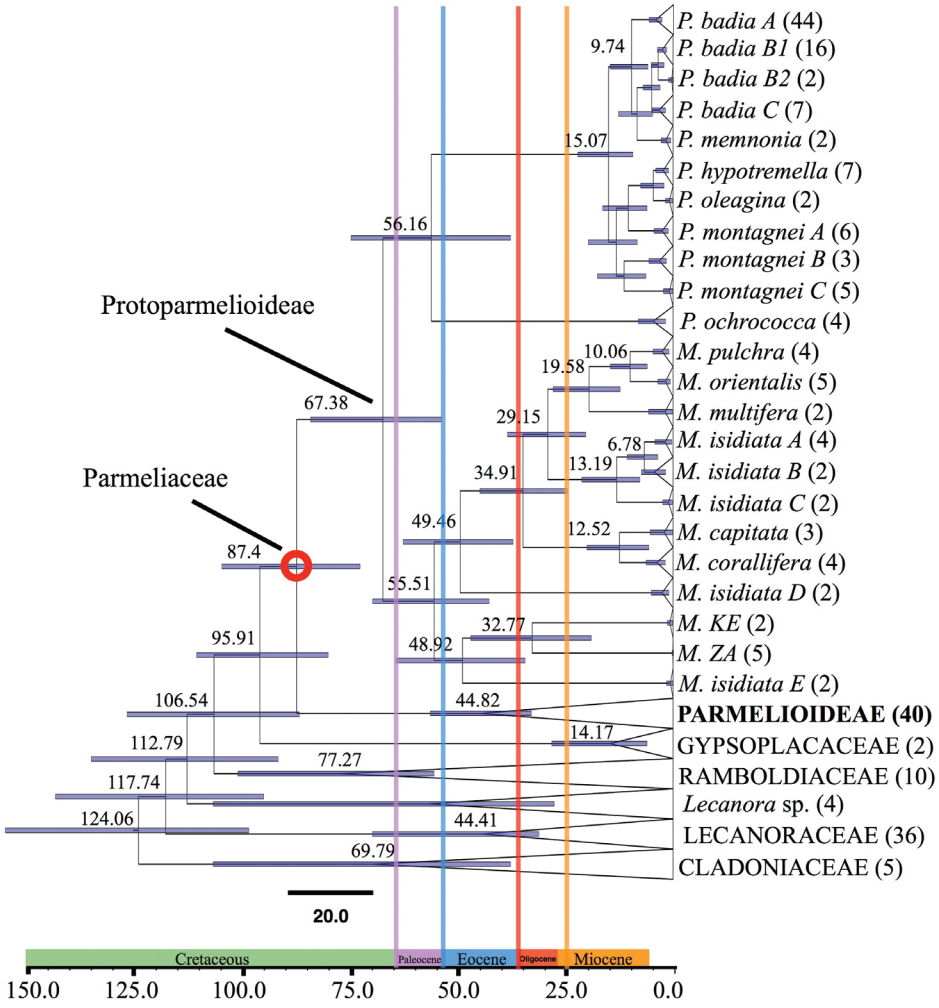

Figure 1. Time-calibrated phylogeny of the major lineages of Lecanorales (Lecanoraceae, Parmeliaceae, Ramboldiaceae, and Gypsoplacaceae), based on a six-locus dataset, dataset 1 (Singh et al. 2015). Cladoniaceae was used as outgroup (Arup et al. 2007, Singh et al. 2013). Mean node age, 95% highest posterior density (HPD) and posterior probability (PP) were mapped on the maximum clade credibility tree. The red circle indicates the calibration point, i.e. the split between Protoparmelioideae and Parmelioideae. Only the strongly supported nodes were considered for divergence time estimates. Geological times are indicated at the axis of the tree. The number of specimens per species is indicated in brackets in front of the taxon names. The scale at the bottom of the tree represents age in millions of years (Ma). Parmelioideae, Gypsoplacaceae, Cladoniaceae, Ramboldiaceae and Lecanoraceae clades are collapsed. In Parmelioideae, *Miriquidica* and *Protoparmelia* s. l. clades are collapsed at the species level.

Divakar et al. 2017). Protoparmelioideae comprises two genera, *Protoparmelia,* which includes taxa with predominantly extra-tropical distribution and *Maronina*, which mainly comprises species with tropical distribution (Divakar et al. 2017). We found

Table 1. The dates of origin of lineages in Protoparmelioideae and the initial divergence of Protoparmelioideae from Parmelioideae (ancestral splits).

Lineage	Mean	Range (95% credibility intervals)
Origin of Ramboldiaceae	106.54	95% HPD = 86.77–126.7
Origin of Gypsoplacaeae	95.91	95% HPD = 80.09–110.59
Parmelioideae-Protoparmelioideae split	87.4	95% HPD = 72.68–104.72
Protoparmelia-Maronina split	67.38	95% HPD = 53.78–84.16
Origin of *Protoparmelia ochrococca*	56.16	95% HPD = 37.8–74.75
Protoparmelia badia A	9.74	95% HPD = 5.94–14.69
Protoparmelia memnonia	8.45	95% HPD = 4.86–12.76
Protoparmelia badia C	5.05	95% HPD = 1.86–5.03
Protoparmelia badia B1	3.57	95% HPD = 2.19–5.17
Protoparmelia badia B2	3.57	95% HPD = 2.19–5.17
Protoparmelia oleagina	11.47	95% HPD = 6.42–17.63
Protoparmelia hypotremella	11.47	95% HPD = 6.42–17.63
Protoparmelia montagnei A	4.68	95% HPD = 2.2–7.64
Protoparmelia montagnei B	4.68	95% HPD = 2.2–7.64
Protoparmelia montagnei C	10.47	95% HPD = 6.15–16.43
Maronina pulchra	10.06	95% HPD = 6.09–14.66
Maronina orientalis	10.06	95% HPD = 6.09–14.66
Maronina multifera	19.58	95% HPD = 12.39–27.91
Maronina isidiata A	6.78	95% HPD = 3.65–10.76
Maronina isidiata B	6.78	95% HPD = 3.65–10.76
Maronina isidiata C	13.19	95% HPD = 7.8–21.26
Maronina capitata	12.52	95% HPD = 5.72–20.07
Maronina corallifera	12.52	95% HPD = 5.72–20.07
Maronina isidiata D	49.46	95% HPD = 37.23–62.68
Maronina isidiata E	48.92	95% HPD = 34.4–64.39
Maronina ZA	32.77	95% HPD = 19.08–47.02
Maronina KE	32.77	95% HPD = 19.08–47.02

that *Protoparmelia* split from *Maronina* around 67 Ma. Our analysis suggests that clade diversification events in *Protoparmelia* and *Maronina* occurred at different geological time scales.

Are tropical taxa older?

Our study suggests that clade diversification events within *Maronina* predate those in *Protoparmelia*. These results are in line with the hypothesis that tropical taxa are older than their arctic/temperate relatives (Dobzhansky 1950, Mittelbach et al. 2007, Schemske 2009). One reason for this is the different climatic history of these regions. Due to major climatic perturbations, the arctic/temperate regions may have suffered waves of extinction. On the contrary, subtropical/tropical regions had a comparatively stable climate and escaped major glaciation events and, thus, did not face major ex-

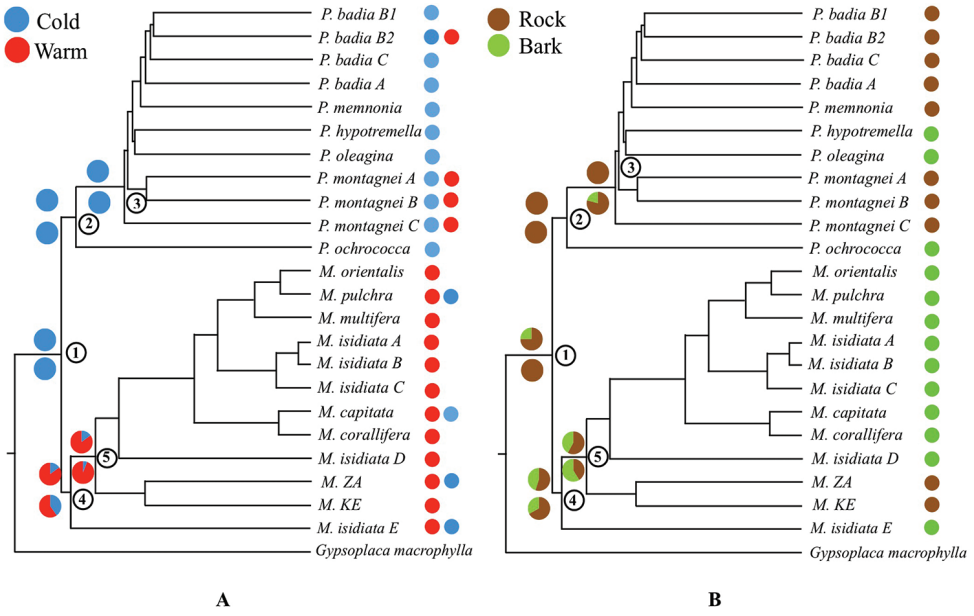

Figure 2. Ancestral states in Protoparmelioideae: Chronogram based on a six-locus dataset, dataset 2 (Singh et al. 2017), representing a species tree of Protoparmelioideae showing the ancestral states at nodes of interest. The topology is derived from the *BEAST species tree. A consensus tree was generated in TreeAnnotator. The current substrate of each species is indicated by the coloured circles in front of the name of the species. Polymorphic taxa have more than one coloured circle. Nodes at which ancestral states are reconstructed are numbered from 1 to 5. Pie charts indicate probabilities of each ancestor being in each of the two potential states at nodes of interest. The circles above the node represent bootstrap support for each character state and the circles at the bottom represent the posterior probability. A) Ancestral habitat: cold (blue), warm (red) and B) Ancestral substrate: rock (brown), bark (green).

Table 2. Results of the character reconstruction for Protoparmelioideae using MCMC and ML methods. We report the posterior probabilities (PP) and likelihoods for the ancestral habitat and substrate at five nodes from Fig. 2. Values with bootstrap support >0.70 and PP >0.95 are marked in bold.

Node	Approach	Habitat		Substrate	
		(P) cold	(P) warm	(P) rock	(P) bark
1	ML	**1.000**	0.000	**0.755**	0.250
	Bayesian	**1.000**	0.000	**1.000**	0.000
2	ML	**0.900**	0.099	**0.780**	0.220
	Bayesian	**1.000**	0.000	0.578	0.422
3	ML	**1.000**	0.000	**0.995**	0.005
	Bayesian	0.060	0.940	0.880	0.120
4	ML	**1.000**	0.000	**0.756**	0.244
	Bayesian	**1.000**	0.000	0.756	0.234
5	ML	0.188	**0.812**	**0.551**	0.449
	Bayesian	0.048	**0.952**	0.700	0.300

tinctions (Willig et al. 2003, Wiens and Donoghue 2004, Mittelbach et al. 2007). Although the tropics escaped glaciation, these regions did face climatic perturbations in the form of severe aridification that impacted species' ranges and also led to extinctions and populations bottlenecks (Demenou et al. 2016, Powell and Glazier 2017). This could explain the comparable species diversity between *Protoparmelia* and *Maronina,* as well as the restricted ranges of *Maronina* species. *Maronina* species, which were thought to have a broad geographic distribution, i.e. *M. isidiata*, have been shown to comprise five distinct lineages/species (Singh et al. 2015). On the contrary, *Protoparmelia badia*, *P. hypotremella* and *P. oleagina* have a broad geographic distribution. A recent study suggested that *P. badia* and *P. montagnei* comprise different morphospecies, however, one lineage of *P. badia* is cosmopolitan and has a broad geographic distribution (Singh et al. 2015). The other putative lineages in *P. badia* and *P. montagnei* are recently discovered and, so far, they have been reported only from Spain and Italy.

Diversification patterns

The diversification of *Protoparmelia* involves an initial "lag phase", indicated by a clade with a long branch (spanning ~50 million years in *Protoparmelia*). However, a long branch might be caused by several factors including extinction of taxa, founder effects or artefacts of the dataset (incomplete sampling etc.). Incomplete sampling might not be the case for the observed long branch in *Protoparmelia* as molecular data is available for most of the taxa and only the taxa forming a monophyletic clade as *Protoparmelia* s. str. (sensu Singh et al. 2013, 2015) were included in this study. These studies showed *Protoparmelia* to be polyphyletic and many taxa have been moved to *Ramboldia (P. plicatula*, *P. petraeoides*), *Maronina* or *Lecanora* (*P. ryaniana*).

Considering the climatic history of the arctic/temperate regions where *Protoparmelia* species are predominantly distributed, extinction could be assumed as the one of the main reasons resulting in the observed long branch in *Protoparmelia*. On the other hand, under comparatively stable climatic conditions, little or no extinction of the early diverging branches might have led to the more even branching pattern in *Maronina*. Thus, past climate, geographic position and geological events might have caused differences in the timing of speciation events between *Protoparmelia* and *Maronina*.

Phylogenetic network

Evolution of organisms is often represented by a phylogenetic tree, which assumes vertical transfer of genetic material from ancestors to descendants. Evolutionary relationships however, might be more complicated and genes may be transferred horizontally between different or reproductively isolated organisms (Lumaret and Jabbour-Zahab 2009, Kol-Maimon et al. 2014). Sharing of genetic material between species may lead to shared characters despite their phylogenetic related nature (Makarenkov and Legendre 2004,

Bapteste et al. 2013). In Protoparmelioideae, *Protoparmelia* is predominantly saxicolous (8 species) with only three corticolous species whereas *Maronina* is predominantly corticolous (10 species) with only two saxicolous species. We inferred whether or not the similar substrates or habitat preference in phylogenetically distant species might be due to the gene flow between them. Our analysis suggests that hybridisation events are unlikely to have occurred between taxa in Protoparmelioideae and the similar substrate and habitat preference between *Protoparmelia* and *Maronina* are probably results of independent evolution of characters.

Ancestral habitat and substrate of Protoparmelioideae

Our results suggest that the ancestors of Protoparmelioideae as well as *Protoparmelia* probably inhabited cold environments (Fig. 2). *Protoparmelia* split from *Maronina* ~67 Ma ago (Fig. 1) and subsequently diversified in arctic/temperate regions in the Northern hemisphere. The cold inhabiting ancestors might have facilitated the diversification in the arctic/temperate regions when presented with novel geographical and ecological opportunities due to mountain uplifts.

Substrate is an important factor determining lichen distribution. For instance, major diversification events within the epiphyte-rich subclasses within Ascomycota occurred in the Jurassic and Cretaceous (Prieto and Wedin 2013), the latter being the period of origin and diversification of angiosperms. In our study, we found evidence that the ancestor of Protoparmelioideae was rock dwelling (Fig. 2). This is connected to the fact that the ancestor of Protoparmelioideae was also inhabiting cold, vegetation-poor, habitats. Substrates other than rock were not available.

Acknowledgements

We thank the curators of the following herbaria for sending the material used in the study: ASCR, BG, CANB, CANL, EA, FR, GZU, HO, LD, MAF, MSC, MSUT, NY, O, OSC, TRH, UPS and UCR and Pieter P. G. van den Boom (Netherlands), Toby Spribille (Austria), Zdenek Palice (Czech Republic) and Victor J. Rico (Spain). We are grateful to PK Divakar (Spain), Dingqiao Wen (USA), Mark Pagel (UK), Vikas Kumar (Germany) and Thorsten Lumbsch (Chicago) for their helpful suggestions. We thank Uwe Hallman (Germany) for helping with GEnS. G.S. was supported by a fellowship from the German Academic Exchange Service (DAAD).

References

Amo de Paz G, Cubas P, Divakar PK, Lumbsch HT, Crespo A (2011) Origin and diversification of major clades in parmelioid lichens (Parmeliaceae, Ascomycota) during the Paleogene

inferred by Bayesian analysis. PLoS ONE 6: e28161. https://doi.org/10.1371/journal.pone.0028161

Aptroot A, Diederich P, Van Herk CM, Spier L, Wirth V (1997) *Protoparmelia hypotremella*, a new sterile corticolous species from Europe, and its lichenicolous fungi. Lichenologist 29: 415–424. https://doi.org/10.1006/lich.1997.0096

Arup U, Ekman S, Grube M, Mattsson J-E, Wedin M (2007) The sister group relation of Parmeliaceae (Lecanorales, Ascomycota). Mycologia 99: 42–49. https://doi.org/10.1080/15572536.2007.11832599

Bapteste E, Van Iersel L, Janke A, Kelchner S, Kelk S, Mcinerney JO, Morrison DA, Nakhleh L, Steel M, Stougie L, Whitfield J (2013) Networks: expanding evolutionary thinking. Trends in Genetics 29: 439–441. https://doi.org/10.1016/j.tig.2013.05.007

Cattin L, Schuerch J, Salamin N, Dubey S (2016) Why are some species older than others? A large-scale study of vertebrates. BMC Evolutionary Biology 16: 90. https://doi.org/10.1186/s12862-016-0646-8. https://doi.org/10.1186/s12862-016-0646-8

Coppins BJ, Chambers SP (2009) *Protoparmelia* M. Choisy (1929). In: CW Smith, et al. (Eds) The lichens of Great Britain and Ireland. London, British Lichen Society, 753–755.

Crespo A, Kauff F, Divakar P (2010) Phylogenetic generic classification of parmelioid lichens (Parmeliaceae, Ascomycota) based on molecular, morphological and chemical evidence. Taxon 59: 1735–1753.

Darriba D, Taboada GL, Doallo R, Posada D (2012) jModelTest 2: more models, new heuristics and parallel computing. Nature Methods 9: 772. http://dx.doi.org/10.1038/nmeth.2109

Demenou BB, Piñeiro R, Hardy OJ (2016) Origin and history of the Dahomey Gap separating West and Central African rain forests: insights from the phylogeography of the legume tree *Distemonanthus benthamianus*. Journal of Biogeography 43: 1365–2699. https://doi.org/10.1111/jbi.12688

Divakar PK, Crespo A, Kraichak E, Leavitt SD, Singh G, Schmitt I, Lumbsch HT (2017) Using a temporal phylogenetic method to harmonize family- and genus-level classification in the largest clade of lichen-forming fungi. Fungal Diversity 84: 101–117. https://doi.org/10.1007/s13225-017-0379-z

Divakar PK, Crespo A, Wedin M, Leavitt SD, Hawksworth DL, Myllys L, McCune B, Randlane T, Bjerke JW, Ohmura Y, Schmitt I, Boluda CG, Alors D, Roca-Valiente B, Del-Prado R, Ruibal C, Buaruang K, Núñez-Zapata J, Amo de Paz G, Rico VJ, Molina MC, Elix JA, Esslinger TL, Tronstad IKK, Lindgren H, Ertz D, Gueidan C, Saag L, Mark K, Singh G, Dal Grande F, Parnmen S, Beck A, Benatti MN, Blanchon D, Candan M, Clerc P, Goward T, Grube M, Hodkinson BP, Hur J-S, Kantvilas G, Kirika PM, Lendemer J, Mattsson J-E, Messuti MI, Miadlikowska J, Nelsen M, Ohlson JI, Pérez-Ortega S, Saag A, Sipman HJM, Sohrabi M, Thell A, Thor G, Truong C, Yahr R, Upreti DK, Cubas P, Lumbsch HT (2015) Evolution of complex symbiotic relationships in a morphologically derived family of lichen-forming fungi. New Phytologist 208: 1217–1226. https://doi.org/10.1111/nph.13553

Divakar PK, Kauff F, Crespo A, Leavitt SD, Lumbsch HT (2013) Understanding phenotypical character evolution in parmelioid lichenized fungi (Parmeliaceae, Ascomycota). PloS ONE 8: e83115. https://doi.org/10.1371/journal.pone.0083115

Dobzhansky T (1950) Evolution in the tropics. American Scientist 32: 209–221.

Drummond AJ, SYW Ho, Phillips MJ, Rambaut A (2006) Relaxed phylogenetics and dating with confidence. PloS Biology 4: 699–710. https://doi.org/10.1371/journal.pbio.0040088

Drummond AJ, Rambaut A (2007) BEAST: Bayesian evolutionary analysis by sampling trees. BMC Evolutionary Biology 7: 214. https://doi.org/10.1186/1471-2148-7-214

Dubey S, Shine R (2011) Geographic variation in the age of temperate-zone reptile and amphibian species: Southern Hemisphere species are older. Biology Letters 7: 96–97. https://doi.org/10.1098/rsbl.2010.0557

Fischer AG (1960) Latitudinal variations in organic diversity. Evolution 14: 64–81. https://doi.org/10.1111/j.1558-5646.1960.tb03057.x

Gaston KJ, Blackburn TM (1996) The tropics as a museum of biological diversity: An analysis of the New World avifauna. Proceedings of the Royal Society of London. Series B: Biological Sciences 263: 63–68. https://doi.org/10.2307/50451

Hijmans RJ, Cameron SE, Parra JL, Jones PG, Jarvis A (2005) Very high resolution interpolated climate surfaces for global land areas. International Journal of Climatology 25: 1965–1978. https://doi.org/10.1002/joc.1276

Kantvilas G, Papong K, Lumbsch HT (2010) Further observations on the genus *Maronina*, with descriptions of two new taxa from Thailand. The Lichenologist 42: 557–561. https://doi.org/10.1017/S0024282910000174

Kaasalainen U, Heinrichs J, Krings M, Myllys L, Grabenhorst H, Rikkinen J, Schmidt AR (2015) Alectorioid morphologies in Paleogene lichens: new evidence and re-evaluation of the fossil *Alectoria succini* Mägdefrau. PLoS ONE 10: e0129526. https://doi.org/10.1371/journal.pone.0129526

Kerkhoff AJ, Moriarty PE, Weiser MD (2014) The latitudinal species richness gradient in New World woody angiosperms is consistent with the tropical conservatism hypothesis. Proceedings of the National Academy of Sciences of the United States of America 111: 8125–8130. https://doi.org/10.1073/pnas.1308932111

Kol-Maimon H, Ghanim M, Franco JC, Mendel Z (2014) Evidence for gene flow between two sympatric mealybug species (Insecta; Coccoidea; Pseudococcidae). PloS ONE 9: e88433. https://doi.org/10.1371/journal.pone.0088433

Kraichak E, Crespo A, Divakar PK, Leavitt SD, Lumbsch HT (2017) A temporal banding approach for consistent taxonomic ranking above the species level. Scientific Reports 7: 2297. https://doi.org/10.1038/s41598-017-02477-7

Kraichak E, Divakar PK, Crespo A, Leavitt SD, Nelsen MP, Lücking R, Lumbsch HT (2015) A tale of two hyper-diversities: diversification dynamics of the two largest families of lichenized fungi. Scientific Reports 5: 10028. http://dx.doi.org/10.1038/srep10028. https://doi.org/10.1038/srep10028

Leavitt SD, Esslinger TL, Divakar PK, Lumbsch HT (2012) Miocene and Pliocene dominated diversification of the lichen-forming fungal genus *Melanohalea* (Parmeliaceae, Ascomycota) and Pleistocene population expansions. BMC Evolutionary Biology 12: 176. https://doi.org/10.1186/1471-2148-12-176

Lendemer JC, Lumbsch HT (2008) *Protoparmelia capitata* sp. nov., and *P. isidiata* Diederich, Aptroot & Sérus., two species of *Protoparmelia* (Lecanorales, Ascomycota) from south-eastern North America. The Lichenologist 40: 329–336. https://doi.org/10.1017/S0024282908007810

Lumbsch HT, Hipp AL, Divakar PK, Blanco O, Crespo A (2008) Accelerated evolutionary rates in tropical and oceanic parmelioid lichens (Ascomycota). BMC Evolutionary Biology 8: 257. https://doi.org/10.1186/1471-2148-8-257

Lumbsch HT (2016) Lichen-Forming Fungi, Diversification of. In: Kliman RM (Ed.) Encyclopedia of Evolutionary Biology. Academic Press, Oxford, 305–311. https://doi.org/10.1016/B978-0-12-800049-6.00249-3

Lumaret R, Jabbour-Zahab R (2009) Ancient and current gene flow between two distantly related Mediterranean oak species, *Quercus suber* and *Q. ilex*. Annals of Botany 104: 725–736. https://doi.org/10.1093/aob/mcp149

Makarenkov V, Legendre P (2004) From a phylogenetic tree to a reticulated network. Journal of Computational Biology 11: 195–212. https://doi.org/10.1089/106652704773416966

Martin SH, Dasmahapatra KK, Nadeau NJ, Salazar C, Walters JR, Simpson F, Blaxter M, Manica A, Mallet J, Jiggins CD (2013) Genome-wide evidence for speciation with gene flow in *Heliconius* butterflies. Genome Research 23: 1817–1828. https://doi.org/10.1101/gr.159426.113

Metzger MJ, Bunce RGH, Jongman RHG, Sayre R, Trabucco A, Zomer R (2013) A high-resolution bioclimate map of the world: a unifying framework for global biodiversity research and monitoring. Global Ecology and Biogeography 22: 630–638. https://doi.org/10.1111/geb.12022

Mittelbach GG, Schemske DW, Cornell H V, Allen AP, Brown JM, Bush MB, Harrison SP, Hurlbert AH, Knowlton N, Lessios HA, McCain CM, McCune AR, McDade LA, McPeek MA, Near TJ, Price TD, Ricklefs RE, Roy K, Sax DF, Schluter D, Sobel JM, Turelli M (2007) Evolution and the latitudinal diversity gradient: speciation, extinction and biogeography. Ecology Letters 10: 315–331. https://doi.org/10.1111/j.1461-0248.2007.01020.x

Moreau CS, Bell CD (2013) Testing the museum versus cradle tropical biological diversity hypothesis: phylogeny, diversification, and ancestral biogeographic range evolution of the ants. Evolution 67: 2240–2257. https://doi.org/10.1111/evo.12105

Nash TH III, Ryan BD, Gries C, Bungartz F (2004) Lichen Flora of the Greater Sonoran Desert Region. Arizona State University Lichen Herbarium, 1–567.

Pagel M, Meade A (2006) Bayesian analysis of correlated evolution of discrete characters by reversible-jump Markov Chain Monte Carlo. The American Naturalist 167: 808–825. https://doi.org/10.1086/503444

Papong K, Kantvilas G, Lumbsch HT (2011) Morphological and molecular evidence places *Maronina* into synonymy with *Protoparmelia* (Ascomycota: Lecanorales). The Lichenologist 43: 561–567. https://doi.org/10.1017/S0024282911000284

Powell M, Glazier DS (2017) Asymmetric geographic range expansion explains the latitudinal diversity gradients of four major taxa of marine plankton. Paleobiology 43: 196–208. https://doi.org/10.1017/pab.2016.38

Prieto M, Wedin M (2013) Dating the diversification of the major lineages of Ascomycota (Fungi). PLoS ONE 8: e65576. https://doi.org/10.1371/journal.pone.0065576

Rambaut A, Suchard MA, Xie D, Drummond AJ (2014) Tracer v1.6.

Richardson JE, Pennington RT (2016) Editorial: Origin of tropical diversity: from clades to communities. Frontiers in Genetics 7: 186. https://doi.org/10.3389/fgene.2016.00186

Rolland J, Condamine FL, Jiguet F, Morlon H (2014) Faster speciation and reduced extinction in the tropics contribute to the mammalian latitudinal diversity gradient. PLoS Biology 12: e1001775. https://doi.org/10.1371/journal.pbio.1001775

Schemske DW (2009) Speciation and patterns of diversity. Butlin R, Bridle J, Schluter D (eds). Cambridge University Press, Cambridge. https://doi.org/10.1017/CBO9780511815683

Singh G, Dal Grande F, Divakar PK, Otte J, Crespo A, Schmitt I (2017) Fungal-algal association patterns in lichen symbiosis linked to macroclimate. New Phytologist 214: 317–329. https://doi.org/10.1111/nph.14366

Singh G, Dal Grande F, Divakar PK, Otte J, Leavitt SD, Szczepanska K, Crespo A, Rico VJ, Aptroot A, Cáceres ME da S, Lumbsch HT, Schmitt I (2015) Coalescent-based species delimitation approach uncovers high cryptic diversity in the cosmopolitan lichen-forming fungal genus *Protoparmelia* (Lecanorales, Ascomycota). PLoS ONE 10: e0124625. https://doi.org/10.1371/journal.pone.0124625

Singh G, Divakar PK, Dal Grande F, Otte J, Parnmen S, Wedin M, Crespo A, Lumbsch HT, Schmitt I (2013) The sister-group relationships of the largest family of lichenized fungi, Parmeliaceae (Lecanorales, Ascomycota). Fungal Biology 117: 715–721. https://doi.org/10.1016/j.funbio.2013.08.001

Than C, Ruths D, Nakhleh L (2008) PhyloNet: a software package for analyzing and reconstructing reticulate evolutionary relationships. BMC Bioinformatics 9: 322. https://doi.org/10.1186/1471-2105-9-322

Thell A, Crespo A, Divakar PK, Kärnefelt I, Leavitt SD, Lumbsch HT, Seaward MRD (2012) A review of the lichen family Parmeliaceae – history, phylogeny and current taxonomy. Nordic Journal of Botany 30: 641–664. https://doi.org/10.1111/j.1756-1051.2012.00008.x

Venables WN, Ripley BD (2002) Modern Applied Statistics with S. Fourth Edition. Springer, New York.

Wallace AR (1878) Tropical nature and other essays. Macmillan, New York. https://doi.org/10.5962/bhl.title.69700

Weir JT, Schluter D (2007) The latitudinal gradient in recent speciation and extinction rates of birds and mammals. Science 315: 1574–1576. https://doi.org/10.1126/science.1135590

Wiens JJ, Donoghue MJ (2004) Historical biogeography, ecology and species richness. Trends in Ecology and Evolution 19: 639–644. https://doi.org/10.1016/j.tree.2004.09.011

Willig MR, Kaufman DM, Stevens RD (2003) Latitudinal gradients of biodiversity: pattern, process, scale, and synthesis. Annual Review of Ecology, Evolution, and Systematics 34: 273–309. https://doi.org/10.1146/annurev.ecolsys.34.012103.144032

Yang Z, Rannala B (2014) Unguided species delimitation using DNA sequence data from multiple loci. Molecular Biology and Evolution 31: 3125–3135. https://doi.org/10.1093/molbev/msu279 PMID: 25274273

Supplementary material 1

Distribution of *Protoparmelia* and *Maronina* species.

Authors: Garima Singh, Francesco Dal Grande, Jan Schnitzler, Markus Pfenninger, Imke Schmitt

Data type: species data

Explanation note: *Protoparmelia* s. str. taxa mainly inhabit arctic/temperate regions and are represented by blue circles. *Maronina* species mainly inhabit subtropical/tropical regions and are represented by red circles. Continuous and dotted line red lines mark tropical and subtropical regions respectively.

Link: https://doi.org/10.3897/mycokeys.36.22548.suppl1

Supplementary material 2

Voucher information

Authors: Garima Singh, Francesco Dal Grande, Jan Schnitzler, Markus Pfenninger, Imke Schmitt

Data type: species data

Explanation note: Voucher information of the samples used in this study (adapted from Singh et al. 2015).

Link: https://doi.org/10.3897/mycokeys.36.22548.suppl2

Supplementary material 3

Genetic characteristics of nuclear loci used in this study

Authors: Garima Singh, Francesco Dal Grande, Jan Schnitzler, Markus Pfenninger, Imke Schmitt

Data type: molecular data

Explanation note: Genetic characteristics of nuclear loci used in this study, including the total number of sequences per locus, length of the alignment and best model of evolution selected using the Akaike information criterion inferred using jModelTest (from Singh et al. 2015).

Link: https://doi.org/10.3897/mycokeys.36.22548.suppl3

Supplementary material 4

Global environmental zones of the *Protoparmelia* and *Maronina* species

Authors: Garima Singh, Francesco Dal Grande, Jan Schnitzler, Markus Pfenninger, Imke Schmitt

Data type: occurence data

Explanation note: Global environmental zones of the *Protoparmelia* and *Maronina* species using the global environmental stratification (GEnS) system, based on statistical clustering of bioclimate data (Metzger et al. 2013). This spatial framework divides the global geographic regions into 18 environmental zones based on the broad set of climate-related variables extracted from the Worldclim database (Hijmans et al. 2005).

Link: https://doi.org/10.3897/mycokeys.36.22548.suppl4

Supplementary material 5

Results of the linear discrimination analysis

Authors: Garima Singh, Francesco Dal Grande, Jan Schnitzler, Markus Pfenninger, Imke Schmitt

Data type: statistical data

Explanation note: A) scree plot summarising the results of principal component analysis for deciding the number of principal components to retain out of 19 bioclimatic variables. The change in slope or the elbow of scree plot occurs at component 4 which is the 4th bioclimatic variable; B) Stacked histogram of the values of the discriminant function for the *Protoparmelia* and *Maronina* species inhabiting warm temperate regions.

Link: https://doi.org/10.3897/mycokeys.36.22548.suppl5

Supplementary material 6

Results of the linear discrimination analysis

Authors: Garima Singh, Francesco Dal Grande, Jan Schnitzler, Markus Pfenninger, Imke Schmitt

Data type: statistical data

Explanation note: Results of the linear discrimination analysis, including the extracted 19 bioclimatic variables, prior probabilities of the *Maronina* and *Protoparmelia*, coefficients of linear discriminants and allocation frequency.

Link: https://doi.org/10.3897/mycokeys.36.22548.suppl6

MycoKeys 36: 21–33 (2018)
doi: 10.3897/mycokeys.36.27094
http://mycokeys.pensoft.net

RESEARCH ARTICLE

A peer-reviewed open-access journal
MycoKeys
Launched to accelerate biodiversity research

A new species of *Rhodocybe* sect. *Rufobrunnea* (Entolomataceae, Agaricales) from Italy

Alfredo Vizzini[1], Renato Jonny Ferrari[2], Enrico Ercole[1], Alessandro Fellin[3]

1 *Department of Life Sciences and Systems Biology, University of Torino, Viale P.A. Mattioli 25, I-10125, Torino, Italy* **2** *Santo Stefano 46, I-39030, San Lorenzo di Sebato (BZ), Italy* **3** *Via G. Canestrini 10/B, I-38028, Revò (TN), Italy*

Corresponding author: *Alfredo Vizzini* (alfredo.vizzini@unito.it)

Academic editor: *M-A Neves* | Received 30 May 2018 | Accepted 30 June 2018 | Published 10 July 2018

Citation: Vizzini A, Ferrari RJ, Ercole E, Fellin A (2018) A new species of *Rhodocybe* sect. *Rufobrunnea* (Entolomataceae, Agaricales) from Italy. MycoKeys 36: 21–33. https://doi.org/10.3897/mycokeys.36.27094

Abstract

Rhodocybe fumanellii is described from Italy as a new species based both on morphological and molecular nrITS/nrLSU data. It belongs in sect. *Rufobrunnea* and is characterised by massive tricholomatoid basidiomata with reddish-brown tinges, adnate and crowded lamellae, an enlarged stipe base with long rhizomorphs, long sinuose slender cheilocystidia, ellipsoid basidiospores and the presence of caulocystidia. Drawings of the main micromorphological features as well as a colour photograph of fresh basidiomata *in situ* are provided and its morphological relationships with allied species are discussed.

Keywords

Agaricomycetes, Basidiomycota, Molecular markers, Phylogeny, Taxonomy

Introduction

Recently, Kluting et al. (2014), using a multigene phylogenetic analysis, redefined the classification of genera within the Entolomataceae. In particular, they proved that the genus *Rhodocybe* Maire, as morphologically delimited (Baroni 1981, Singer 1986, Noordeloos 1988, 2012) is heterogeneous, and it actually consisted of four lineages, of which *Rhodocybe* s.s., *Clitocella* Kluting, T.J. Baroni & Bergemann, *Clitopilopsis* Maire and *Rhodophana* Kühner should be considered as separate genera. *Rhodocybe*

was restricted to the species possessing variable basidiomata (pleurotoid, collybioid, mycenoid, clitocyboid or tricholomatoid), variously coloured, white, grey, brown, pinkish, reddish, yellowish or combinations of these colours; lamellae variously attached, ranging from adnexed to adnate or (sub-)decurrent; basidiospores are thin-walled and evenly cyanophilic, angular in polar view with 6–12 facets and have pronounced undulate pustulate ornamentations in face and profile views. Hymenial cystidia are present or absent and, when present, they can be as pseudocystidia with brightly coloured contents or as hyaline leptocystidia found as cheilocystidia and sometimes as pleurocystidia and clamp connections are absent.

Within *Rhodocybe* s.s., section *Rufobrunnea*, typified by *R. roseiavellanea* (Murrill) Singer, is characterised by a reddish-beige, salmon pink, pinkish-brown or ochre pileus, adnate or decurrent lamellae and absence of pseudocystidia (Baroni 1981, Singer 1986, Noordeloos 2008, 2012). The section was later shown to be natural (monophyletic), also on a molecular basis (Kluting et al. 2014, Sesli and Vizzini 2017). The aim of the present paper is to describe a new species of *Rhodocybe* sect. *Rufobrunnea* from Italy circumscribed on both morphological and molecular data.

Materials and methods

Morphology

Macroscopic description was based from detailed field notes on fresh basidiomata. Colour terms in capital letters (e.g. Pompeian Red, Plate XIII) are those of Ridgway (1912). Fresh basidiomata were photographed *in situ* with a Nikon D5600 digital camera and then dried, while the photos of the microscopical structures, on which the line drawings were based, were obtained through a Zeiss Axiolab light microscope and an OPTIKAM B5 digital camera.

Micromorphologic features were observed on fresh and dried material; sections were rehydrated in distilled water or 3% NH_4OH and then mounted in anionic Congo red as universal dye, lactic Cotton blue to test for cyanophily and Melzer's reagent to determine amyloidity, separately.

All microscopic measurements were carried out with a 1000× oil immersion objective using the Optika Vision Lite 2.1 software. Basidiospores were measured from hymenophores of mature basidiomes and dimensions (hilar appendix excluded) are given as: (minimum–) average minus standard deviation – *average* – average plus standard deviation (–maximum) of length × (minimum–) average minus standard deviation – *average* – average plus standard deviation (–maximum) of width, Q = (minimum–) average minus standard deviation – *average* – average plus standard deviation (–maximum) of ratio length/width. Spore statistics were produced with R version 3.4.4 (R Core Team 2018). The following abbreviations are used: L = number of lamellae reaching the stipe, l = number of lamellulae between each pair of lamellae, Q = the basidiospore quotient (length/width ratio). Herbarium acronyms follow Thiers (2018).

DNA extraction, PCR amplification, and DNA sequencing

Total DNA was extracted from a dry basidioma (MCVE 29550) by blending a portion of it (about 20 mg) with the aid of a micropestle in 600 µl CTAB buffer (CTAB 2%, NaCl 1.4 M, EDTA pH 8.0 20 mM, Tris-HCl pH 8.0 100 mM). The resulting mixture was incubated for 15 min at 65°C. A similar volume of chloroform:isoamyl alcohol (24:1) was added and carefully mixed with the samples until their emulsion. It was then centrifuged for 10 min at 13,000 g, and the DNA in the supernatant was precipitated with a volume of isopropanol. After a new centrifugation of 15 min at the same speed, the pellet was washed in cold ethanol 70%, centrifuged again for 2 min and dried. It was finally re-suspended in 200 µl ddH_2O. PCR amplification was performed with the primers ITS1F and ITS4 (White et al. 1990, Gardes and Bruns 1993) for the nrITS region, while LR0R and LR5 (Vilgalys and Hester 1990) were used to amplify the nrLSU region (28S). PCR reactions were performed under a programme consisting of a hot start at 95 °C for 5 min, followed by 35 cycles at 94 °C, 54 °C and 72 °C (45, 30 and 45 s respectively) and a final 72 °C step for 10 min. PCR products were checked in 1% agarose gel and positive reactions were sequenced with primer ITS4. Chromatograms were checked by searching for putative reading errors and these were corrected. The PCR products were purified with the Wizard SV Gel and PCR Clean-UP System (Promega) following manufacturer's instructions and sequenced by MACROGEN Inc. (Seoul, Republic of Korea). Sequences were checked and assembled using Geneious 5.3 (Drummond et al. 2010) and submitted to GenBank (http://www.ncbi.nlm.nih.gov/genbank/). Accession numbers are reported in Figs 1–3.

Sequence alignment, dataset assembly and phylogenetic analysis

Sequences obtained in this study were compared to those available in the GenBank (http://www.ncbi.nlm.nih.gov/) and UNITE (http://unite.ut.ee/) databases by using the Blastn algorithm (Altschul et al. 1990). Based on the Blastn results, sequences were selected according to the outcomes of recent phylogenetic studies incorporating *Rhodocybe* s.l. taxa (Kluting et al. 2014, Crous et al. 2017, Sesli and Vizzini 2017). The nrITS and nrLSU datasets were analysed separately. The combined nrITS/nrLSU phylogeny was not performed as most *Rhodocybe* s.l. collections in GenBank are not provided with both molecular markers. Alignments were generated for each nrITS and nrLSU dataset using MAFFT (Katoh et al. 2002) with default conditions for gap openings and gap extension penalties. The two alignments were imported into MEGA 6.0 (Tamura et al. 2013) for manual adjustment. The best-fit substitution model for each single alignment was estimated by both the Akaike Information Criterion (AIC) and the Bayesian Information Criterion (BIC) with jModelTest 2 (Darriba et al. 2012). The GTR + G model was chosen for both the nrITS and nrLSU alignments. Two Lyophyllaceae, *Rugosomyces* (*Calocybe*) *carneus* (AF357028 and AF223178) and *Lyophyllum leucophaeatum* (AF357032 and AF223202) were used as outgroup taxa in

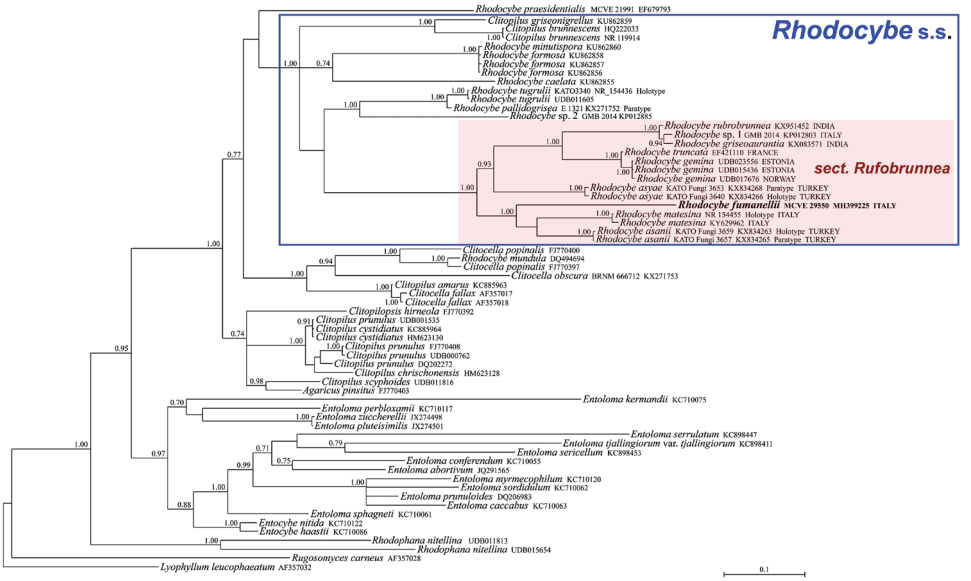

Figure 1. Bayesian phylogram based on the nrITS sequences of Entolomataceae, with *Rugosomyces* (*Calocybe*) *carneus* and *Lyophyllum leucophaeatum* as outgroup taxa. Only BPP values ≥ 0.70 are shown. The newly sequenced collection is in bold.

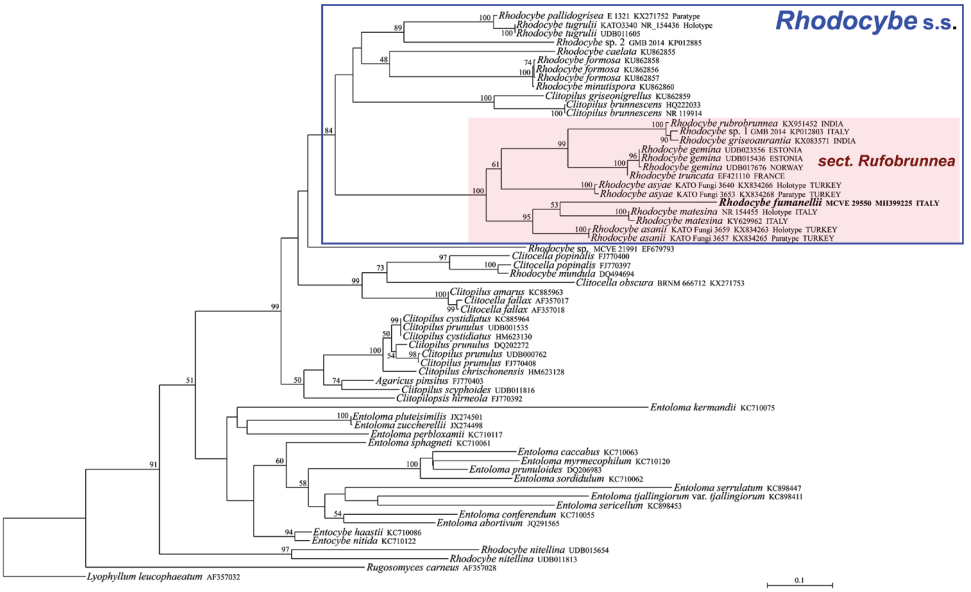

Figure 2. Maximum Likelihood phylogram based on the nrITS sequences of Entolomataceae, with *Rugosomyces* (*Calocybe*) *carneus* and *Lyophyllum leucophaeatum* as outgroup taxa. Only MLB values ≥ 50% are shown. The newly sequenced collection is in bold.

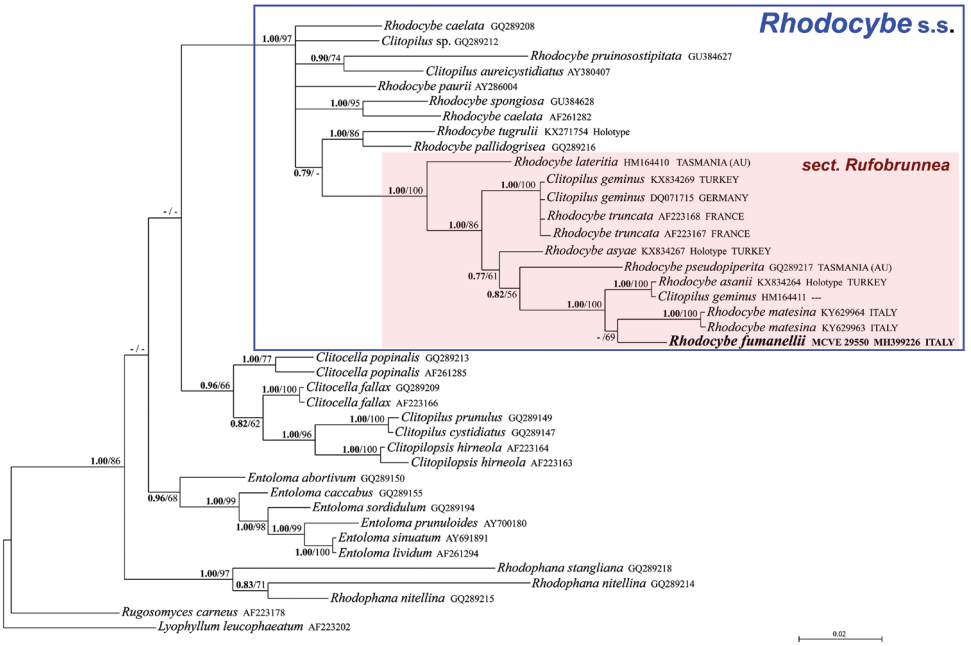

Figure 3. Bayesian phylogram based on the nrLSU sequences of Entolomataceae, with *Rugosomyces* (*Calocybe*) *carneus* and *Lyophyllum leucophaeatum* as outgroup taxa. Only BPP values ≥ 0.70 and MLB values ≥ 50% are shown. The newly sequenced collection is in bold.

both the nrITS and nrLSU analyses following Crous et al. (2017) and Sesli and Vizzini (2017). The nrITS dataset was partitioned into ITS1, 5.8S and ITS2 subsets.

Phylogenetic hypotheses were constructed with Bayesian inference (BI) and Maximum Likelihood (ML) criteria. The BI was performed with MrBayes 3.2.6 (Ronquist et al. 2012) with one cold and three incrementally heated simultaneous Monte Carlo Markov Chains (MCMC) run for 10 million generations, under the selected evolutionary model. Two simultaneous runs were performed independently. Trees were sampled every 1,000 generations, resulting in overall sampling of 10,001 trees per single run; the first 2,500 trees (25%) were discarded as burn-in. For the remaining trees of the two independent runs, a majority rule consensus tree showing all compatible partitions was computed to obtain estimates for Bayesian Posterior Probabilities (BPP).

ML estimation was performed through RAxML 7.3.2 (Stamatakis 2006) with 1,000 bootstrap replicates (Felsenstein 1985) using the GTRGAMMA algorithm to perform a tree inference and search for a good topology. Support values from bootstrapping runs (MLB) were mapped on the globally best tree using the "-f a" option of RAxML and "-x 12345" as a random seed to invoke the novel rapid bootstrapping algorithm. BI and ML analyses were run on the CIPRES Science Gateway web server (Miller et al. 2010). Only BPP and MLB values ≥ 0.70 and ≥ 50%, respectively, are reported in the resulting trees (Figs 1–3). Branch lengths were estimated as mean values over the sampled trees.

Results

Phylogenetic analyses

The nrITS data matrix comprised 64 sequences (1 from the newly sequenced collection, 54 from GenBank and 9 from UNITE). The nrLSU data matrix comprised 40 sequences (1 from the newly sequenced collection and 39 from GenBank). As the Bayesian and Maximum Likelihood analyses of the nrITS sequences are conflicting with each other regarding the precise position of our species, it was decided to show them both (Figs 1–2); on the contrary, BI and ML analyses of the nrLSU sequences produced comparable and congruent topologies and, consequently, only the BI phylogram, with both BPP and MLB values is shown (Fig. 3). Both in the nrITS and nrLSU analysis, our collection clusters in the genus *Rhodocybe* s.s. within the section *Rufobrunnea* (Figs 1–3). In particular, it forms a strongly supported clade together with *R. asanii* Seslı & Vizzini and *R. matesina* Picillo & Vizzini where it occupies an independent but uncertain position with regard to the other two species.

Taxonomy

Rhodocybe fumanellii **Ferrari, Vizzini & Fellin, sp. nov.**
MycoBank MB825646
Figs 4–5

Holotype. Italy. Veneto, Venezia, Chioggia, Riserva Naturale Integrale Bosco Nordio, 45°7'19.563"N, 12°15'38.046"E, 4 m a.s.l., mixed broadleaved forest with *Fraxinus ornus* and *Quercus ilex*, on consolidated dunes, 10 November 2017, Renato Jonny Ferrari & Enrico Bizio (MCVE 29550).

Etymology. dedicated to Ezio Fumanelli, Italian mycologist, naturalist and photographer.

Habit tricholomatoid (Fig. 4). *Pileus* 35–100 mm diam, at first convex with large central umbo, soon plane, irregular, with margin slightly inrolled when young, soon plane, strongly undulate, lobate when old, not striate, surface smooth, dry, greasy when wet, not or very slightly hygrophanous, at first reddish-brown (Nopal Red, Brazil Red, Plate I; Pompeian Red, Plate XIII; *Vinaceous-Rufous, Plate XIV) then brick-red (*Brick Red, Plate XIII), light orange to ochre (Flesh Ocher, Apricot Buff, Plate XIV) when old. *Lamellae* narrow, adnate, quite crowded (L = 60–80), intermixed with lamellulae of variable length [l = 1–3(–4)], up to 3–4 mm high, at first whitish-cream (Seashell Pink, Plate XIV; Pale Ochraceous-Salmon, Plate XV), finally pinkish (Pale Salmon Colour, Pale Flesh Colour, Plate XIV) when very old, with an irregular-eroded concolorous edge. *Stipe* 40–70 × 5–15 mm, cylindrical-clavate (at base to 20–28 mm broad), central, solid, pinkish (Light Corinthian Red, Plate XXVII; Light Congo Pink, *Vinaceous-Pink, Plate XXVIII), covered with a white flocculent-pruinosity, denser

Figure 4. *Rhodocybe fumanellii* (MCVE 29550). Fresh basidiomes *in situ*. Scale bar: 50 mm. Picture by R.J. Ferrari.

towards the apex, the base with a white dense mycelial tomentum and numerous thick white rhizomorphs. *Context* whitish, pink shaded, marbled, thicker (up to 9 mm) in the disc and thinner in the rest of the pileus, *odour* aromatic of walnut kernel, a little floury, *taste* mild, flour-aromatic, not astringent. *Spore-print* pinkish. *Macrochemical reactions* (on fresh material): 30% KOH on context and pileus surface negative.

Basidiospores (5.3–)5.68–*6.26*–6.83(–7.3) × (3.5–)3.93–*4.26*–4.58(–5.1) µm (n = 40), Q = (1.22–)1.34–*1.47*–1.60(–1.78), ellipsoid, colourless under the light microscope, finely warty, pustulate, with a wavy profile (angular in polar view with 8–12 facets), walls cyanophilic, inamyloid (Fig. 5a). Lamella edge heterogeneous. *Basidia* 30–40 × 6.5–7 µm, clavate, 4-spored, thin-walled, sterigmata up to 5 µm long. *Basidioles* 30–45 × 4.5–6 µm, clavate. *Cheilocystidia* 35–95 × 3–6.5 µm, scattered, slender, flexuose-cylindrical, sometimes with protuberances and 1–2-septate, thin-walled (Fig. 5c). *Pleurocystidia* absent. *Hymenophoral trama* subregular, consisting of cylindrical parallel hyphae (2.5–5 µm) mixed with short, inflated, up to 13 µm wide elements. *Pileipellis* as a xerocutis, made up of subparallel, thin-walled hyphae, 2−5 µm wide, orange-brown (in H_2O), with presence of granular epiparietal pigment (observable in H_2O and NH_4OH), terminal elements obtuse (Fig. 5c). *Caulocystidia* (25–)30–50(–69) × (2.5–)3–4(–5) µm, slender with a cylindrical-irregular shape, thin-walled (Fig. 5b). *Clamp-connections* absent everywhere.

Habit, habitat and distribution. In small groups (gregarious), in the litter of broadleaved trees on sandy soil. So far, known only from the type locality.

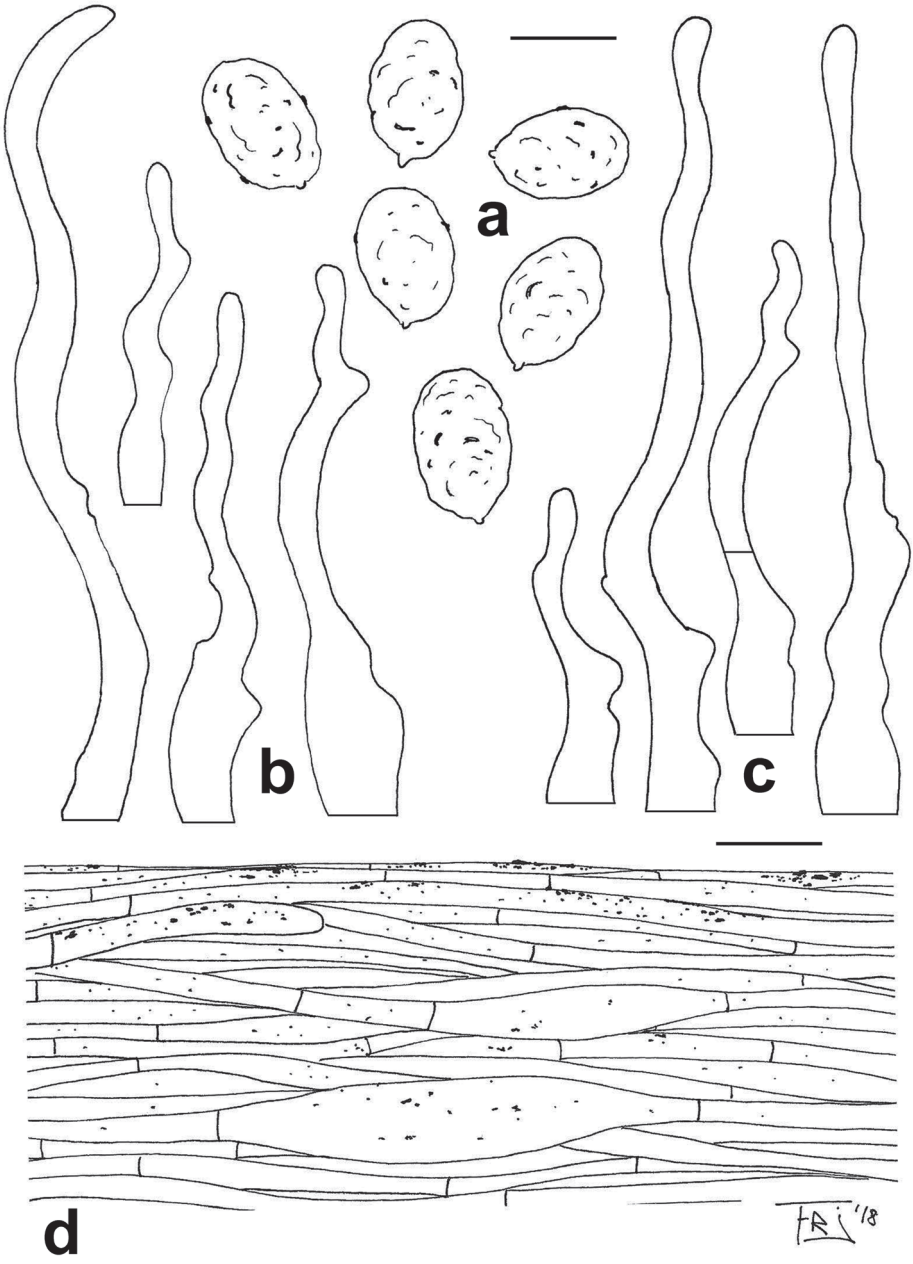

Figure 5. *Rhodocybe fumanellii* (MCVE 29550). Microscopical features. **a** Basidiospores **b** caulocystidia **c** cheilocystidia **d** pileipellis. Scale bars: 5 µm. Line drawings by R.J. Ferrari.

Discussion

Section *Rufobrunnea* is a character-poor taxon with many species macroscopically very similar (cryptic species) and differing only in very subtle features (e.g. habit, basidioma colour, type of lamellae insertion, odour, taste, presence/absence of rhizomorphs) (Baroni 1981, Sesli and Vizzini 2017). To what extent these characters can be influenced by the environmental factors still remains to be verified. Also microscopic identification depends on observations of a rather limited set of characters, such as presence/absence of cheilocystidia, cystidial shape, spore size and ornamentation and pileipellis structure and pigmentation. From a traditional morphological perspective, this often makes species identification difficult or even daunting. Despite this, the species in this section are quite distinct if analysed in light of ribosomal sequences (Crous et al. 2017, Sesli and Vizzini 2017).

Rhodocybe fumanellii has proved to be an independent and distinct species within this section based on molecular analyses (Figs 1–3). Morphologically, it is circumscribed in having robust and massive basidiomata with a tricholomatoid habit and reddish-brown tinges, adnate not decurrent and crowded lamellae, an enlarged stipe base with evident long rhizomorphs, very long and slender cheilocystidia (up to 95 µm long), ellipsoid basidiospores (average Q = 1.47) and presence of caulocystidia.

The phylogenetically closest species to *R. fumanellii* are the recently described *R. matesina* and *R. asanii*. *Rhodocybe matesina* from Italy differs in a collybioid and slender habit (stipe up to 9 mm broad), thin context, a strongly hygrophanous pileus without reddish tinges, a smell similar to *Hygrophorus penarioides* Jacobsson & E. Larss., bitter and astringent taste, absence of rhizomorphs and an olive-green reaction on the pileus surface with KOH; microscopically *R. matesina* is distinguished due to shorter cheilocystidia (16.5–23 × 3–6.5 µm), the absence of caulocystidia and the presence in the pileipellis of rare pseudoclamps (Crous et al. 2017). *Rhodocybe asanii* from Turkey has a collybioid habit with a 20–45 mm broad pileus, thin and very fragile context (up to 4 mm thick at pileus centre), quite distant sinuate lamellae (L = 40–50), a stipe without rhizomorphs, indistinct odour and taste, smaller spores (5.8 × 4.1 µm on average, apiculus included), no cheilocystidia and caulocystidia and growth between debris and grass in coniferous woods (*Pinus* L., *Picea* A. Dietr., *Abies* Mill.) (Sesli and Vizzini 2017).

Hereafter, distinctive features of the species in the section *Rufobrunnea* that somehow morphologically resemble *R. fumanellii*, are provided. *Rhodocybe lateritia* T.J. Baroni & G.M. Gates described from Tasmania, is circumscribed by a burnt sienna or reddish-brown cup-shaped, up to 120 mm broad pileus, large, 5.5–11 × 4.5–7.5 µm basidiospores and ascending, cystidioid elements (pileocystidia) in the pileipellis (Baroni and Gates 2006, Noordeloos and Gates 2012). *Rhodocybe alutacea* Singer from North America has a smaller umbilicate hygrophanous pileus (up to 35 mm diam and up to 2 mm thick context) minutely erect-squamulose to subtomentose-squamulose at centre and thinner stipe (2.5–5 mm broad), a pileus margin remaining inrolled to incurved, decurrent lamellae, a farinaceous odour and taste (mild), larger spores (up to 8 × 5.5 µm) and shorter septate cheilocystidia (20–35 × 6.5–7 µm) with often capitulate terminal elements (Singer 1946, Baroni 1981, Baroni and Horak 1994). *Rhodocybe asyae*

Seslı & Vizzini from Turkey differs in having smaller basidiomes (pileus up to 30 mm diam and stipe up to 5 mm diam), decurrent lamellae, stipe without rhizomorphs, mainly 2-spored basidia, no caulocystidia, less elongated basidiospores (average Q = 1.3) and grows in the litter of coniferous trees (*Pinus*, *Picea*, *Abies*) (Sesli and Vizzini 2017). *Rhodocybe incarnata* T.J. Baroni & Halling, from cloud forests in Venezuela, mainly differs by a pileus at first fire red, flame red, flame scarlet then becoming paler, matted subtomentose to matted pubescent, white to yellowish-white lamellae, shorter basidiospores (5.7 µm long on average) and cheilocystidia (14.6–25.9 × 2.4–4 µm) and pileipellis as a trichoderm (Baroni and Halling 1992). *Rhodocybe pseudopiperita* T.J. Baroni & G.M. Gates from Tasmania is distinguished by a weakly umbonate pileus with shallow depression around the umbo, indistinct odour or like mown grass, the presence of scattered cystidioid elements in the pileipellis and dimorphic basidiospore morphology with most of them being distinctly undulate-pustulate and smaller (5.5–6.5 × 4–5 µm) while ca. 30–45% of the basidiospores are almost smooth and distinctly larger (7–9 × 5–5.5 µm) (Baroni and Gates 2006, Noordeloos and Gates 2012). The North American *R. roseiavellanea* shares with *R. fumanellii* a robust habitus (not hygrophanous thick-fleshed pileus 35–70 mm broad and stipe 30–60 × 10–25 mm), a mild taste, a growth under oaks, but is distinguished by short decurrent to decurrent lamellae, a stipe without rhizomorphs, shorter cheilocystidia, 12–25 × 2–4 µm and large ellipsoid to subamygdaliform spores, (6.5–)7–9(–10) × (4–)5–5.5(–7) µm (Baroni 1981). *Rhodocybe gemina* (Paulet) Kuyper & Noordel. from Europe, Algeria, Morocco and Turkey differs considerably in having broadly adnate to subdecurrent lamellae, subglobose to broadly ellipsoid, 5–6.5(–7) × 4–5(–5.5) µm basidiospores and mainly growing in montane coniferous forests (above all *Picea* spp.) (Maire 1924, Malençon and Bertault 1975, Watling and Gregory 1977, Baroni 1981, Breitenbach and Kränzlin 1995, Noordeloos 1988, 2012, Sesli and Vizzini 2017). *Rhodocybe gemina* var. *mauretanica* (Maire) Bon and var. *subvermicularis* (Maire) Quadr. & Lunghini [= *Rhodocybe subvermicularis* (Maire) Ballero & Contu] from European Mediterranean areas, Algeria and Morocco show a collybioid to clitocyboid habit with a pileus up to 50 mm broad and decurrent lamellae and no evident cheilo- and caulocystidia (Maire 1924, Malençon and Bertault 1975, Baroni 1981, Bon 1990, Ballero et al. 1992). Finally, *R. nuciolens* (Murrill) Singer from North America shows slender basidiomes with short decurrent subdistant lamellae, a 2–9 mm broad stipe, context up to 3 mm thick at pileus centre, large ellipsoid to amygdaliform basidiospores 5.5–8(–9) × (3–)4–5(–5.5) µm, and it grows in humus, sandy soil or on decaying wood under *Pseudotsuga menziesii*, *Sequoia sempervirens*, *Abies* sp., or *Arbutus menziesii* (Murrill 1913, Singer 1946, Baroni 1981).

Acknowledgements

We want to thank Enrico Bizio and Gabriele Cacialli for their helpful suggestions and collaboration and the Bresadola Mycological Association (AMB) of Brunico (BZ) for its support.

References

Altschul SF, Gish W, Miller W, Myers EW, Lipman DJ (1990) Basic local alignment search tool. Journal of Molecular Biology 215: 403–410. http://dx.doi.org/10.1016/S0022-2836(05)80360-2

Ballero M, Contu M, Fogu MC (1992) Contributo alla conoscenza dei macromiceti presenti nei cisteti della Sardegna. Revista Iberoamericana de Micología 9(3): 58–60.

Baroni TJ (1981) A revision of the genus *Rhodocybe* Maire (Agaricales). Beihefte zur Nova Hedwigia 67: 1–198.

Baroni TJ, Gates GM (2006) New species and records of *Rhodocybe* (Entolomataceae, Agaricales) from Tasmania. Australian Systematic Botany 19: 343–358. http://dx.doi.org/10.1071/SB06002

Baroni TJ, Halling RE (1992) New species of *Rhodocybe* from South America with a key to species. Mycologia 84(3): 411–421. http://dx.doi.org/10.2307/3760194

Baroni TJ, Horak E (1994) Entolomataceae in North America III: new taxa, new combinations and notes on species of *Rhodocybe*. Mycologia 86(1): 138–145. http://dx.doi.org/10.2307/3760730

Bon M (1990) Flore mycologique du littoral - 04. Documents Mycologiques 20(78): 53–60.

Breitenbach J, Kränzlin F (1995) Champignons de Suisse, tome 4. Mykologia, Lucerne.

Crous PW, Wingfield MJ, Burgess TI, Hardy GEStJ, Barber PA, Alvarado P, Barnes CW, Buchanan PK, Heykoop M, Moreno G, Thangavel R, Van der Spuy S, Barili A, Barrett S, Cacciola SO, Cano-Lira JF, Crane C, Decock C, Gibertoni TB, Guarro J, Guevara-Suarez M, Hubka V, Kolařík M, Lira CRS, Ordoñez ME, Padamsee M, Ryvarden L, Soares AM, Stchigel AM, Sutton DA, Vizzini A, Weir BS, Acharya K, Aloi F, Baseia IG, Blanchette RA, Bordallo JJ, Bratek Z, Butler T, Cano-Canals J, Carlavilla JR, Chander J, Cheewangkoon R, Cruz RHSF, Da Silva M, Dutta AK, Ercole E, Escobio V, Esteve-Raventós F, Flores JA, Gené J, Góis JS, Haines L, Held BW, Horta Jung M, Hosaka K, Jung T, Jurjević Ž, Kautman V, Kautmanova I, Kiyashko AA, Kozanek M, Kubátová A, Lafourcade M, La Spada F, Latha KPD, Madrid H, Malysheva EF, Manimohan P, Manjón JL, Martín MP, Mata M, Merényi Z, Morte A, Nagy I, Normand A-C, Paloi S, Pattison N, Pawłowska J, Pereira OL, Petterson ME, Picillo B, Raj KNA (2017) Fungal Planet description sheets: 558–624. Persoonia 38: 240–384. https://doi.org/10.3767/003158517X698941

Darriba D, Taboada GL, Doallo R, Posada D (2012) jModelTest 2: more models, new heuristics and parallel computing. Nature Methods 9(8): 772. https://doi.org/10.1038/nmeth.2109

Drummond AJ, Ashton B, Cheung M, Heled J, et al. (2010) Geneious v5.3. Available from http://www.geneious.com/

Gardes M, Bruns TD (1993) ITS primers with enhanced specificity for basidiomycetes – application to the identification of mycorrhizae and rusts. Molecular Ecology 2: 113–118. https://doi.org/10.1111/j.1365-294x.1993.tb00005.x

Katoh K, Misawa K, Kuma K, Miyata T (2002) MAFFT: a novel method for rapid multiple sequence alignment based on fast Fourier transform. Nucleic Acids Research 30: 3059–3066. https://doi.org/10.1093/nar/gkf436

Kluting KL, Baroni TJ, Bergemann SE (2014) Toward a stable classification of genera within the Entolomataceae: a phylogenetic re-evaluation of the *Rhodocybe-Clitopilus* clade. Mycologia 106(6): 1127–1142. https://doi.org/10.3852/13-270

Maire R (1924) Études mycologiques (fascicule 2). Bulletin de la Société Mycologique de France 40(3): 293–317.

Malençon G, Bertault R (1975) Flore des Champignons supérieurs du Maroc. Tome II. Institut scientifique Chérifien, Rabat.

Miller MA, Pfeiffer W, Schwartz T (2010) Creating the CIPRES Science Gateway for inference of large phylogenetic trees. Proceedings of the Gateway Computing Environments Workshop (GCE), 14 November 2010, New Orleans, LA, 1–8. https://doi.org/10.1109/gce.2010.5676129

Murrill WA (1913) The Agaricaceae of the Pacific Coast: IV. New Species of *Clitocybe* and *Melanoleuca*. Mycologia 5(4): 206–223.

Noordeloos ME (1988) *Rhodocybe* Maire. In: Bas C, Kuyper TW, Noordeloos ME, Vellinga EC (Eds) Flora Agaricina Neerlandica. I. A.A. Balkema, Rotterdam, 77–82.

Noordeloos ME (2012) *Rhodocybe* Maire. In: Knudsen H, Vesterholt J (Eds) Funga Nordica, 2nd edition. Nordsvamp, Copenhagen, 576–579.

Noordeloos ME, Gates GM (2012) The Entolomataceae of Tasmania. Fungal Diversity Research Series 22: 1–400.

R Core Team (2018) R: a language and environment for statistical computing, version 3.4.4. http://www.R-project.org

Ridgway R (1912) Color standards and color nomenclature. Self-published, Washington DC.

Ronquist F, Teslenko M, van der Mark P, Ayres DL, Darling A, Höhna S, Larget B, Liu L, Suchard MA, Huelsenbeck JP (2012) MrBayes 3.2: efficient Bayesian phylogenetic inference and model choice across a large model space. Systematic Biology 61: 539–542. https://doi.org/10.1093/sysbio/sys029

Sesli E, Vizzini A (2017) Two new *Rhodocybe* species (sect. *Rufobrunnea*, Entolomataceae) from the East Black Sea coast of Turkey. Turkish Journal of Botany 41: 200–210. https://doi.org/10.3906/bot-1607-1

Singer R (1946) Two new species in the Agaricales. Mycologia 38(6): 687–690. https://doi.org/10.2307/3755310

Singer R (1986) The Agaricales in modern taxonomy. 4th ed. Koeltz scientific Books, Koenigstein.

Stamatakis A (2006) RAxML-VI-HPC: Maximum likelihood-based phylogenetic analyses with thousands of taxa and mixed models. Bioinformatics 22: 2688–2690. https://doi.org/10.1093/bioinformatics/btl446

Tamura K, Stecher G, Peterson D, Filipski A, Kumar S (2013) MEGA 6: molecular evolutionary genetics analysis version 6.0. Molecular Biology and Evolution 30(12): 2725–2729. https://doi.org/10.1093/molbev/mst197

Thiers B [continuously updated] Index Herbariorum: A global directory of public herbaria and associated staff. New York Botanical Garden's Virtual Herbarium. http://sweetgum.nybg.org/science/ih/ [Accessed 25 May 2018]

Vilgalys R, Hester M (1990) Rapid genetic identification and mapping of enzymatically amplified ribosomal DNA from several *Cryptococcus* species. Journal of Bacteriology 172: 4238–4246. https://doi.org/10.1128/jb.172.8.4238-4246.1990

Watling R, Gregory NM (1977) Larger fungi from Turkey, Iran and neighbouring countries. Karstenia 17: 59–72. https://doi.org/10.29203/ka.1977.125

White TJ, Bruns T, Lee S, Taylor JW (1990) Amplification and direct sequencing of fungal ribosomal RNA genes for phylogenetics. In: Innis MA, Gelfand DH, Sninsky JJ, White TJ (Eds) PCR protocols: a guide to methods and applications. Academic Press Inc., New York, 315–322. https://doi.org/10.1016/b978-0-12-372180-8.50042-1

MycoKeys 36: 35–43 (2018)
doi: 10.3897/mycokeys.36.25986
http://mycokeys.pensoft.net

RESEARCH ARTICLE

A peer-reviewed open-access journal
MycoKeys
Launched to accelerate biodiversity research

Fomitiporia rhamnoides sp. nov. (Hymenochaetales, Basidiomycota), a new polypore growing on *Hippophae* from China

Tie-Zhi Liu[1], Qian Chen[2], Mei-Ling Han[3], Fang Wu[2]

1 *College of Life Sciences, Chifeng University, Chifeng, Inner Mongolia 024000, China* **2** *Institute of Microbiology, Beijing Forestry University, Beijing 100083, China* **3** *College of Life Science, Langfang Normal University, Langfang 065000, China*

Corresponding author: *Fang Wu* (fangwubjfu2014@yahoo.com)

Academic editor: *A. Vizzini* | Received 9 April 2018 | Accepted 3 July 2018 | Published 13 July 2018

Citation: Liu T-Z, Chen Q, Han M-L, Wu F (2018) *Fomitiporia rhamnoides* sp. nov. (Hymenochaetales, Basidiomycota), a new polypore growing on *Hippophae* from China. Title. MycoKeys 36: 35–43. https://doi.org/10.3897/mycokeys.36.25986

Abstract

Based on morphology and phylogenetic analysis, *Fomitiporia rhamnoides* sp. nov. is described. It is characterised by perennial, pileate basidiomata, distinctly shining poroid surface, a zonate context, 11–13 pores per mm, parallel tramal hyphae and regularly arranged contextual hyphae, the presence of cystidioles, globose, hyaline, thick-walled, smooth, dextrinoid, strongly cyanophilous basidiospores measuring 5.8–7 × 5.4–6.5 µm and growing on *Hippophae rhamnoides* in northern China. *Fomitiporia rhamnoides* differs from other *Fomitiporia* species growing on *Hippophae* by its smaller pores (11–13 per mm vs. <10 per mm).

Keywords

Hymenochaetaceae, taxonomy, wood-inhabiting fungi

Introduction

Fomitiporia Murrill (Murrill 1907), typified by *F. langloisii* Murrill, is an important genus in Hymenochaetaceae because some species are pathogens of trees (Dai et al. 2007, Rajchenberg and Robledo 2013, Ota et al. 2014) whereas some other species

are claimed to be medicinal (Dai et al. 2009). *Fomitiporia* is easy to distinguish from other members of Hymenochaetaceae in having subglobose to globose, hyaline, thick-walled, strongly dextrinoid and cyanophilous basidiospores (Fiasson and Niemelä 1984, Amalfi and Decock 2013, Chen and Cui 2017).

During investigations on wood-inhabiting fungi in northern China, in Hebei and Shanxi provinces, some specimens of a *Fomitiporia* species were collected on living *Hippophae rhamnoides*. They are characterised by distinctly small pores which make them different from other *Fomitiporia* species growing on *Hippophae*.

To understand their taxonomic placement, phylogenetic analysis was carried out based on the nuc rDNA regions of the 5.8S rDNA (ITS) and nuc 28S rDNA D1-D2 domains. Molecular analyses showed that the sampled specimens are clustered into a lineage representing an unknown species of *Fomitiporia*.

Materials and methods

The studied specimens are deposited at the herbarium of the Institute of Microbiology, Beijing Forestry University (BJFC). The microscopic procedure follows Zhou et al. (2016a). The following abbreviations are used: IKI = Melzer's reagent, IKI– = both inamyloid and indextrinoid, KOH = 5% potassium hydroxide, CB = Cotton Blue, CB+ = cyanophilous, CB– = acyanophilous, L = mean spore length (arithmetic average of all spores), W = mean spore width (arithmetic average of all spores), Q = variation in the L/W ratios between the specimens studied and n = number of spores measured from a given number of specimens. Special colour codes followed Petersen (1996).

CTAB rapid plant genome extraction kit-DN14 (Aidlab Biotechnologies Co. Ltd, Beijing) was used to obtain PCR products from dried specimens according to the manufacturer's instructions with some modifications. Two DNA gene fragments, ITS and 28S were amplified using respectively the primer pairs ITS5/ITS4 (White et al. 1990) and LR0R/LR7 (http://www.biology.duke.edu/fungi/mycolab/primers.htm). The PCR procedures for ITS and 28S followed Zhou et al. (2016b). DNA sequencing was performed at the Beijing Genomics Institute and newly generated sequences were deposited in the GenBank database.

Sequences generated for this study and additional sequences downloaded from GenBank were aligned using BioEdit (Hall 1999) and ClustalX (Thompson et al. 1997).

In the study, nuclear ribosomal RNA genes were used to determine the phylogenetic position of the new species. *Phellinus uncisetus* Robledo, Urcelay & Rajchenb. was designated as an outgroup following Decock et al. (2007).

Maximum parsimony analysis was applied to the combined dataset of ITS+28S sequences using PAUP* version 4.0b10 (Swofford 2002). All characters were equally weighted and gaps were treated as missing data. Trees were inferred using the heuristic search option with TBR branch swapping and 1000 random sequence additions. Max-trees were set to 5000, branches of zero length were collapsed and all parsimonious trees were saved. Clade robustness was assessed using bootstrap analysis with 1000

replicates (Felsenstein 1985). Descriptive tree statistics tree length (TL), consistency index (CI), retention index (RI), rescaled consistency index (RC) and homoplasy index (HI) were calculated for each maximum parsimonious tree generated. The Maximum likelihood (ML) tree was constructed using raxmlGUI 1.2 (Stamatakis 2006, Silvestro and Michalak 2012) with GTR+I+ G model and auto FC option (Pattengale 2010) in bootstrap (BS) replicates.

MrModeltest 2.3 (Posada and Crandall 1998, Nylander 2004) was used to determine the best-fit evolution model for the combined dataset of ITS+28S sequences for running Bayesian inference (BI). BI was calculated with MrBayes 3.1.2 (Ronquist and Huelsenbeck 2003). Four Markov chains were run for two runs from random starting trees for 2 million generations for the combined dataset of ITS+28S sequences and trees were sampled every 100 generations. The first quarter of the generations were discarded as burn-in. The majority rule consensus tree of all remaining trees was calculated. Branches that received bootstrap support for Maximum parsimony (BP), Maximum likelihood (BS) and Bayesian posterior probabilities (BPP) greater than or equal to 50% (BP/BS) and 0.95 (BPP), respectively, were considered as significantly supported.

Phylogeny results

The combined ITS+28S dataset includes 78 specimens and resulted in an alignment of 1737 characters, of which 1124 characters are constant, 98 are variable and parsimony-uninformative and 515 are parsimony-informative. Maximum parsimony analysis yielded 28 equally parsimonious trees (TL = 1515, CI = 0.549, HI = 0.451, RI = 0.813, RC = 0.446). The best model for the combined dataset, estimated and applied in the Bayesian analysis, is GTR+I+G, lset nst = 6, rates = invgamma; prset statefreqpr = dirichlet (1,1,1,1). Bayesian analysis and ML analysis resulted in a similar topology to MP analysis, with an average standard deviation of split frequencies = 0.007191 (BI). Therefore, only the MP tree was presented and BP, BS and BPP values simultaneously above 50%, 50% and 0.95, respectively, were indicated at the nodes (Fig. 1). The phylogeny shows that the three newly sequenced specimens gathered with *F. guoshangensis* S. Guo & L. Zhou in a single, isolated, variably supported (68%/71%/1.00) clade (Fig. 1).

Taxonomy

Fomitiporia rhamnoides **T.Z. Liu & F. Wu, sp. nov.**
MycoBank: MB825105
Figs 2, 3

Holotype. CHINA. Hebei Province, Zuolu County, Xiaowutai Nature Reserve, Shanjiankou, on living tree of *Hippophae rhamnoides*, 10.IX.2017, *Dai 18091* (BJFC025621).

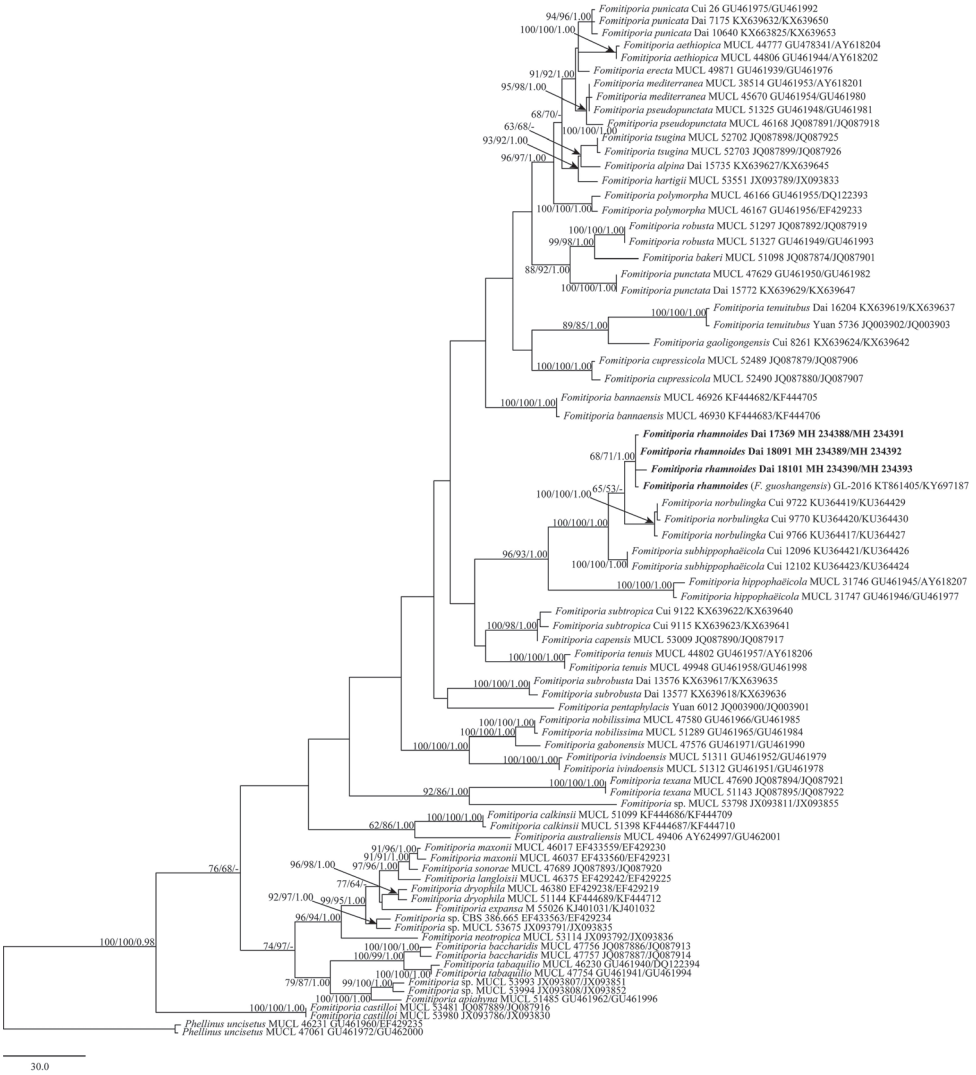

Figure 1. Phylogenetic tree inferred from maximum parsimony (MP) analysis based on the combined dataset of ITS and 28S. Only maximum parsimony (BP), maximum likelihood (BS) and Bayesian posterior probabilities (BPP) greater than or equal to 50% (BP), 50% (BS) and 0.95 (BPP) are reported on the branches.

Etymology. *Rhamnoides* (Lat.) refers to the species growing on *Hippophae rhamnoides*.

Basidiomata perennial, pileate, solitary or a few imbricated, hard corky and without odour or taste when fresh, woody hard and medium in weight when dry; pilei dimidiate to ungulate, triquetrous in section, projecting up to 5 cm, 7 cm wide and 2.5 cm thick at base; pileal surface yellowish-brown, greyish-brown to dark brown, concentrically sulcate, at first velutinate, becoming glabrous and slightly cracked with age; margin obtuse. Poroid surface clay-buff to yellowish-brown when fresh, becoming

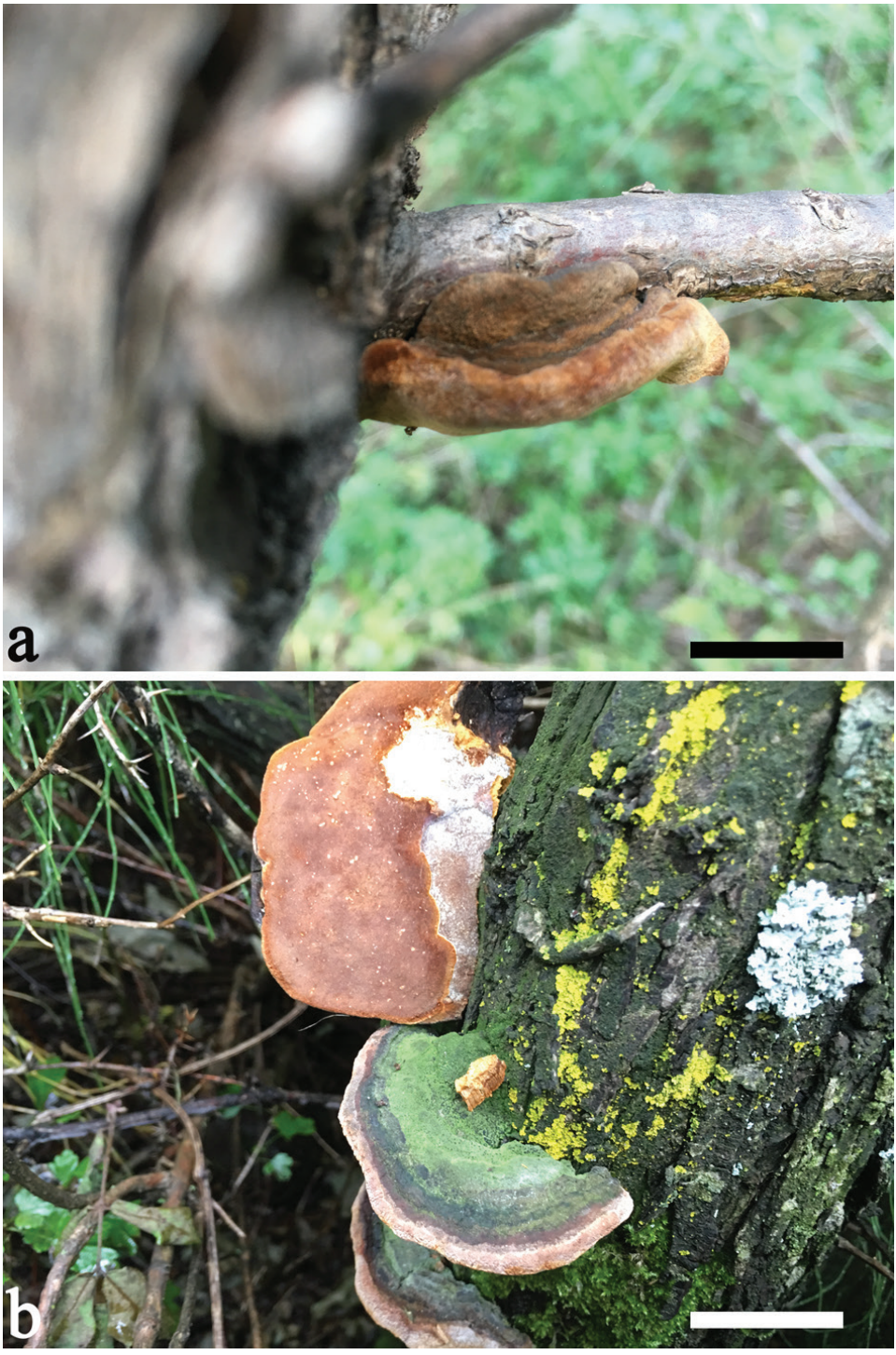

Figure 2. Basidiocarps of *Fomitiporia rhamnoides* (**a** Dai 18087 showing a juvenile basidiomata **b** Dai 18100 showing the mature basidiomata; Scale bars: 3 cm).

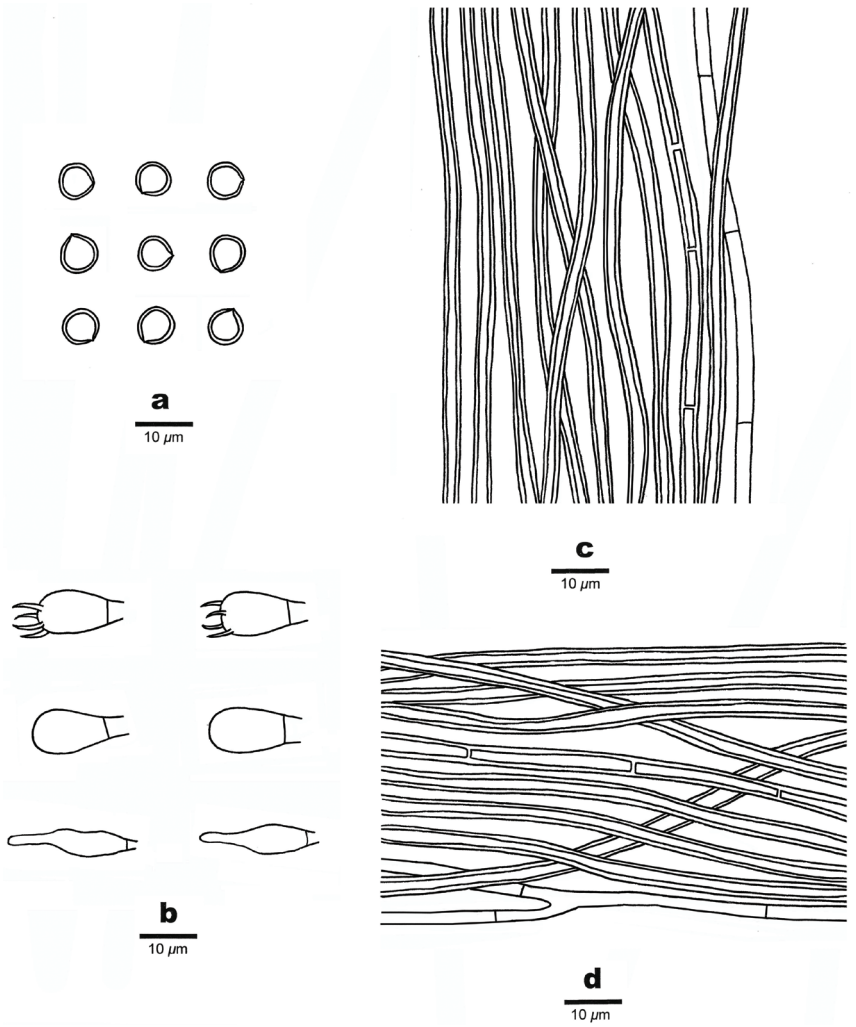

Figure 3. Microscopic structures of *Fomitiporia rhamnoides* (from the holotype). **a** Basidiospores **b** Basidia, basidioles and cystidioles **c** Hyphae from trama **d** Hyphae from context.

orange brown to snuff brown when dry, shining; sterile margin yellowish-brown, up to 3 mm wide; pores circular, 11–13 per mm, dissepiments entire. Context yellowish-brown, zonate, woody hard, up to 1.5 cm thick; tubes greyish-brown, paler than context, hard corky to brittle, up to 1 cm long, annual layers indistinct.

Hyphal structure. Hyphal system dimitic; generative hyphae simple septate; tissue darkening but otherwise unchanged in KOH.

Context. Generative hyphae hyaline to pale yellow, thin- to slightly thick-walled, occasionally branched, frequently septate, 3–4 μm in diam., skeletal hyphae yellowish-brown, thick-walled with a wide lumen, unbranched, occasionally septate, straight, regularly arranged, 4.5–6 μm in diam.

Trama of the tubes. Generative hyphae hyaline to pale yellowish, thin-walled, occasionally branched, frequently septate, 2–3 μm in diam., skeletal hyphae dominant, yellowish-brown, thick-walled with a wide lumen, unbranched, occasionally septate, straight, parallel along the tubes, 2.5–4 μm in diam. Setae absent; cystidioles present, more or less ventricose, hyaline, thin-walled, 12–20 × 3–6 μm; basidia subglobose to barrel-shaped, with four sterigmata and a simple septum at the base, 8–16 × 6–10 μm; basidioles dominant in hymenium, in shape similar to basidia, but slightly smaller; big rhomboid crystals present amongst hymenium.

Spores. Basidiospores globose, hyaline, thick-walled, smooth, dextrinoid in Melzer's reagent, strongly CB+, (5.2–)5.8–7(–7.3) × (5–)5.5–6.5(–6.8) μm, L = 6.47 μm, W = 6.06 μm, Q = 1.06–1.08 (n=60/2).

Additional specimens (paratypes) examined. CHINA. Hebei Province, Zuolu County, Xiaowutai Nature Reserve, Shanjiankou, on living tree of *Hippophae rhamnoides*, 10.IX.2017, *Dai 18087* (BJFC025617), *Dai 18088* (BJFC025618), *Dai 18090* (BJFC025620), *Dai 18100* (BJFC025630), *Dai 18101* (BJFC25631). Shanxi Province, Zuoyun County, Santun, on living tree of *Hippophae rhamnoides*, 19.V.2017, *Dai 17368* (BJFC024903), *Dai 17369* (BJFC024904), *Dai 17370* (BJFC024905).

Type of rot. Causing a white rot.

Discussion

Fomitiporia rhamnoides is characterised by its very small pores (11–13 per mm) and growing on *Hippophae rhamnoides*. It has the same sequences of *Fomitiporia guoshangensis*, an illegitimate name (art. 7, 8, 32A, code of nomenclature) also described based in Chinese collections (Guo et al. 2016).

Three species of *Fomitiporia*, *F. hippophaëicola* (H. Jahn) Fiasson & Niemelä, *F. norbulingka* B.K. Cui & Hong Chen, *F. subhippophaëicola* B.K. Cui & H. Chen, have been reported on *Hippophae* (Chen et al. 2016, Chen and Cui 2017, Ryvarden and Melo 2017). Amongst them, *F. hippophaëicola* has a distribution in Europe whereas *F. norbulingka* and *F. subhippophaëicola* have, so far, been found in Tibet, China (Chen et al. 2016). *Fomitiporia hippophaëicola* was previously recorded in China (Dai 2010), but the voucher specimens were re-identified as *F. subhippophaëicola*. The main characters of *F. hippophaëicola*, *F. norbulingka* and *F. subhippophaëicola* were given by Chen et al. (2016).

Fomitiporia rhamnoides resembles *F. hippophaëicola*, *F. norbulingka* and *F. subhippophaëicola* by sharing similar basidiomata and basidiospores, but it can be distinguished from these three species by smaller pores (11–13 per mm, vs. 5–7 per mm in *F. hippophaëicola*, 6–9 per mm in *F. norbulingka*, 8–10 per mm in *F. subhippophaëicola*). Phylogenetically, *F. rhamnoides* forms a single lineage and is closely related to *F. norbulingka*.

Fomes yasudae Lloyd was originally described from Japan on an angiosperm trunk (Lloyd 1915) and Ryvarden (1989) considered it as a synonym of *Fomitiporia robusta* (P. Karst.) Fiasson & Niemelä. *Fomes yasudae* may be confused with *Fomitiporia rhamnoides* because of its small pores, but it has distinct smaller basidiospores (3.5–4 μm in

diam.) and uncracked upper surface (Lloyd 1915). *Fomes yasudae* is most probably an independent species rather than *Fomitiporia robusta* because the latter has larger basidiospores (5.8–7.3 × 5.3–6.8 μm, Niemelä 2005).

Acknowledgements

We would like to express our deep thanks to Prof. Yu-Cheng Dai (Beijing Forestry University) who allowed us to study his specimens. This study was supported by the National Natural Science Foundation of China (Nos. 31700024 and 31760004).

References

Amalfi M, Decock C (2013) *Fomitiporia castilloi* sp. nov. and evidence for multiples clades around *F. apiahyna* in Meso- and South America, representing potential species. Mycologia 105: 873–887. https://doi.org/10.3852/11-423

Chen H, Cui BK (2017) Multi-locus phylogeny and morphology reveal five new species of *Fomitiporia* (Hymenochaetaceae) from China. Mycological Progress 16: 687–701. https://doi.org/10.1007/s11557-017-1306-0

Chen H, Zhou JL, Cui BK (2016) Two new species of *Fomitiporia* (Hymenochaetales, Basidiomycota) from Tibet, southwest China. Mycologia 108: 1010–1017. https://doi.org/10.3852/16-011

Dai YC (2010) Hymenochaetaceae (Basidiomycota) in China. Fungal Diversity 45: 131–343. https://doi.org/10.1007/s13225-010-0066-9

Dai YC, Cui BK, Yuan HS, Li BD (2007) Pathogenic wood-decaying fungi in China. Forest Pathology 37: 105–120. https://doi.org/10.1111/j.1439-0329.2007.00485.x

Dai YC, Yang ZL, Cui BK, Yu CJ, Zhou LW (2009) Species diversity and utilization of medicinal mushrooms and fungi in China (Review). International Journal of Medicinal Mushrooms 11: 287–302. https://doi.org/10.1615/IntJMedMushr.v11.i3.80

Decock C, Herrera FS, Robledo G, Castillo G (2007) *Fomitiporia punctata* (Basidiomycota, Hymenochaetales) and its presumed taxonomic synonyms in America: taxonomy and phylogeny of some species from tropical/subtropical areas. Mycologia 99: 733–752. https://doi.org/10.3852/mycologia.99.5.733

Felsenstein J (1985) Confidence intervals on phylogenetics: an approach using bootstrap. Evolution 39: 783–791. https://doi.org/10.2307/2408678

Fiasson JL, Niemelä T (1984) The Hymenochaetales: a revision of the European poroid taxa. Karstenia 24: 14–28. https://doi.org/10.29203/ka.1984.224

Guo S, Pang R, Guo LH, Li YT, Xu LN, Nan XJ, Liu XG (2016) Analysis on nutrition and acute toxicity of a new species of the *Fomitiporia* sp. Edible Fungi of China 35(4): 54–57.

Hall TA (1999) BioEdit: a user-friendly biological sequence alignment editor and analysis program for Windows 95/98/NT. Nucleic Acids Symposium Series No. 41: 95–98.

Lloyd CG (1915) Synopsis of the genus *Fomes*. Mycological Writings 4: 209–288.

Niemelä T (2005) Polypores, lignicolous fungi. Norrlinia 13: 1–320.

Nylander JAA (2004) MrModeltest v2. Program distributed by the author. Evolutionary Biology Centre, Uppsala University, Uppsala.

Ota Y, Hattori T, Nakamura H, Terashima Y, Lee SS, Miyuki Y, Sotome K (2014) Taxonomy and phylogenetic position of *Fomitiporia torreyae*, a causal agent of trunk rot on Sanbusugi, a cultivar of Japanese cedar (*Cryptomeria japonica*) in Japan. Mycologia 106: 66–76. https://doi.org/10.3852/13-045

Pattengale ND, Alipour M, Bininda-Emonds ORP, Moret BME, Stamatakis A (2010) How many bootstrap replicates are necessary? Journal of Computational Biology 17: 337–354. https://doi.org/10.1089/cmb.2009.0179

Petersen JH (1996) Farvekort. The Danish Mycological Society´s color-chart. Foreningen til Svampekundskabens Fremme, Greve.

Posada D, Crandall KA (1998) Modeltest: Testing the model of DNA substitution. Bioinformatics 14: 817–818. https://doi.org/10.1093/bioinformatics/14.9.817

Rajchenberg M, Robledo G (2013) Pathogenic polypores in Argentina. Forest Pathology 43: 171–184. https://doi.org/10.1111/efp.12032

Ronquist F, Huelsenbeck JP (2003) MrBayes 3: Bayesian phylogenetic inference under mixed models. Bioinformatics 19: 1572–1574. https://doi.org/10.1093/bioinformatics/btg180

Ryvarden L (1989) Type studies in the Polyporaceae 21. Species described by C.G. Lloyd in *Cyclomyces*, *Daedalea*, *Favolus*, *Fomes* and *Hexagonia*. Mycotaxon 35: 229–236

Ryvarden L, Melo I (2017) Poroid fungi of Europe, 2nd edition. Synopsis Fungorum 37: 1–431.

Silvestro D, Michalak I (2012) raxmlGUI: a graphical front-end for RAxML. Organisms Diversity & Evolution 12: 335–337. https://doi.org/10.1007/s13127-011-0056-0

Stamatakis A (2006) RAxML-VI-HPC: maximum likelihood-based phylogenetic analyses with thousands of taxa and mixed models. Bioinformatics 22: 2688–2690. https://doi.org/10.1093/bioinformatics/btl446

Swofford DL (2002) PAUP*: Phylogenetic analysis using parsimony (*and other methods). Version 4.0b10. Sinauer Associates, Sunderland, Massachusetts.

Thompson JD, Gibson TJ, Plewniak F, Jeanmougin F, Higgins DG (1997) The Clustal_X windows interface: flexible strategies for multiple sequence alignment aided by quality analysis tools. Nucleic Acids Research 25: 4876–4882. https://doi.org/10.1093/nar/25.24.4876

White TJ, Bruns TD, Lee S, Taylor J (1990) Amplification and direct sequencing of fungal ribosomal RNA genes for phylogenetics. In: Innis MA, Gelfand DH, Sninsky JJ, White TJ (Eds) PCR protocols, a guide to methods and applications. Academic, San Diego, 315–322. https://doi.org/10.1016/B978-0-12-372180-8.50042-1

Zhou LW, Vlasák J, Decock C, Assefa A, Stenlid J, Abate D, Wu SH, Dai YC (2016a) Global diversity and taxonomy of the *Inonotus* linteus complex (Hymenochaetales, Basidiomycota): *Sanghuangporus* gen. nov., *Tropicoporus excentrodendri* and *T. guanacastensis* gen. et spp. nov., and 17 new combinations. Fungal Diversity 77: 335–347. https://doi.org/10.1007/s13225-015-0335-8

Zhou LW, Vlasák J, Qin WM, Dai YC (2016b). Global diversity and phylogeny of the *Phellinus igniarius* complex (Hymenochaetales, Basidiomycota) with the description of five new species. Mycologia 108: 192–204. https://doi.org/10.3852/15-099

MycoKeys 36: 45–82 (2018)
doi: 10.3897/mycokeys.36.27002
http://mycokeys.pensoft.net

RESEARCH ARTICLE

A peer-reviewed open-access journal
MycoKeys
Launched to accelerate biodiversity research

Cryptic species diversity in polypores: the *Skeletocutis nivea* species complex

Aku Korhonen[1,2], Jaya Seelan Sathiya Seelan[3], Otto Miettinen[1]

1 *Finnish Museum of Natural History, University of Helsinki, PO Box 7, 00014 University of Helsinki, Finland*
2 *Natural Resources Institute Finland (Luke), PO Box 2 (Latokartanonkaari 9), FI-00791, Helsinki, Finland*
3 *Mycology and Pathology Laboratory, Institute for Tropical Biology and Conservation (ITBC), Universiti Malaysia Sabah, 88400 Kota Kinabalu, Sabah, Malaysia*

Corresponding author: *Aku Korhonen* (aku.korhonen@helsinki.fi)

Academic editor: *R.H. Nilsson* | Received 27 May 2018 | Accepted 7 July 2018 | Published 18 July 2018

Citation: Korhonen A, Seelan JSS, Miettinen O (2018) Cryptic species diversity in polypores: the *Skeletocutis nivea* species complex. MycoKeys 36: 45–82. https://doi.org/10.3897/mycokeys.36.27002

Abstract

We propose a taxonomic revision of the two closely related white-rot polypore species, *Skeletocutis nivea* (Jungh.) Jean Keller and *S. ochroalba* Niemelä (Incrustoporiaceae, Basidiomycota), based on phylogenetic analyses of nuclear ribosomal internal transcribed spacer (ITS) and translation elongation factor EF-1α sequences. We show that prevailing morphological species concepts of *S. nivea* and *S. ochroalba* are non-monophyletic and we delineate new species boundaries based on phylogenetic inference. We recognise eleven species within the prevailing species concept of *S. nivea* (*S. calida* **sp. nov.**, *S. coprosmae* comb. nov., *S. futilis* **sp. nov.**, *S. impervia* **sp. nov.**, *S. ipuletii* **sp. nov.**, *S. lepida* **sp. nov.**, *S. nemoralis* **sp. nov.**, *S. nivea* sensu typi, *S. semipileata* comb. nov., *S. unguina* **sp. nov.** and *S. yuchengii* **sp. nov.**) and assign new sequenced epitypes for *S. nivea* and *S. semipileata*. The traditional concept of *S. ochroalba* comprises two independent lineages embedded within the *S. nivea* species complex. The Eurasian conifer-dwelling species *S. cummata* **sp. nov.** is recognised as separate from the North American *S. ochroalba* sensu stricto. Despite comprehensive microscopic examination, the majority of the recognised species are left without stable diagnostic character combinations that would enable species identification based solely on morphology and ecology.

Keywords

cryptic species, fungal taxonomy, Incrustoporiaceae, phylogenetic species, polypores

Introduction

Species delimitation in macrofungi has traditionally been based on morphology of fruiting bodies. Yet, their structure is often relatively simple and taxonomically useful characters are scarce. Even with rigorous microscopic inspection of hyphal structures and spores, true species diversity in macrofungi appears to be concealed by limited morphological resolution.

In polypores (a form group of primarily wood-decaying Basidiomycota with poroid hymenophores), numerous DNA-based studies have reported unaccounted species diversity within previously recognised morphospecies: e.g. *Antrodia crassa* (Spirin et al. 2015), *Heterobasidion insulare* (Chen et al. 2014, Dai and Korhonen 2009), *Laetiporus sulphureus* (Banik et al. 2010, Vasaitis et al. 2009), *Phellinus igniarius* (Tomovský et al. 2010, Zhou et al. 2016) and *Porodaedalea pini* (Brazee and Lindner 2013). In the above-mentioned cases, the newly discovered species can be, and mostly were, characterised morphologically. It should be noted however that much of morphological taxonomy, including our work, is conducted today as follows: first sequence your material, postulate phylogenetically supported species and then see if you can spot morphological and ecological differences between these phylogenetic species.

A handful of studies have documented morphologically indistinguishable, cryptic species diversity, for instance, in the fleshy fungus *Sparassis crispa* (Hughes et al. 2014), the polypore genus *Heterobasidion* (Otrosina and Garbelotto 2010) and the corticioid genera *Coniophora* (Kauserud et al. 2007), *Peniophorella* (Hallenberg et al. 2007) and *Sebacina* (Riess et al. 2013). However, there is no clear distinction when a species is morphologically cryptic. In our own experience, while *Antrodiella* spp. and *Skeletocutis* spp. may be identifiable to a few experts with the aid of a phase-contrast microscope, they are cryptic to many mycologists without access to material for comparison (Miettinen and Niemelä 2018, Miettinen et al. 2006). To us, it would appear that truly cryptic species are a small minority in polypores and corticioid fungi—morphological differences can be detected even between closely related species.

Morphological resolution is of significance when we need to link old names and unsequenced historical specimens to modern species concepts. In these cases, the question about morphologically indistinguishable, cryptic species becomes relevant.

Here, we demonstrate previously unrecognised cryptic diversity in a polypore species complex comprising the morphospecies *Skeletocutis nivea* (Jungh.) Jean Keller and *S. ochroalba* Niemelä in the family Incrustoporiaceae Jülich (Polyporales, Basidiomycota). Despite in-depth morphometrics, extensive material and the best of our expertise, we have not been able to find reliable morphological differences between most species in this complex. Species identification is thus reliant on DNA markers only and we have taken the necessary step to provide sequenced types for all known taxa whenever possible.

According to the prevailing, morphology-based circumscription, *S. nivea* is a cosmopolitan white-rot polypore species, distributed in tropical and temperate zones on both hemispheres, growing on dead angiosperm wood. *S. nivea* was originally described from the Island of Java (Indonesia) (Junghuhn 1838) and subsequently basionyms

Polyporus semipileatus Peck from North America and *Poria coprosmae* G. Cunn. from New Zealand have been widely accepted as synonyms of *S. nivea*. A species currently known as *S. diluta* (Rajchenb.) A. David & Rajchenb. was originally described as a subspecies of *S. nivea* but ITS sequences have shown it to be distinct from *S. nivea* and more closely related to other *Skeletocutis* species (Vlasák et al. 2011).

S. ochroalba, described from boreal North America (Niemelä 1985), is very similar to *S. nivea* but grows on coniferous wood. Subsequent findings, identified as this species, have been reported mainly from Eurasia. The morphospecies *S. nivea* and *S. ochroalba* are distinguished from other species of *Skeletocutis* Kotl. & Pouzar by their hyphal structure, which is usually characterised as trimitic in context and monomitic in trama and the very small size of pores and basidiospores. We use the collective term *S. nivea* complex to refer to both morphospecies.

In this study, we resolve the diversity within the *S. nivea* complex by phylogenetic analyses of two genetic markers, viz. the nuclear ribosomal internal transcribed spacer (ITS) region and the translation elongation factor EF-1α (*tef1*), complemented by microscopic study of specimens. We have sampled *S. nivea* and *S. ochroalba* widely over their known distributions and combine our newly generated data with previously published sequences. Based on our results, we propose a taxonomic revision of the *S. nivea* complex.

Materials and methods

DNA extraction, amplification and sequencing

In total, 92 ITS and 33 *tef1* DNA sequences were generated for this study. In addition, we included sequences publicly available in the International Nucleotide Sequence Database Collaboration database (INSDC). To elucidate the relationship of the *S. nivea* complex to other taxa in the family Incrustoporiaceae, we also amplified the nuclear large subunit (LSU) region of the rRNA operon from representatives of the *S. nivea* complex and retrieved LSU sequences of relevant outgroup taxa from the INSDC. LSU is highly conserved within the *S. nivea* complex but enables comparisons to more distantly related taxa. All of the newly generated sequences were deposited in the INSDC. Voucher data for all included sequences are provided in Suppl. material 1.

DNA was extracted from dried herbarium samples of basidiocarps and mycelia from agar cultures using the E.Z.N.A. Forensic DNA kit (Omega Bio-tek). Pieces of the sample were cut out with a scalpel and then homogenised with a mortar and pestle in a 1.5 ml centrifuge tube. Further steps were performed according to the kit manufacturer's protocol.

The primers ITS5 and ITS4 (White et al. 1990) were used for amplifying and sequencing the ITS1–5.8S–ITS2 region of the nuclear rRNA operon. The primers EF1-983.2f (5'-GCH YCH GGN CAY CGT GAY TTY AT-3') (modified from Matheny et al. 2007) and EF1-G2r (5'-GCD ATR TGN GCR GTR TGR CAR TC-3')

(modified from Rehner 2001) were used for the *tef1*. The LSU region was amplified with the primers CTB6 (Haynes et al. 1995) and LR7 (Vilgalys and Hester 1990) and sequenced with the primers CTB6-LR5 (Vilgalys and Hester 1990) and LR3R (5'-GTC TTG AAA CAC GGA CC-3')-LR7.

Polymerase chain reactions (PCRs) were carried out with either the Illustra PureTaq Ready-To-Go PCR Beads (GE Healthcare), DreamTaq Green PCR mix (Thermo Scientific) or Phire Tissue Direct PCR Master Mix (Thermo Scientific). A touchdown style PCR programme (designed by Zheng Wang http://wordpress.clarku.edu/polypeet/datasets/primer-information/) was applied for *tef1* amplification. The resulting products were sequenced with BigDye v.3.1 and ABI3730XL analyser (Applied Biosystems) by Macrogen and FIMM. The electropherograms of forward and reverse sequences were aligned against each other using Sequencher v. 5.0 (Gene Codes Corporation). The aligned electropherograms were then visually inspected to ensure good sequence quality and ambiguous sequence reads were discarded. Double peaks were interpreted as true base ambiguities when they were detected in both forward and reverse sequencing electropherograms.

Alignments and phylogenetic analysis

For an outgroup analysis, a combined ITS–LSU dataset was assembled with representatives of the *S. nivea* complex (18 sequences) and outgroups (14 sequences from 11 species). The resulting trees were rooted with *Tyromyces merulinus* (a possible sister to Incrustoporiaceae) following Justo et al. (2017). The *Tef1* (34 sequences) and ITS (139 sequences) datasets were analysed to investigate the phylogeny of the *S. nivea* complex in more detail and to delineate species within the complex. *Tyromyces globosporus* (JN710734) was used as an outgroup in the *tef1* analysis and *Skeletocutis chrysella* (JQ673126) in the ITS analysis.

Sequences were aligned using PRANK v.140603 (Löytynoja and Goldman 2010) with default settings. These alignments were checked by eye and alignment errors were corrected manually. In the ITS-LSU analysis, parts of the ITS region were so divergent between distantly related taxa that they could not be credibly aligned and those sections (131/706, 18.6% of aligned positions) were excluded from the ITS–LSU analysis. The alignments and trees were deposited in TreeBASE (22552).

Phylogenetic trees were constructed using the maximum likelihood (ML) and Bayesian inference (BI) methods. ML trees were reconstructed with RAxML 8.2.10 (Stamatakis 2014) with GTR+G set as the evolutionary model and alignments partitioned according to Table 1. The rapid bootstrap with MRE-based bootstopping criterion option was used for branch support estimation.

The substitution models for BI were selected for each partition (Table 1) with JModelTest2 v.2.1.6 (Guindon and Gascuel 2003, Darriba et al. 2012) prior to the run. When evaluating models, the number of substitution schemes was set to 3 and models with equal/unequal base frequencies (+F), with/without a proportion of invari-

Table 1. Sequence partitions and substitution models.

Analysis	Gene	Partition in model estimation	Model selected for Bayesian analysis	Sub-partition	Length in alignment	Number of parsimony informative sites in alignment
outgroup	nrRNA	ITS1 and ITS2	GTR+G	ITS1	215	62
				ITS2	206	67
		5.8S and LSU	K80+G	5.8S	154	8
				LSU	1460	91
ingroup		ITS1 and ITS2	HKY+G	ITS1	257	57
				ITS2	262	73
		5.8S	K80		154	0
	tef1	1. codon position	F81+G		231	13
		2. codon position	JC+G		231	11
		3. codon position	HKY+G		231	87
		introns	HKY+I		188	79

able sites (+I) and with/without rate variation amongst sites (+G) (nCat = 25), were included. Models were selected according to Bayesian information criterion.

BI analyses were performed in MrBayes v.3.2.6 (Ronquist et al. 2012) in two independent runs with 4 chains for 10 million generations for the analysis of ITS sequences and 1 million generations for *tef1* and ITS–LSU analyses. Upon run completion, the first 25% of the trees were discarded as burn-in. By then, the average standard deviation of split frequencies had reached a value lower than 0.01.

All analyses were performed through the Cipres Science Gateway v.3.3 interface (Miller et al. 2010).

The numbers of base substitutions per site within and between the inferred species were calculated in MEGA v.7.0.25 (Kumar et al. 2016) by averaging over all sequence pairs in an analysis with Maximum Composite Likelihood model (Tamura et al. 2004). The rate variation amongst sites was modelled with a gamma distribution (shape parameter = 4). The differences in the composition bias amongst sequences were considered in evolutionary comparisons (Tamura and Kumar 2002). Standard error estimates were obtained by a bootstrap procedure (500 replicates).

Microscopic study

The majority of studied materials are dried specimen collections stored in herbarium H (Helsinki). Type material and reference specimens from herbaria BPI, H, L, O and PDD were also studied. Herbarium acronyms are given according to Thiers (2017).

Pore measurements (12 per specimen) were done under a stereomicroscope (Wild M54) by counting the number of pores per 1 mm; only pores aligned in straight rows were selected for this purpose. Microscopic structures were studied and measured with Leitz Diaplan and Leica DMBL microscopes (×1250 magnification). Microscopic routines used in this study follow Miettinen et al. (2006, 2012). Measurements were made

and illustrations were drawn in Cotton Blue using phase contrast illumination and oil immersion (with a subjective accuracy of 0.1 μm; Miettinen et al. 2006).

In microscopic descriptions, the following abbreviations are used: L – mean spore length; W – mean spore width; Q – mean L/W ratio; n – pore counts, spores or hyphae measured / number of specimens. For presenting a variation of basidiospores and hyphae, 5% of measurements were excluded from each end of the range and are given in parentheses. The respective cut-off for reported pore measures is 20%.

Results

Sequences and phylogeny

Intragenomic variation of ITS sequences, as discussed by Lindner and Banik (2011) and Lindner et al. 2013, was found to be common and widespread in the *S. nivea* complex. Variation consisted mainly of single nucleotide polymorphisms (SNP) and short length variations of one or a few base pairs. In our analyses and INSDC submission, we always used the shortest alleles.

Phylogenetic analyses of the ITS–LSU dataset (Fig. 1) show that the *S. nivea* complex forms a monophyletic assemblage of closely related species in the family Incrustoporiaceae. The genus *Skeletocutis* in its current circumscription is non-monophyletic and the *S. nivea* complex belongs to a clade that is separate from the type species of the genus, *S. amorpha* (Fr.) Kotl. & Pouzar. When the generic limits within the family are clarified in the future, the *S. nivea* complex should be assigned to a different genus.

Some segments of ITS sequences proved difficult to align unequivocally even within the *S. nivea* complex. While the composition of the clades which we interpret as species was not affected, the topologies of deeper nodes were found to be somewhat sensitive to small adjustments of the alignment in those variable segments.

Despite partially contrasting topology of inter-group relationships, the phylogenetic analyses of both *tef1* (Fig. 2) and ITS (Fig. 3) datasets were concordant in grouping terminals into 13 clades that we interpret and describe here as species. Analysis of the ITS dataset revealed an additional 14th clade (*S.* aff. *futilis*) not included in our *tef1* sampling, which may represent a separate species.

All recognised species were strongly supported in the analyses of the *tef1* dataset. Corresponding support from the ITS data was strong for all but *S. nivea*, which lacks true synapomorphic characters in relation to *S. lepida* and *S. yuchengii* in that genetic marker.

Average estimated intraspecific sequence divergence in the ITS dataset was up to 0.32% (SE=0.12) (in *S. nivea*) and in the *tef1* dataset up to 4.2% (SE=0.8) (in *S. yuchengii*). Average estimated genetic distances between species varied from 1.3% (SE=0.4) between *S. lepida* and *S. nivea*, to 10.3% (SE=1.1) between *S. calida* and *S.* aff. *futilis* in the ITS dataset and from 3.7% (SE=0.7) between *S. impervia* and *S. lepida*, to 16.9% (SE=2.1) between *S. futilis* and *S. ochroalba* in the *tef1* dataset. The genetic divergence within and between species was generally higher in *tef1* than ITS

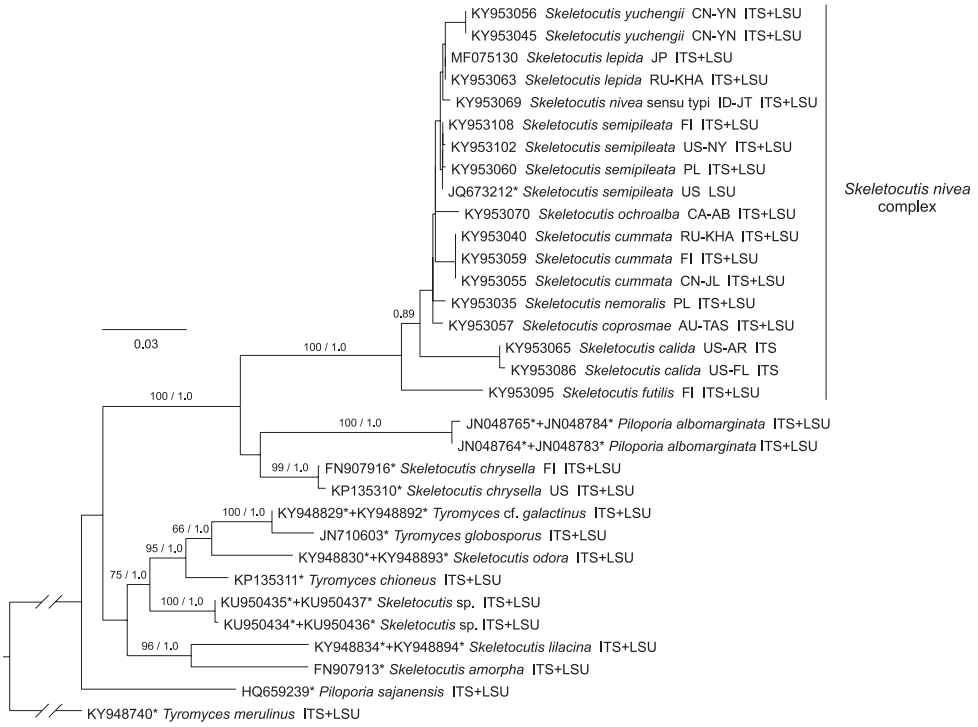

Figure 1. Phylogenetic tree from ML analysis of the ITS–LSU dataset. Bootstrap support values (up to 100) and respective Bayesian posterior probabilities (up to 1) are shown beside branches (bs / pp) where bs > 50 or pp ≥0.80. Terminal labels include INSDC accession number(s), species name, (area of origin, in ISO 3166 code) and gene regions included. * = sequence retrieved from the INSDC.

sequences. The full set of estimates of genetic divergence between and within species is provided in Suppl. materials 2–4.

Morphology, ecology and distribution

Morphometrics for each species are reported in Table 2. Characteristics and ecology of the species are summarised in Table 3. Distribution maps depicting the approximate collection localities of specimens are provided in Supplement S5A–C.

Discussion

Phylogeny and species diversity in the *Skeletocutis nivea* complex

Interspecies relationships were not clearly resolved by our data and analyses of the ITS and *tef1* datasets resulted in partially contrasting topologies. *Skeletocutis futilis*

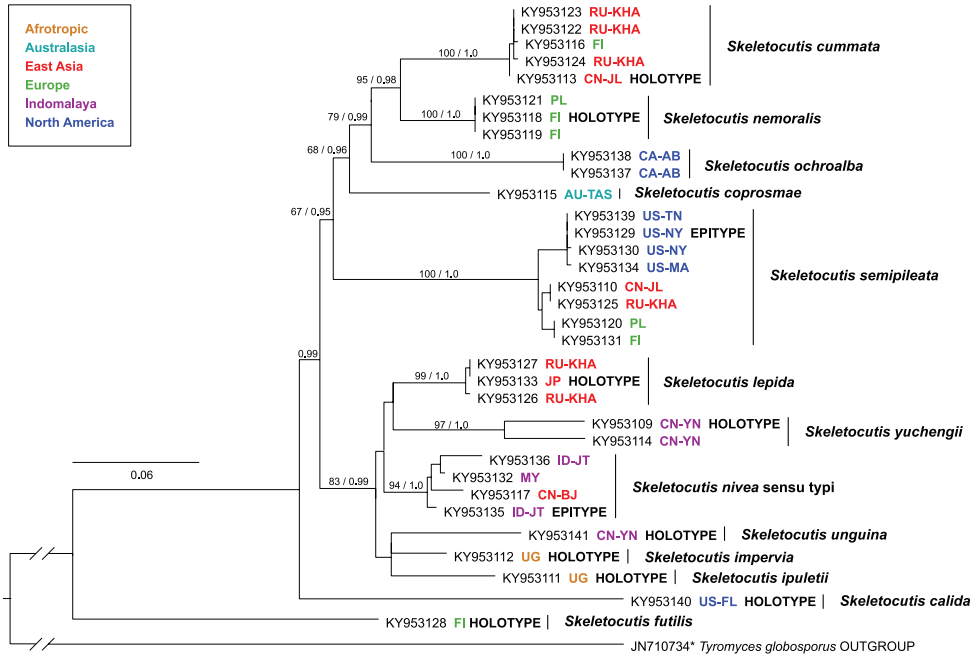

Figure 2. Phylogenetic tree from ML analysis of the *tef1* dataset. Bootstrap support values (up to 100) and respective Bayesian posterior probabilities (up to 1) are shown beside branches (bs / pp) for all nodes that delimit species and for deeper nodes where bs >50 or pp ≥0.95. Terminal labels include INSDC accession number, species name, area of origin (in ISO 3166 code) and indication of type status. * = sequence retrieved from the INSDC.

(together with *S.* aff. *futilis*) and *S. calida* represent long, divergent branches which are consistently positioned as early diverging lineages in our analyses. However, the position of *S. calida* was found to be sensitive to slight alterations of alignment in some variable segments of ITS, alternative positions being within the crown group.

The crown group is characterised by relatively short internodes and poor interspecies resolution. However, *S. lepida*, *S. nivea* and *S. yuchengii* were consistently grouped together. Weak support (bs=9, pp=0.30) for *S. nivea* in the ITS data could be explained by incomplete lineage sorting in this genetic marker after relatively recent speciation. The loss of ancestral alleles can be expected to be slower in the widely distributed *S. nivea,* which probably comprises a larger population than the regionally endemic *S. lepida* or *S. yuchengii*.

Despite their ecological and morphological similarities, the conifer-dwelling species *S. cummata* and *S. ochroalba* were recovered as sister species only in the Bayesian analysis of the ITS–LSU dataset. Even then, the support was minimal (pp=0.151).

Our results with the *S. nivea* complex are in line with other molecular systematic studies in *Polyporales* (e.g. Carlson et al. 2014, Miettinen et al. 2018) who conclude that *tef1* is more variable between species than ITS and provides greater resolution in separating species. Still, unique character state combinations can be identified from ITS

Table 2. Pore and spore measurements of species in the *Skeletocutis nivea* complex. Spore measures in bold-face are accumulated statistics from specimens below.

Specimen	Pores/mm (min–median–max)	n	Spore length (µm)	L	Spore width (µm)	W	Q'	Q	n
***Skeletocutis calida* sp. nov.**			**2.5–3.1(–3.3)**	**2.86**	**0.5–0.6(–0.7)**	**0.55**	**(4.0–)4.3–6.0(–6.9)**	**5.18**	**60/2**
holotype	8–**9**–10	12	2.8–3.0	2.92	0.5–0.6(–0.7)	0.56	(4.3–)4.8–5.8(–6.0)	5.22	30
Miettinen 17466	8–**9**–11	12	2.5–3.2(–3.3)	2.79	0.5–0.7	0.54	(4.0–)4.2–6.4(–6.9)	5.13	30
***S. coprosmae* comb. nov.**			**2.8–3.2(–3.3)**	**2.98**	**0.5–0.7**	**0.57**	**(4.0–)4.3–6.0(–6.4)**	**5.19**	**60/2**
holotype	6–**8**–9	12	2.8–3.2(–3.3)	3	0.5–0.7	0.57	4.3–6.2(–6.4)	5.3	30
Gates 1898	7–**8**–9	12	2.8–3.1	2.95	0.5–0.7	0.58	(4.0–)4.3–6.0	5.09	30
***S. cummata* sp. nov.**			**(2.8–)2.9–3.4(–3.9)**	**3.1**	**0.5–0.8(–0.9)**	**0.66**	**(3.3–)3.8–6.0(–6.6)**	**4.68**	**270/9**
holotype	5–**6**–7	12	2.9–3.3	3.05	0.6–0.8(–0.9)	0.74	(3.3–)3.6–5.2(–5.5)	4.14	30
Niemelä 9088	6–**7**–8	12	3.0–3.3(–3.5)	3.09	0.6–0.7	0.66	4.3–5.3	4.71	30
Spirin 3857	7–**8**–9	12	(2.9–)3.0–3.9	3.13	0.5–0.8	0.63	4.3–6.0	4.94	30
Spirin 4170	7–**9**	12	2.9–3.7(–3.9)	3.18	0.5–0.7(–0.8)	0.58	4.4–6.4(–6.6)	5.48	30
Spirin 4897	6–**7**–8	12	2.8–3.4(–3.5)	3.05	0.5–0.7	0.6	(4.1–)4.3–6.0	5.11	30
Spirin 5430	5–**6**–8	12	3.0–3.4	3.1	0.5–0.8	0.66	(3.9–)4.0–6.0	4.68	30
Spirin 5472	6–**7.5**–9	12	3.0–3.4(–3.5)	3.09	0.6–0.8(–0.9)	0.74	3.8–5.0	4.18	30
Spirin 5484	7–**10**–13	12	2.9–3.2(–3.3)	3.05	0.6–0.8	0.67	3.6–5.2(–5.3)	4.52	30
Spirin 5676		12	2.8–3.4(–3.5)	3.12	0.6–0.8	0.67	(3.5–)3.9–5.7	4.63	30
***S. futilis* sp. nov.**	6–**7**–8	9	3.0–4.0	3.33	0.7–0.9	0.81	(3.3–)3.4–5.1	4.13	30
***S. impervia* sp. nov.**	7–**8.5**–10	12	(2.8–)2.9–3.1	2.97	0.5–0.8	0.61	(3.6–)3.8–6.0(–6.2)	4.85	30
***S. ipuletii* sp. nov.**	9–**10**–11	12	2.8–3.4	2.96	0.5–0.7(–0.8)	0.6	(4.0–)4.1–6.0(–6.2)	4.97	30
***S. lepida* sp. nov.**			**(2.8–)2.9–3.0(–3.1)**	**2.95**	**0.5–0.6**	**0.55**	**4.8–6.0**	**5.36**	**90/3**
holotype	7–**8**–9	12	2.9–3.1	2.98	0.5–0.6	0.54	4.8–6.0	5.55	30
Spirin 4989	7–**9**–10	12	(2.8–)2.9–3.0	2.94	0.5–0.6	0.56	4.8–6.0	5.22	30
Spirin 3964	7–**9**–10	12	2.8–3.0	2.93	0.5–0.6	0.55	4.8–6.0	5.3	30
***S. nemoralis* sp. nov.**			**(2.8–)2.9–3.2(–4.0)**	**3.04**	**(0.4–)0.5–0.6(–0.7)**	**0.56**	**(4.1–)4.8–6.3(–7.8)**	**5.47**	**390/13**
holotype	6–**7.5**–9	12	2.9–3.2(–3.3)	3.06	0.5–0.7	0.57	4.3–6.2	5.4	30
Brandrud 149–04	7–**8**–9	12	(2.9–)3.0–3.4(–3.8)	3.13	0.4–0.7	0.55	(4.6–)4.9–7.2(–7.5)	5.66	30
Gaarder 5257	8–**8.5**–9	12	(2.9–)3.0–3.8(–4.0)	3.17	(0.4–)0.5–0.7	0.57	(4.6–)4.7–6.7(–7.5)	5.59	30
Klepsland JK06–S080	7–**8**–9	12	2.8–3.0(–3.2)	2.94	0.5–0.7	0.57	4.1–6.0	5.16	30
Korhonen 28	7–**8**–9	12	2.9–3.1(–3.3)	3.02	0.4–0.6(–0.7)	0.54	(4.7–)4.8–7.2(–7.8)	5.56	30

Specimen	Pores/mm (min–median–max)	n	Spore length (µm)	L	Spore width (µm)	W	Q'	Q	n
Korhonen 31	6–**7**–9	12	2.9–3.1(–3.5)	3.02	0.5–0.7	0.58	4.3–6.0(–6.2)	5.18	30
Korhonen 35		12	(2.8–)2.9–3.2(–3.3)	3.06	0.5–0.6	0.54	(4.8–)5.0–6.4(–6.6)	5.71	30
Korhonen 83	6–**8**–9	12	2.9–3.1	3	0.5–0.6(–0.7)	0.55	(4.3–)4.8–6.2	5.46	30
Korhonen 86	7–**8**–10	12	2.9–3.1	3	0.5–0.6	0.57	4.8–6.0(–6.2)	5.3	30
Korhonen 89	7–**8**–9	12	2.9–3.1(–3.2)	3.05	0.5–0.6	0.56	4.8–6.2	5.45	30
Korhonen 93	6–**7**–8	12	3.0–3.1	3.05	0.4–0.6	0.53	5.0–7.5(–7.8)	5.79	30
Korhonen 100	7–**8**	12	2.9–3.1(–3.2)	3.02	0.5–0.6	0.56	4.8–6.2	5.43	30
Korhonen 103	6–**7**–8	12	(2.8–)2.9–3.2(–3.8)	3.04	(0.4–)0.5–0.6	0.55	(4.7–)4.8–6.4(–7.2)	5.52	30
S. nivea			**(2.7–)2.8–3.2(–3.7)**	**2.96**	**0.5–0.7(–0.8)**	**0.56**	**(3.9–)4.3–6.0(–6.2)**	**5.27**	**125/5**
holotype	8–**10**–13	5	–	–	–	–	–	–	–
epitype	8–**10**–11	12	(2.7–)2.8–3.4(–3.7)	2.96	0.5–0.7(–0.8)	0.56	(4.3–)4.4–6.0	5.32	30
Miettinen 10579.1	7–**8**–9	12	2.7–3.0	2.91	0.5–0.7	0.57	(3.9–)4.0–6.0	5.08	30
Miettinen 18255	–	–	3.0–3.2	3.12	0.5–0.6	0.56	5.2–6.2	5.57	5
Miettinen 16350	9–**10**–11	12	2.7–3.1	2.91	0.5–0.7	0.55	4.3–6.2	5.33	30
Ryvarden 38177	7–**8**–10	12	2.8–3.5(–3.7)	3.02	0.5–0.7	0.57	(4.1–)4.3–6.0	5.3	30
S. ochroalba			**(2.8–)2.9–3.7(–4.0)**	**3.1**	**0.5–0.8**	**0.67**	**3.8–6.0(–7.0)**	**4.65**	**70/3**
Niemelä 2689	6–**7.5**–9	12	2.9–3.7(–4.0)	3.1	(0.5–)0.6–0.8	0.67	(3.8–)4.1–5.2(–7.0)	4.63	35
Spirin 8854a	6–**7**–9	22	(2.8–)2.9–3.2(–3.3)	3.04	0.5–0.8	0.67	3.8–6.0(–6.2)	4.56	30
Spirin 8854b		9	3.2–3.8	3.48	0.6–0.7	0.66	4.7–5.5	5.27	5
S. semipileata **comb. nov.**			**(2.3–)2.8–3.1(–3.3)**	**2.97**	**0.4–0.6(–0.7)**	**0.55**	**(4.1–)4.7–7.0(–7.5)**	**5.43**	**450/15**
lectotype	8–**8.5**–11	10	–	–	–	–	–	–	–
epitype	7–**8**–10	12	2.8–3.1	2.98	0.5–0.7	0.57	4.4–6.0	5.22	30
Gaarder 5136	7–**8**–10	12	(2.8–)2.9–3.1(–3.3)	2.98	0.5–0.7	0.58	(4.1–)4.4–6.0	5.17	30
Korhonen 76	7–**9**–10	12	(2.6–)2.8–3.1	2.98	0.4–0.6(–0.7)	0.53	(4.1–)4.8–7.2	5.62	30
Miettinen 6694	7–**8**–10	12	(2.7–)2.8–3.2	2.97	0.5–0.6	0.58	4.8–6.0	5.16	30
Miettinen 14114	7–**8**–10	12	2.8–3.0(–3.1)	2.94	0.5–0.6	0.56	4.8–6.0	5.28	30
Miettinen 14917.4	8–**9**–10	12	(2.8–)2.9–3.1	3	(0.4–)0.5–0.6	0.55	(4.7–)4.8–6.2(–7.5)	5.42	30
Miettinen 15715		12	(2.3–)2.4–3.0	2.79	(0.4–)0.5–0.6	0.53	(4.5–)4.6–5.8(–7.0)	5.26	30
Miettinen 15835	8–**9**–11	12	(2.8–)2.9–3.2(–3.3)	3.02	(0.4–)0.5–0.6	0.54	5.0–6.2(–7.0)	5.56	30
Miettinen 16693.1		12	2.9–3.2(–3.3)	3.01	0.4–0.6(–0.7)	0.52	(4.3–)4.8–7.5	5.75	30
Miettinen 16823	8–**9**–11	12	2.8–3.0	2.93	0.4–0.6	0.49	4.8–7.5	5.93	30

Specimen	Pores/mm (min–median–max)	n	Spore length (µm)	L	Spore width (µm)	W	Q'	Q	n
Miettinen 17074	8–**9**–11	12	2.8–3.0	2.93	0.4–0.7	0.56	(4.1–)4.3–7.2	5.27	30
Miettinen 17135	7–**9**–10	12	2.9–3.0(–3.1)	2.99	(0.4–)0.5–0.6	0.54	5.0–6.0(–7.5)	5.5	30
Ryvarden 47279	7–**8**–10	12	2.9–3.1	3.02	0.5–0.7	0.58	(4.3–)4.4–6.0(–6.2)	5.21	30
Spirin 2326	7–**8**–9	12	2.8–3.1	2.96	0.4–0.6	0.53	(4.7–)4.8–7.0(–7.2)	5.59	30
Spirin 5142		12	2.9–3.0(–3.1)	2.98	0.4–0.6	0.53	(4.8–)5.0–7.2	5.59	30
***S. unguina* sp. nov.**	7–**8**–9	12	2.9–3.2(–3.3)	3.04	(0.4–)0.5–0.6(–0.7)	0.55	(4.6–)4.8–6.4(–7.5)	5.49	30
***S. yuchengii* sp. nov.**			**(2.7–)2.8–3.1(–3.2)**	**2.96**	**(0.4–)0.5–0.7**	**0.59**	**(4.0–)4.1–6.0(–7.2)**	**4.99**	**90/3**
holotype	8–**8.5**–11	12	(2.8–)2.9–3.2	3.01	0.5–0.7	0.62	(4.0–)4.1–6.0(–6.4)	4.86	30
Miettinen 10150.2	–	–	2.7–3.1	2.93	0.5–0.7	0.59	(4.0–)4.1–6.0(–6.2)	5	30
Miettinen 10366.1	8–**9**–11	12	(2.8–)2.9–3.0(–3.1)	2.95	(0.4–)0.5–0.7	0.58	(4.0–)4.1–6.0(–7.2)	5.11	30

Table 3. Distribution, ecology and habit of species in the *Skeletocutis nivea* complex.

Host	Species	Distribution	Characteristics and ecology
angiosperm	*Skeletocutis calida* sp. nov.	subtropical N America	annual; basidiocarps small individual pilei; on fallen twigs
	S. coprosmae comb. nov.	Tasmania, New Zealand	**potentially perennial**; basidiocarps becoming large and sturdy when growing on coarse wood
	S. futilis sp. nov.	Finland	annual; basidiocarps small; **spores over 0.7 µm thick**; on fallen twigs
	S. impervia sp. nov.	Uganda	likely annual
	S. ipuletii sp. nov.	Uganda	likely annual
	S. lepida sp. nov.	temperate East Asia (Russian Far East, Japan)	annual; basidiocarps small individual pilei when growing on thin branches, sturdier on coarse wood
	S. nemoralis sp. nov.	temperate Eurasia	annual; basidiocarps often sturdy and large; on fallen branches; **prefers *Fraxinus***
	S. nivea	China, SE Asia, New Zealand	annual; basidiocarps potentially quite large; on fallen branches or logs
	S. semipileata comb. nov.	temperate – south-boreal northern hemisphere	annual; basidiocarps often quite large; on fallen twigs, branches or logs of various woody angiosperms
	S. unguina sp. nov.	China (Yunnan)	annual; basidiocarps small individual pilei; on fallen twigs
	S. yuchengii sp. nov.	China (Yunnan)	annual; basidiocarps small; on fallen twigs
conifer	*S. cummata* sp. nov.	(oro)boreal Eurasia	annual; basidiocarps small, pileus surface and margin slightly pubescent; on downed conifer logs, usually *Picea*
	S. ochroalba	boreal N America	potentially perennial; basidiocarps small, pileus surface and margin slightly pubescent; on downed logs of *Picea*

sequences even for the most closely related species in the *S. nivea* complex. Intraspecific sequence variation in *tef1* was generally larger but roughly corresponding to the variation observed in the ITS region. However, in *S. yuchengii,* the *tef1* sequences show striking divergence in contrast to ITS. To clarify interspecies relationships within the *S. nivea* complex, additional genetic markers such as the *rpb1* will need to be sequenced.

Geographic patterns of diversity

Our sampling is concentrated in the northern temperate zone, where most species of the *S. nivea* complex appear to be restricted to a single continent or region. This is in accordance with other comparable studies on polypores (e.g. Otrosina and Garbelotto 2010, Spirin et al. 2015, Han et al. 2016, Song and Cui 2017, Spirin et al. 2017, Miettinen et al. 2018). Notable exceptions here include *S. semipileata*, which has a circumpolar distribution and *S. nivea*, which ranges longitudinally from northern China to New Zealand.

The greatest species diversity is found in Eurasia and particularly in East Asia with three species unique to the region: *S. lepida* in Northeast Asia and *S. unguina* and *S. yuchengii* in southern China. *S. futilis* is thus far known only from northern Europe but the closely related *S.* aff. *futilis* occurs in North America. *S. cummata* and *S. nemoralis* have continent-wide distributions in Eurasia.

North American species include *S. calida* in southern U.S.A. and *S.* aff. *futilis* in northern U.S.A. The conifer-dwelling *S. ochroalba* represents the North American parallel of the Eurasian *S. cummata* with boreal, continent-wide distribution.

Wide and disjunct distributions of species like *S. semipileata*, *S. nivea* and *S. coprosmae* indicate that species distributions are not necessarily limited by dispersal ability. Spores in the *S. nivea* complex are exceedingly small and their theoretical dispersal ability along air currents is practically unlimited (Wilkinson et al. 2012). Yet, the actual dispersal ability may be severely limited by the survivability of the delicate spores during long distance transport and their ability to establish after deposition on a new substrate (Norros et al. 2015).

The generalist ecology of *S. semipileata* may have facilitated its dispersal over the northern hemisphere, while some of the more restricted species may be limited by low establishment probability imposed by stricter specialisation. Geographic structuring within *S. semipileata*, particularly evident in the *tef1* data – where differentiation between North America and Eurasia and furthermore East Asian and European populations emerges – suggests that gene flow across long distances in this species is somewhat restricted. Similarly, geographic isolation is likely driving the differentiation between *S. futilis* and *S.* aff. *futilis*, be that inter or intraspecific.

Our sampling from the low latitudes and southern hemisphere was sporadic but yielded a proportionately large number of species, most of which were represented by only one or a few specimens. Specimens collected from a relatively small area in Yunnan, southern China fall into three species, two of which (*S. unguina* and *S. yuchengii*) are known only from that area.

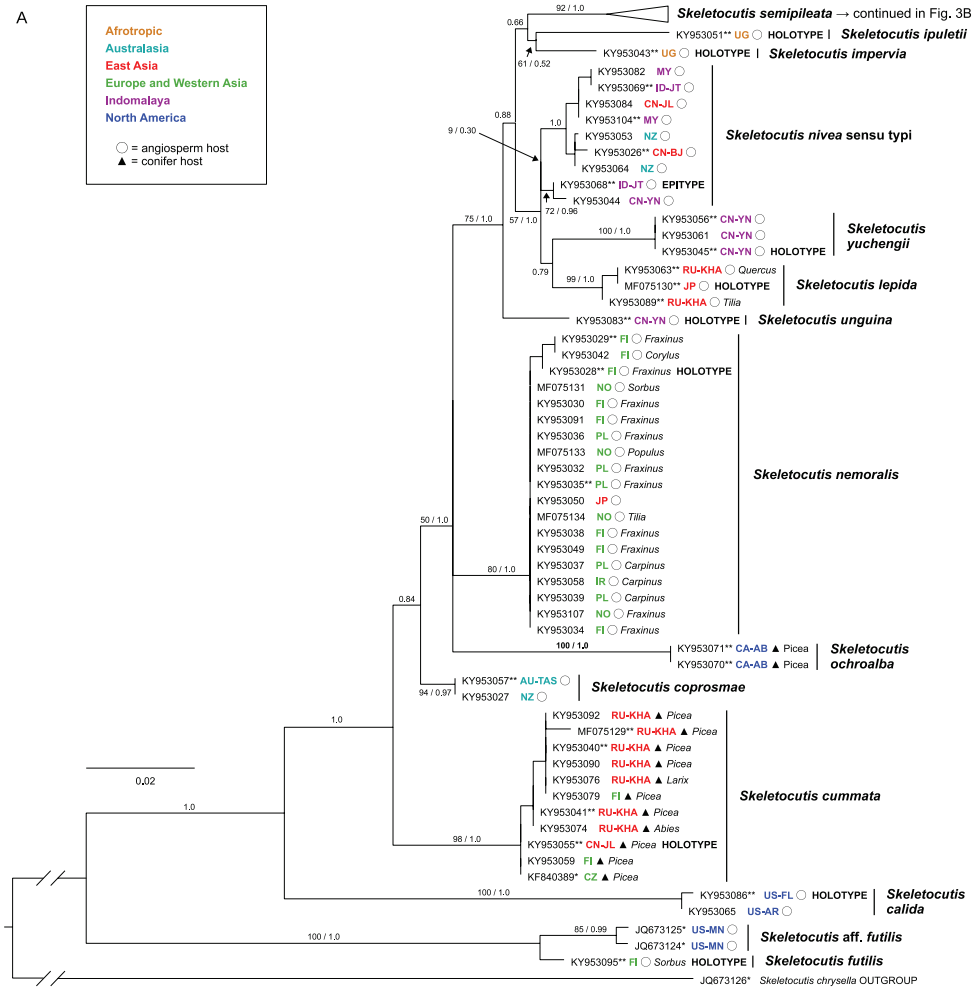

Figure 3. Phylogenetic tree from ML analysis of the ITS dataset. Bootstrap support values (up to 100) and Bayesian posterior probabilities (up to 1) are shown beside branches (bs / pp) for all nodes that delimit species and deeper nodes where bs >50 or pp ≥0.95. Terminal labels include INSDC accession number, species name, area of origin (in ISO 3166 code), host tree and indication of type status. * = sequence retrieved from the INSDC. ** = *tef1* sampled from corresponding specimen. (A) All terminals shown except *Skeletocutis semipileata*; (B) terminals within *S. semipileata*.

The only two African specimens, both from Uganda, proved to represent separate species, *S. impervia* and *S. ipuletii*. Another new species, *S. afronivea* Ryvarden, morphologically close to the *S. nivea* complex, was recently described from Uganda (Ryvarden 2018). Sequence data for *S. afronivea* is not available, so its affinity to the *S. nivea* complex cannot be verified. However, the larger spore size distinguishes *S. afronivea* as separate from *S. impervia*, *S. ipuletii* and most other species of the *S. nivea* complex.

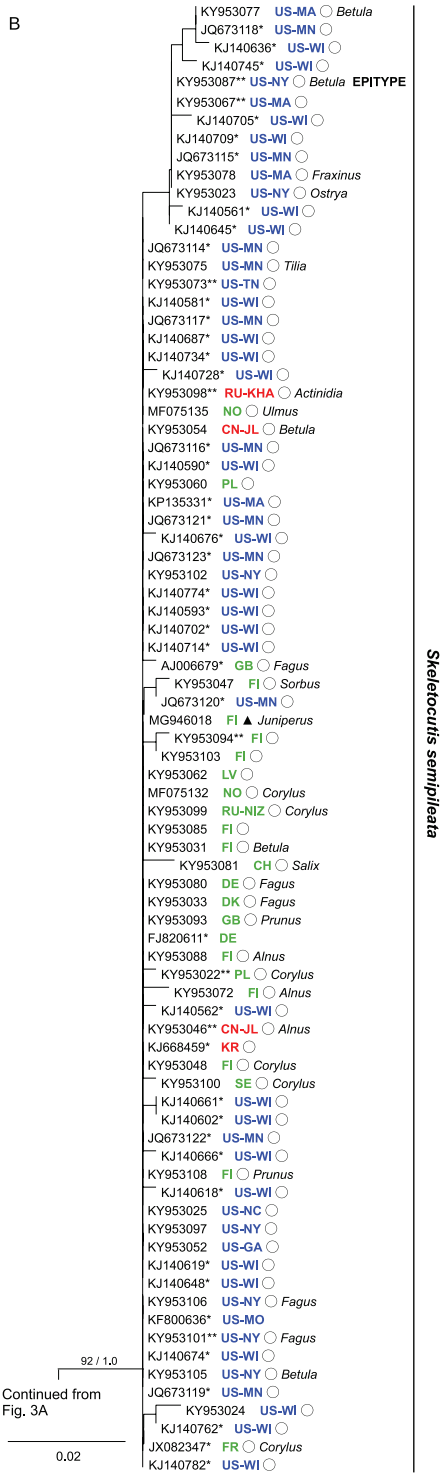

Figure 3. Continued.

We anticipate that further studies are likely to reveal even more diversity within the *S. nivea* complex. Potential hotspot areas include the montane forests of the tropics as well as the temperate forests in mid-latitudes. For instance, Western North America and large parts of the southern hemisphere were not sampled in this study.

Ecology and host tree associations

Ecologically, *S. nivea* complex can be divided into conifer-dwelling species (*S. cummata* and *S. ochroalba*) and angiosperm-dwelling species. The lack of support for a sister species relationship between *S. cummata* and *S. ochroalba* suggests that host switching may have happened more than once during the diversification of the *S. nivea* complex. Both *S. cummata* and *S. ochroalba* have remarkably similar fruiting body morphology characterised by small size, pileate form with pubescent pileus surface and the occasional salmon colour on the pore surface as well as spore dimensions that are distinct from most angiosperm-dwelling species. Better phylogenetic resolution of the *S. nivea* complex would be required to discern whether these shared traits represent homologies or independently derived ecological adaptations.

The host range of the conifer-dwelling species remains unresolved. They are most commonly found on logs of *Picea*, but *S. cummata* in the Russian Far East has been collected from *Abies* and *Larix* as well. We also studied a specimen from China (L. Ryvarden 21394 (H)), labelled as *S. nivea* from *Pinus*, but close inspection revealed the spores to be too small for *S. cummata*. The specimen was not sequenced so its true species identity remains unverified. In North America, Overholts (1953) and Lowe (1966) report *S. semipileata* (*P. semipileatus*) as sometimes growing on conifers such as *Picea*, *Pinus* and *Thuja*. It is possible that the referenced specimens belong to *S. ochroalba*, but we have not confirmed their identity. However, we have confirmed one Finnish collection of *S. semipileata* (O. Miettinen 21003 (H)) from *Juniperus communis*, proving that occasional crossovers of angiosperm-dwelling species to conifer hosts sometimes occur.

Several of the angiosperm-dwelling species are so far known only from one or a few specimens and detailed substrate data were often not available. Our records of *S. lepida*, *S. nemoralis* and *S. semipileata* suggest that individual species are able grow on a wide diversity of woody angiosperms. A preference for *Fraxinus* wood is evident in *S. nemoralis*, whereas *S. semipileata* appears to be rather indifferent in this respect. All species can be found on thin branches, but some (*S. nivea* and *S. semipileata*) have also been recorded from coarse woody debris (>20 cm Ø). The examples presented above indicate that ecological specialisation amongst the angiosperm-dwelling species is relatively weak. However, generalisations from common and widespread species, such as *S. semipileata*, are likely to be biased. Some degree of niche partitioning could be expected at least locally, where two or more species co-occur.

The observed pattern of overlapping species distributions in the *S. nivea* complex indicates that effective hybridisation barriers are in place between species. The mechanisms of reproductive isolation and the evolutionary processes that have led to their

formation are thus far unverified. The existence of possible innate reproductive barriers that prevent hybridisation on shared substrates could be investigated by mating experiments. However, in order to conduct such studies, fresh material will need to be collected to establish living cultures of the species in the *S. nivea* complex. Further ecological study is also required to elucidate possible higher resolution patterns of distribution and substrate use. Special care should be taken to record detailed collection data including the species, size class, quality, position and decay stage (following e.g. Söderström (1988)) of the substrate.

Crypticity in the *Skeletocutis nivea* complex

After macroscopic and microscopic study of 60 specimens representing 13 species (more than 700 pores, 1700 spores and 3000 hyphae measured), the majority of the species in the *S. nivea* complex are left without reliable morphological diagnosis. Intraspecific variability in basidiocarp phenology appears to be too wide to infer interspecific differences. On the other hand, the microscopic structures of the hyphal system are remarkably uniform across species. Easily measurable quantitative characters such as the spore dimension provide only minimal differentiation, if any. Identification is particularly problematic amongst the angiosperm-dwelling species, many of which clearly have overlapping distributions; only *S.* (aff.) *futilis* is distinguished by distinctly larger spores.

Taxonomy

A collective description of the *S. nivea* complex is provided below. Individual species descriptions focus on relevant specifications for each species.

Skeletocutis nivea complex

Description. Basidiocarps (Fig. 4) annual to sometimes perennial; half-resupinate (resupinate with a pileate edge) to resupinate; hard when dry; surface of pileus white to ochraceous, sometimes turning black when old (Fig. 4C); pore surface cream coloured with ochraceous tints, bluish or greenish colour sometimes develops in the tubes (Fig. 4E); context and subiculum with coriaceous consistency and whitish colour; pores 6–10 per mm; tube layer darker than context.

Hyphal structure: context and subiculum seemingly trimitic (Fig. 5C); hyphae are parallel near cap surface, forming a homogenous, coriaceous texture; skeletal hyphae prevailing, unbranched, thick-walled and often solid, refractive; generative hyphae relatively scarce, clamped, sometimes with (unevenly and irregularly) thickened walls and rarely with sandy encrustation, rarely producing generocystidia (encrusted tips of generative hyphae) with thorny encrustation; 'binding hyphae' (Fig. 5C–D) 1–2–4 μm

Figure 4. Fruiting bodies of the *Skeletocutis nivea* complex. **A** *S. nemoralis*, Korhonen 86 **B** *S. nemoralis*, Korhonen 89 **C** *S. nivea*, epitype **D** *S. nivea*, Miettinen 16350 **E** *S. semipileata* with a characteristic bluish colour on pore surface, epitype **F** *S. unguina*, holotype.

wide, arbuscule-like, simple-septate side-branches of generative hyphae, thin-walled to solid and refractive, developing later than skeletal hyphae and sometimes missing in young parts of context/subiculum but becoming dominant in older parts, sometimes filling up the old tube layer.

Trama (Fig. 5G) monomitic to dimitic; hyphae interwoven, tightly subparallel; generative hyphae 1–3 µm wide, usually prevailing, clamped, thin-walled or sometimes with slightly thickened walls; skeletal hyphae (Fig. 6A–C) looking different from those in context and subiculum, sparse, sometimes apparently missing, originating from tramal generative hyphae, winding and irregularly wide (up to 5+ µm) with spacious lumen, walls usually only slightly thickened, slightly refractive; generative hyphae in dissepiment

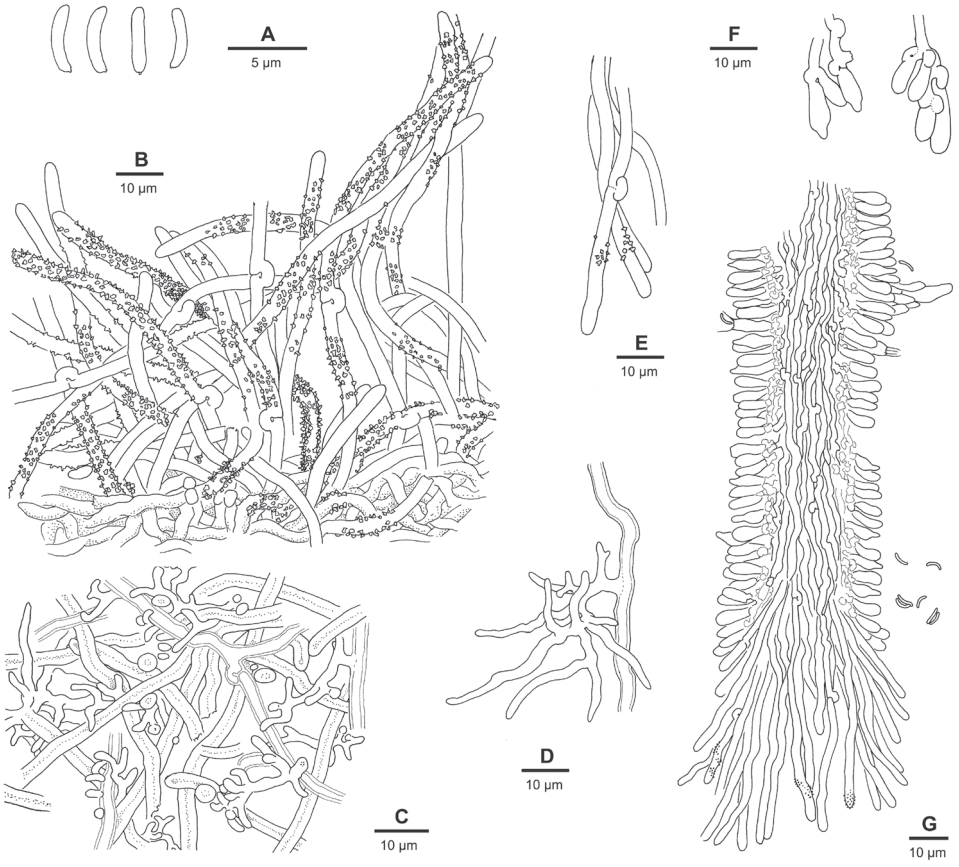

Figure 5. Microscopic structures of *Skeletocutis ochroalba* (reproduced after Niemelä (1985)). **A** spores **B** encrusted tomentum hyphae arising from dense cortical tissue **C** section through context, showing generative and skeletal hyphae and ramified side-branches resembling binding hyphae **D** ramified arbuscule-like binding hypha, arising from a generative hypha **E** dissepiment edge hyphae **F** cystidioles and basidioles **G** vertical section through a dissepiment edge, showing trama, hymenium with a hyphal peg and sparsely encrusted dissepiment edge hyphae.

edges (Fig. 5E and G) ca. 2 µm wide, thin-walled, slightly undulating, often somewhat irregularly shaped towards the tips, bare to richly encrusted with sandy crystals.

Hymenium with fusiform cystidiols (Fig. 5F), often weakly differentiated and inconspicuous but sometimes with strongly elongated apices; hyphal pegs (Fig. 5G) common; heavily encrusted, thorny generocystidia (Fig. 6D) originating from subhymenial hyphae and emerging through hymenium, common especially in older parts of hymenium but sometimes forming amongst dissepiment edge hyphae; basidia (Fig. 6E–G) (5–)6–9(–10) ×(2.2–)2.7–3.7(–4) µm wide, tetrasterigmatic.

Basidiospores (Fig. 7) narrowly allantoid, 2.5–4.0×0.4–0.9 µm, Q'=3.4–7.0, IKI-, CB- (contents CB+).

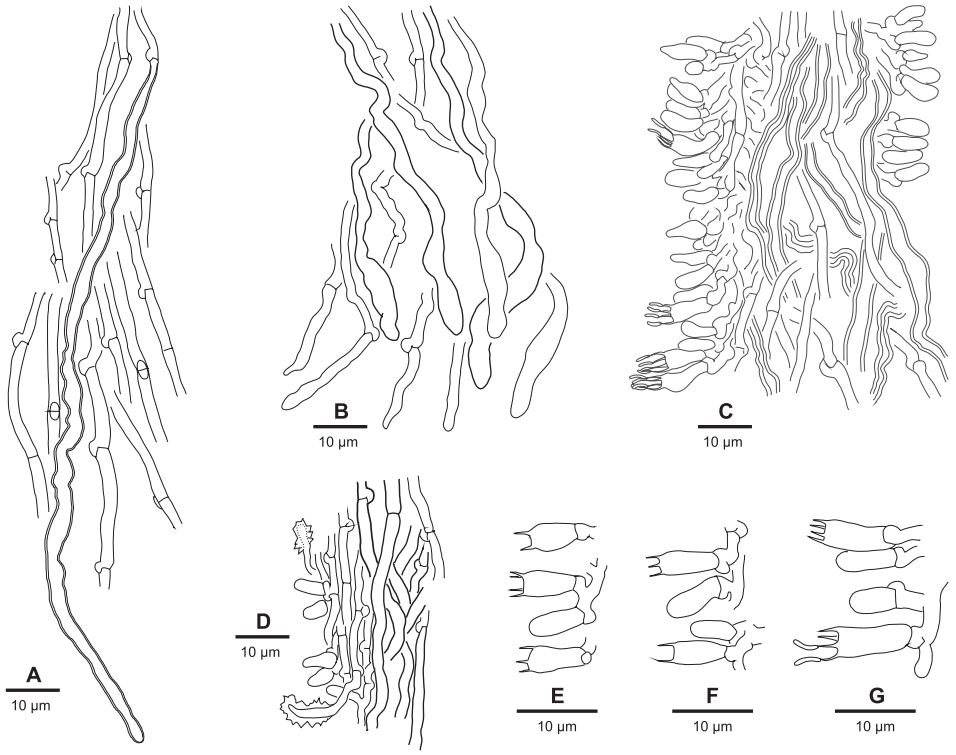

Figure 6. Microscopic structures of the *Skeletocutis nivea* complex. **A** *S. lepida*, tramal skeletal hypha amongst generative hyphae (holotype) **B** *S. semipileata*, ends of generative and skeletal hyphae in trama (Miettinen 17135) **C** *S. nemoralis*, tube trama and hymenium (holotype) **D** *S. nivea*, tube trama and hymenium with encrusted generocystidia (epitype) **E** *S. nivea*, basidia (Miettinen 16350) **F** *S. semipileata*, basidia (epitype) **G** *S. cummata*, the largest basidia in the the *S. nivea* complex (Niemelä 9088).

Discussion. The tramal hyphal structure in *S. nivea* and *S. ochroalba* has traditionally been described as monomitic. However, our microscopic study revealed two distinct hyphal types existing in the trama of all species in the *S. nivea* complex. Amongst the normal clamped and thin-walled generative hyphae, there are usually at least some notably wider and slightly thick-walled hyphae which seem to lack clamps. We call these special hyphae tramal skeletal hyphae. They appear to originate from the generative hyphae in the trama and reach down almost to the pore mouths. Usually the lack of clamps, greater width and thicker walls help to tell them apart from generative hyphae in the trama. Although the tramal skeletal hyphae are usually wide and only slightly thick-walled, some specimens of *S. nivea* had narrower and solid skeletal hyphae in the trama.

Sometimes the tramal hyphal structure is dominated by the skeletal hyphae but sometimes they seem to be missing completely or occur only sporadically in otherwise

monomitic tramal structure (at least in *S. nemoralis* and *S. semipileata*). They can also be difficult to detect when the whole tramal structure becomes sclerified and generative hyphae also develop thickened walls, which was observed in some specimens of *S. nivea*. In general, clear detection of tramal skeletal hyphae is easiest in a squash mount from very thin longitudinal slices of the tube layer which have been properly thinned to an almost disintegrated state.

The nature of the arbuscule-like 'binding hyphae' has been discussed by David (1982) and Niemelä (1985) and both express some reservations about using the term 'trimitic' to describe the *S. nivea* complex. They point out that the 'binding hyphae' in the morphospecies *S. nivea* and *S. ochroalba* originate as clampless side-branches of the generative hyphae and, hence, they are not binding hyphae proper, such as those of *Trametes*. David (1982) studied the staining reactions of the hyphal walls and noted that the walls of the 'binding hyphae' are congophilic and non-metachromatic whereas the walls of the skeletal hyphae are non-congophilic and metachromatic. Our observations confirm that all species in the *S. nivea* complex appear to be similar in this respect.

***Skeletocutis calida* Miettinen & A. Korhonen, sp. nov.**
MycoBank No. MB822242
Figure 7

Holotype. U.S.A. Florida: Alachua County, Gainesville, indet. angiosperm wood, 20 Nov 2013 Miettinen 17761 (H 7008665, isotype FLAS).

Description. Basidiocarps annual; half-resupinate; up to 1.5 cm wide and 2 mm thick; hard when dry but easy to break apart; pilei thin, protruding up to 5 mm; margin incurved; upper surface minutely rough, matted, white to cream coloured when young, turning ochraceous; context up to 1.5 mm thick, faintly zonate in longitudinal section with thin dark lines separating layers of growth; tube layer up to 0.5 mm thick; pores 8–10(–11) per mm.

Hyphal structure: skeletal hyphae in context / subiculum (1.0–)2.0–2.9(–3.5) µm wide, in trama (1.0–)2.0–4.1(–5.2) µm wide, generative hyphae in trama 1.0–2.0(–2.9) µm wide.

Basidiospores 2.5–3.1(–3.3)×0.5–0.6(–0.7) µm, L=2.86 µm, W=0.55 µm, Q'=(4.0–)4.3–6.0(–6.9), Q=5.18, n=60/2.

Distribution and ecology. The species is known only from two specimens from southern U.S.A., collected from warm temperate deciduous forests where specimens were growing on rather thin twigs of unidentified woody angiosperm.

Etymology. Calidus (Lat.), warm, refers to the southern distribution.

Specimens examined. U.S.A. Arkansas: Marion County, Yellville, indet. angiosperm wood, 25 Oct 2013 Miettinen 17466 (H, FLAS); Florida: (holotype, see above).

***Skeletocutis coprosmae* (G. Cunn.) A. Korhonen & Miettinen, comb. nov.**
MycoBank No. MB822243

Basionym. *Poria coprosmae* G. Cunn., Bulletin of the New Zealand Department of Industrial Research 72: 38 (1947).

Holotype. New Zealand. Westland: Lake Mapourika, *Coprosma*, Nov 1946 J.M.Dingley (PDD 5252, studied).

Description. Basidiocarps possibly perennial; resupinate to half-resupinate; up to 6 cm wide and 8 mm thick; hard when dry, breaking apart neatly; pilei fleshy, protruding up to 1.7 cm; margin blunt with narrow, sterile ridge on the underside; upper surface minutely rough, matted, white to cream coloured when young, turning ochraceous brown and finally blackish with age; pore surface sometimes with greenish-grey tints deep within the tubes in pileate part; context and subiculum whitish-cream colour to light greyish-brown near contact with substrate (in thick basidiocarps); context up to 5 mm thick, azonate; tube layer from 0.5–1.5 up to 6 mm thick and zonate in perennial basidiocarp, lighter horizontal zones appear where tubes are filled with arbuscule-like 'binding hyphae'; pores (6–)7–8(–9) per mm.

Hyphal structure: skeletal hyphae in context 2.0–4.3(-5.3) µm wide, in subiculum (1.0–)2.0–3.5(–4.2) µm wide, in trama 2.0–4.0(–5.0) µm wide, generative hyphae in trama 1.0–2.3(–3.0) µm wide.

Basidiospores 2.8–3.2(–3.3)×0.5–0.7 µm, L=2.98 µm, W=0.57 µm, Q'=(4.0–)4.3–6.0(–6.4), Q=5.19, n=60/2.

Distribution and ecology. Available material is very limited but suggests a rather wide, temperate Australasian distribution from Tasmania to southern New Zealand.

Specimens examined. AUSTRALIA. Tasmania: Huon Valley, indet. angiosperm wood, 21 Nov 2006 Gates 1898 (H). NEW ZEALAND. Westland: (holotype, see above).

Discussion. After examining the type, we have chosen to use a previously published name *Poria coprosmae* as the basionym for this Australasian species. *P. coprosmae* was described by Cunningham (1947) from Westland, New Zealand. He (Cunningham 1965) later concluded that his *P. coprosmae* was the same as *Polyporus semipileatus* Peck but he treated them mistakenly under the name *Tyromyces chioneus* (Fr.) P. Karst., as explained by Buchanan and Ryvarden (1988).

In their type studies of *Polyporaceae* species described by Cunningham, Buchanan and Ryvarden (1988) place *P. coprosmae* in the genus *Ceriporiopsis* Dom., rejecting placement in *Incrustoporia* or *Skeletocutis* based on the absence of encrusted hyphae. Rajchenberg (1995), on the other hand, found the hyphal structure in the holotype and other collections of *P. coprosmae* in PDD more in line with that of *S. nivea*. Our studies of the holotype confirm this view with the addition that we also observed encrusted generocystidia and thin-walled skeletal hyphae in the trama, which are characteristic for the *S. nivea* complex. Macroscopically, the only other studied specimen from Tasmania looks quite different from the type. However, we could not identify any clear microscopic differences and cannot rule out the possibility that the macroscopic

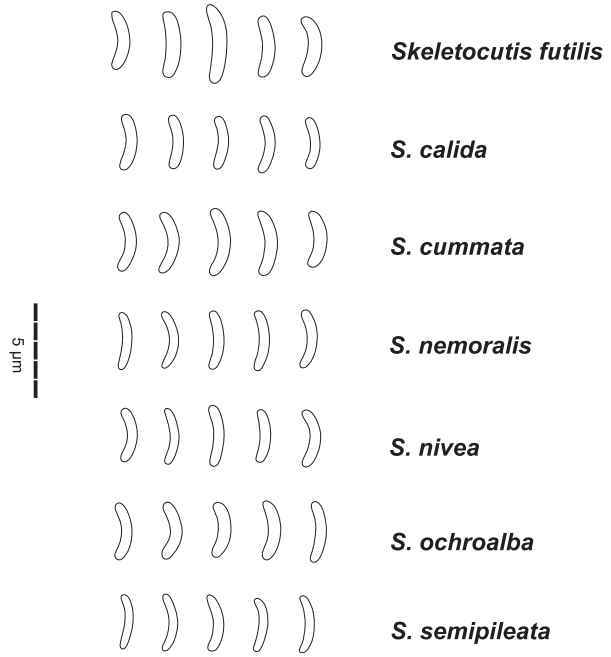

Figure 7. Spores of selected species in the *Skeletocutis nivea* complex.

differences represent variation between developmental stages. Nevertheless, considering the level of crypticity in the *S. nivea* complex, we have reservations in stating that our sequenced specimens are truly conspecific with the old type. Thus, we refrain from assigning an epitype for now.

S. nivea occurs in the North Island of New Zealand and it is possible that these two species could overlap as *S. nivea* has been shown to extend respectively far into the temperate zone in the northern hemisphere. The type specimen is a thin and resupinate basidiocarp on a fallen branch of a *Coprosma* shrub. The Tasmanian specimen, on the other hand, has evidently been growing on coarse wood and is unique in having a clearly perennial habit with a zonate tube layer.

***Skeletocutis cummata* A. Korhonen & Miettinen, sp. nov.**
MycoBank No. MB822244
Figures 6G, 7

Holotype. China. Jilin: Antu, Changbai Mountains, alt. 1300 m, *Picea jezoënsis*, 18 Sep 1998 Niemelä 6408 & Dai (H 7008666).

Description. Basidiocarps annual; half-resupinate to pileate; up to 3 cm wide and (pilei) up to 1 cm thick; hard when dry but easy to break apart; pilei nodulous or thick but steeply sloping, protruding up to 1 cm; margin of pileus curved downwards,

blunt, with narrow, woolly ridge on the underside; upper surface matted to minutely pubescent, white to cream coloured when young, turning ochraceous with almost orange hues; pore surface with ochraceous or sometimes salmon/peach coloured tints, sometimes a greenish-grey tint is visible in the tubes; context and subiculum finally coriaceous but looser and fibrous near cap edge and surface; context faintly zonate in longitudinal section with thin dark lines separating layers of growth; tube layer up to 1 mm thick; pores (5–)7–8(–13) per mm.

Hyphal structure: the outer layer of context typically with a loose, fibrous texture composed of radially orientated encrusted hyphae (tomentum). Skeletal hyphae in context / subiculum (1.0–)2.0–3.5(–5.0) µm wide, in trama 2.0–4.0(–5.0) µm wide, generative hyphae in trama 1.0–2.0(–2.6) µm wide.

Basidiospores (2.8–)2.9–3.4(–3.9)×0.5–0.8(–0.9) µm, L=3.1 µm, W=0.66 µm, Q'=(3.3–)3.8–6.0(–6.6), Q=4.68, n=270/9.

Distribution and ecology. Boreal, Eurasian taiga; known from Fennoscandia, Czech Republic and Far East. The species seems to be rather rare in Europe but possibly more common in the Far East where Spirin (H) has collected it abundantly. The species has been found growing on fallen spruce logs (*Picea abies*, *P. jezoënsis*) but also on *Abies nephrolepis* and *Larix* sp.

Etymology. Cummatus (Lat.), resinous, refers to the brown upper surface of basidiomes.

Specimens examined. CHINA. Jilin: (holotype, see above). FINLAND. Etelä-Häme: Hämeenlinna, *P. abies* (fallen, fairly thin, still corticated tree), 17 Sep 2013 Niemelä 9088 & Spirin (H). RUSSIA. Khabarovsk Reg.: Khabarovsk Dist., Levyi Ulun, *P. jezoënsis*, 21 Aug 2012 Spirin 5472 (H); 5484 (H); Malyi Kukachan, *Larix* sp., 19 Aug 2012 Spirin 5430 (H); Malyi Niran, *P. jezoënsis*, 6 Aug 2012 Spirin 4897 (H); Ulun, *P. jezoënsis*, 26 Aug 2012 Spirin 5676 (H); Solnechny Dist., Igdomi, *Abies nephrolepis*, VIII.2011 Spirin 3857; Suluk-Makit, *P. jezoënsis*, 17 Aug 2011 Spirin 4170 (H).

Discussion. *S. cummata* is most notably distinguished from other Eurasian species in the *S. nivea* complex by its occurrence on conifer wood. Spores of *S. cummata* are also larger than those of angiosperm-dwelling species apart from *S. futilis*. The pubescence on pileus surface in pileate specimens provides an additional identification cue. Very wide but thin-walled tramal skeletal hyphae seem to be particularly pronounced in this species. All distinctive features of *S. cummata* are shared with the North American conifer-dwelling species *S. ochroalba*.

Skeletocutis futilis **Miettinen & A. Korhonen, sp. nov.**
MycoBank No. MB822245
Figure 7

Holotype. Finland. Uusimaa: Helsinki, *Sorbus aucuparia*, 24 Sep 2012 Miettinen 15745 (H 7008667).

Description. Basidiocarps annual; half-resupinate; small, up to 5 mm wide and 1.5 mm thick; hard when dry but easy to break apart; pilei very small and nodulous; upper surface white when young, turning yellowish-brown; context and subiculum white; tube layer up to 0.2 mm thick; pores 6–8 per mm.

Hyphal structure: skeletal hyphae in context / subiculum (1.0–)2.0–3.0(–3.3) µm wide, in trama scarce, (1.0–)2.0–3.9(–4.9) µm wide, generative hyphae in trama 1.0–2.0(–3.2) µm wide.

Basidiospores 3.0–4.0×0.7–0.9 µm, L=3.33 µm, W=0.81 µm, Q'=(3.3–)3.4–5.1, Q=4.13, n=30.

Distribution and ecology. The species is known only from the type specimen which was collected from a *Betula* stand on a disturbed site near the seashore in Helsinki, Finland (hemiboreal zone) where it was growing on rather thin twigs of *Sorbus aucuparia*.

Etymology. Futilis (Lat.), fragile, insignificant.

Specimen examined. FINLAND: Uusimaa: (holotype, see above).

Discussion. While macroscopic features may be quite scanty, characteristic trimitic-looking subiculum, skeletal hyphae in trama and encrustations of dissepiment edge hyphae reveal *S. futilis* to be a member of the *S. nivea* complex. *S. futilis* can be distinguished from other species in the complex by thicker spores.

In our analyses, *S. futilis* constitutes a sister taxon to the rest of the *S. nivea* complex. The clade also includes *S.* aff. *futilis* in North America. Owing to the limited material available, we refrain from judging whether they represent geographic variation within one species or vicariant sister species. The voucher specimens of *S.* aff. *futilis* (Lindner DLL2009-067; -068 (CFMR)) are in a rather poor condition, but it seems that the small size of basidiocarps and thick spores are as characteristic for *S.* aff. *futilis* as they are for *S. futilis*.

Skeletocutis impervia **Miettinen & A. Korhonen, sp. nov.**
MycoBank No. MB822246

Holotype. Uganda. Western Reg.: Kabale Dist., Bwindi Impenetrable National Park, indet. angiosperm wood, 18 Nov 2002 Ipulet F1104 (O 918073, isotype H 7017125).

Description. Basidiocarps annual; half-resupinate; up to 6 mm thick; hard when dry, breaking apart neatly; pilei fleshy, protruding up to 5 mm; margin blunt; upper surface almost smooth, matted, white to cream coloured when young, turning ochraceous brown and finally blackish with age; context and subiculum whitish-cream to light greyish-brown; context up to 5 mm thick, zonate in longitudinal section with thin dark lines separating layers of growth; tube layer from up to 1 mm thick; pores (7–)8–9(–10) per mm.

Hyphal structure: skeletal hyphae in context 2.0–3.2(–4.1) µm wide, in subiculum (1.0–)2.0–3.0(–3.8) µm wide, in trama (1.0–)2.0–3.5(–4.9) µm wide, generative hyphae in trama 1.0–2.0 µm wide.

Basidiospores (2.8–)2.9–3.1×0.5–0.8 µm, L=2.97 µm, W=0.61 µm, Q'=(3.6–)3.8–6.0(–6.2), Q=4.85, n=30.

Distribution and ecology. The species is known only from the type specimen, collected from Bwindi Impenetrable National Park in Uganda where it was reportedly growing on rotting branches.

Etymology. Impervius (Lat.), impenetrable; the species is morphologically indistinguishable from its kins.

Specimen examined. UGANDA. Western Reg.: (holotype, see above).

***Skeletocutis ipuletii* Miettinen & A. Korhonen, sp. nov.**
MycoBank No. MB822247

Holotype. Uganda. Western Reg.: Kabarole Dist., Kibale National Park, indet. angiosperm wood (leaning dead branch), 28 Oct 2002 Ipulet F761 (H 7017127, isotype O 918074).

Description. Basidiocarps annual; half-resupinate; up to 2.5 cm wide and 6 mm thick; hard when dry, breaking apart neatly; pilei fleshy, protruding up to 5 mm; margin blunt; upper surface almost smooth, matted, white to cream coloured when young, turning ochraceous brown; pore surface cream coloured with greyish tint deep within the tubes; context and subiculum whitish-cream to light greyish-brown; context up to 5 mm thick, faintly zonate in longitudinal section with thin dark lines separating layers of growth; tube layer up to 1.5 mm thick; pores 9–10(–11) per mm.

Hyphal structure: skeletal hyphae in context / subiculum 2.0–3.0(–3.6) µm wide, in trama (1.0–)2.0–4.1(–5.0) µm wide, generative hyphae in trama 1.0–2.0(–2.2) µm wide.

Basidiospores 2.8–3.4×0.5–0.7(–0.8) µm, L=2.96 µm, W=0.6 µm, Q'=(4.0–)4.1–6.0(–6.2), Q=4.97, n=30.

Distribution and ecology. The species is known only from the type specimen, collected from Kibale National Park in Uganda, where it was reportedly growing on a leaning, dead branch.

Etymology. Named in honour of the pioneering Ugandan mycologist Perpetua Ipulet, who collected the type of this species.

Specimen examined. UGANDA. Western Reg.: (holotype, see above).

***Skeletocutis lepida* A. Korhonen & Miettinen, sp. nov.**
MycoBank No. MB822248
Figure 6A

Holotype. Japan. Kansai Reg.: Shiga Prefecture, Otsu, indet. angiosperm wood, 7 Nov 2013 Schigel 7684 & Nakamori, Tanaka, Nakano (H 7008661, isotype TFM).

Description. Basidiocarps annual; half-resupinate; pilei up to 3 cm wide, nodulous or up to 4 mm thick and fleshy, blunt edged; upper surface slightly rough, matted, white to cream coloured when young, turning ochraceous; context faintly zonate in longitudinal section with thin dark lines separating layers of growth; tube layer up to 1 mm thick; pores (7–)8–9(–10) per mm.

Hyphal structure: skeletal hyphae in context / subiculum (1.0–)2.0–3.3(–4.0) µm wide, in trama (1.0–)2.0–3.5(–4.9) µm wide, generative hyphae in trama 1.0–2.2(–3.0) µm wide.

Basidiospores See general description of microscopic structures; (2.8–)2.9–3.0(–3.1)×0.5–0.6 µm, L=2.95 µm, W=0.55 µm, Q'=4.8–6.0, Q=5.36, n=90/3.

Distribution and ecology. Available material is limited but suggests a temperate East Asian distribution. Russian specimens represent rather small basidiocarps that were collected from thin, fallen angiosperm branches. The holotype from Japan is a sturdier basidiocarp that was probably growing on a thick branch or a log.

Etymology. Lepidus (Lat.), charming, nice, elegant.

Specimens examined. JAPAN. Kansai Reg.: (holotype, see above). RUSSIA. Khabarovsk Reg.: Khabarovsk Dist., Malyi Niran, *Tilia amurensis*, 7 Aug 2012 Spirin 4989 (H); Solnechny Dist., Boktor, *Quercus mongolica*, 8 Aug 2011 Spirin 3964 (H).

***Skeletocutis nemoralis* A. Korhonen & Miettinen, sp. nov.**
MycoBank No. MB822249
Figures 4A–B, 6C, 7

Holotype. Finland. Åland: Lemland, Nåtö, *Fraxinus excelsior* (fallen branch), 9 Oct 2012 Korhonen 90 (H 7008662).

Basidiocarps annual; resupinate to half-resupinate; bone hard when dry, breaking apart neatly; resupinate basidiocarps up to 10+ cm wide; pilei nodulous to shelf-shaped, often laterally fused and fleshy, protruding up to 1.3 cm; sterile margin often quite pronounced especially in resupinate part; upper surface slightly rough, matted, white to cream coloured when young, turning ochraceous and finally blackish with age; pore surface sometimes with a greenish-grey or turquoise tint emerging within the tubes especially in the pileate part but sometimes in scattered blotches; context sometimes faintly zonate in longitudinal section; tube layer up to 2 mm thick; pores (6–)7–8(–10) per mm.

Hyphal structure: skeletal hyphae in context / subiculum (1.0–)2.0–3.0(–4.0) µm wide, in trama (1.0–)2.0–3.9(–5.0) µm wide, generative hyphae in trama 1.0–2.2(–2.9) µm wide.

Basidiospores (2.8–)2.9–3.2(–4.0)×(0.4–)0.5–0.6(–0.7) µm, L=3.04 µm, W=0.56 µm, Q'=(4.1–)4.8–6.3(–7.8), Q=5.47, n=390/13.

Distribution and ecology. Temperate Eurasia, found in Europe, Iran and Japan; on angiosperm wood, especially *Fraxinus*, preferring coarse substrates like thick branches or even logs.

Etymology. Refers to the distribution area of the species in the nemoral zone.

Specimens examined. FINLAND. Åland: Jomala, Ramsholm, *Fraxinus excelsior* (fallen branch), 10 Oct 2012 Korhonen 100 (H); *103* (H); Lemland, Nåtö, *F. excelsior* (fallen branch) 9 Oct 2012 Korhonen 86 (H); 89 (H); (holotype, see above); *Corylus*

avellana (fallen branch) Korhonen 93 (H). NORWAY. Møre og Romsdal: Sunndal, *Populus tremula*, 24 Sep 2008 Gaarder 5257 (O 288578); Nord-Trøndelag: Verdal, *Sorbus aucuparia*, 30 Aug 2006 Klepsland JK06-S080 (O 284195); Sogn og Fjordane: Aurland, *Tilia cordata*, 10 Jul 2004 Brandrud 149-04 (O 166204). POLAND. Podlaskie Voivodeship: Białowieża National Park, *Carpinus betulus* (fallen branch), 15 Sep 2012 Korhonen 35 (H); *F. excelsior* (fallen branch), 15 Sep 2012 Korhonen 28 (H); 31 (H); 18 Sep 2012 Korhonen 83 (H).

Discussion. *S. nemoralis* shares its wide distribution in Eurasia with similar-looking *S. semipileata*. Both species tend to form rather large, half-resupinate basidiocarps with fleshy pilei. *S. nemoralis* has slightly larger spores and pores than *S. semipileata*, but the distinction is probably too small for definitive identification.

In Europe, *S. nemoralis* does not reach as far to the northeast as *S. semipileata* and appears to be missing in continental Finland. At its north-eastern outpost in Åland Islands, *S. nemoralis* is rather common, especially in old coppice meadows where it prefers the wood of *Fraxinus*.

***Skeletocutis nivea* (Jungh.) Jean Keller, Persoonia 10(3): 353 (1979).**
Figures 4C–D, 6D–E, 7

Basionym. *Polyporus niveus* Jungh. Praemissa in floram cryptogamicam Javae insulae: 48 (1838).

Holotype. Indonesia. Central Java: Mount Merapi, Junghuhn 44 (L).

Epitype. Indonesia. Central Java: Mount Lawu, alt. 2130 m, old-growth montane forest dominated by *Castanopsis javanica*, indet. angiosperm wood (fallen branch), 22 May 2014 Miettinen 18217 (BO, designated here, duplicate H 7008663). MycoBank No. MBT378098

Description. Basidiocarps annual; half-resupinate; hard when dry, breaking apart neatly; pilei nodulous to shelf-shaped, sometimes laterally fused and quite fleshy, up to 2 cm wide and 5 mm thick, protruding up to 1.3 cm, often connected to wider resupinate part; upper surface almost smooth to slightly rough, matted, white to cream coloured when young, turning ochraceous and finally blackish with age; pore surface often with a greenish-grey or turquoise tint emerging within the tubes particularly in the pileate part but often in scattered blotches; context and subiculum coriaceous, white; context sometimes faintly zonate in longitudinal section; tube layer up to 1 mm thick; pores (7–)8–10(–13) per mm.

Hyphal structure: trama dimitic but sometimes seemingly monomitic with slightly sclerified generative hyphae or sometimes clearly dimitic with solid skeletal hyphae; skeletal hyphae in context / subiculum (1.0–)2.0–3.0(–3.9) µm wide, in trama (1.0–)2.0–3.5(–4.9) µm wide, but only 2–3 µm wide and solid in specimens from New Zealand, generative hyphae in trama 1.0–2.3(–2.8) µm wide.

Basidiospores (2.7–)2.8–3.2(–3.7)×0.5–0.7(–0.8) µm, L=2.96 µm, W=0.56 µm, Q'=(3.9–)4.3–6.0(–6.2), Q=5.27, n=125/5.

Distribution and ecology. From tropical southeast Asia to subtropical New Zealand in the south and temperate China in the north, on angiosperm wood.

Specimens examined. CHINA. Jilin: Antu, Changbai Mountains, alt. 1100 m, *Alnus* sp. (fallen tree crown), 27 Aug 2015 Miettinen 10579.1 (H). INDONESIA. Central Java: (epitype, see above); alt. 2180 m, old-growth montane forest dominated by *Castanopsis javanica*, indet. angiosperm wood (fallen tree), 22 May 2014 Miettinen 18255 (ANDA, H); (holotype, see above). MALAYSIA. Sabah: Kinabalu Park, alt. 1675 m, lower montane forest, indet. angiosperm wood, 17 Jun 2013 Miettinen 16350 (SNP, H). NEW ZEALAND. Auckland: Hunua Ranges, indet. angiosperm wood, 19 Mar 1996 Ryvarden 38171 (O 916495); 38177 (O 916496).

Discussion. The holotype of *S. nivea* is sterile but it possesses the encrusted generocystidia and arbuscule-like 'binding hyphae' characteristic to the *S. nivea* complex. Specimens from New Zealand represent a disjunct population and exhibit aberrant hyphal morphology with clearly dimitic trama. However, they do not stand out phylogenetically (in ITS) from the rest of *S. nivea*.

Skeletocutis ochroalba Niemelä, Naturaliste Canadien 112: 466 (1985).

Figures 5, 7

Holotype. Canada. Northern Quebec: Poste-de-la-Baleine, *Picea* sp., 7 Aug 1982 Niemelä 2695 (H 7017091)

Description. Basidiocarps annual or possibly perennial; half-resupinate to pileate; up to 3 cm wide and (pilei) up to 8 mm thick; hard when dry but easy to break apart; pilei nodulous or thick but steeply sloping, protruding up to 1 cm; margin of pileus curved downwards, blunt, with narrow, woolly, ridge on the underside; upper surface matted to minutely pubescent, white or cream coloured when young, turning ochraceous brown; pore surface cream coloured with ochraceous or sometimes salmon/peach coloured tints, sometimes a greenish-grey tint is visible in the tubes; context and subiculum finally coriaceous but looser and fibrous near cap edge and surface; context faintly zonate in longitudinal section with thin dark lines separating layers of growth; tube layer up to 1 mm thick, sometimes divided by a thin white layer where tubes are filled with arbuscule-like 'binding hyphae', otherwise pale buff; pores (6–)7–8(–10) per mm.

Hyphal structure: the outer layer of context typically has a loose, fibrous texture composed of radially orientated hyphae. Skeletal hyphae in context / subiculum (1.0–)2.0–3.5(–4.0) µm wide, in trama 2.0–4.6(–6.2) µm wide, generative hyphae in trama 1.0–2.2(–2.9) µm wide.

Basidiospores (2.8–)2.9–3.7(–4.0)×0.5–0.8 µm, L=3.1 µm, W=0.67 µm, Q'=3.8–6.0(–7.0), Q=4.65, n=70/3.

Distribution and ecology. Boreal North America, possibly quite rare, findings from Northern Quebec and Alberta in Canada; growing on fallen *Picea* logs.

Specimens examined. CANADA. Alberta: William A. Switzer Provincial Park, *Picea* sp., 24 Jul 2015 Spirin 8854a (H); 8854b (H); Northern Quebec: Poste-de-la-Baleine, *Picea* sp., 7 Aug 1982 Niemelä 2689.

Discussion. *S. ochroalba* is most notably distinguished from other North American species of the *S. nivea* complex by its occurrence on conifer wood. Surface of the pileus is characteristically pubescent in this species. The spores of *S. ochroalba* are also thicker than those of North American angiosperm-dwelling species apart from *S.* aff. *futilis*. Resemblance to the Eurasian conifer-dwelling *S. cummata* is strong both in phenology and microscopic structure.

***Skeletocutis semipileata* (Peck) Miettinen & A. Korhonen, comb. nov.**
MycoBank No. MB822250
Figures 4E; 6B, F

Basionym. *Polyporus semipileatus* Peck, Annual Report on the New York State Museum of Natural History 34: 43 (1881).

Lectotype. U.S.A. New York: Catskill Mountains, *Acer spicatum*, Aug 1880 Peck (BPI 220657 ISOTYPE, designated here). MycoBank No. MBT381253

Epitype. U.S.A. New York: Essex County, Huntington Wildlife Forest, Betula sp. (branch), 15 Aug 2012 Miettinen 15536 (H 7008664, designated here, duplicate in BPI)**.** MycoBank No. MBT381348

Description. Basidiocarps annual; resupinate to half-resupinate; hard when dry, breaking apart neatly; resupinate basidiocarps up to 10+ cm wide; pilei nodulous to shelf-shaped, often laterally fused, up to 4 mm thick and protruding up to 1.5 cm, sometimes rather fleshy but often thin and sharp-edged with slightly incurved margin or with narrow, sterile ridge on the underside; upper surface slightly rough, matted, white to cream coloured when young, turning ochraceous and finally blackish with age; pore surface cream coloured with ochraceous or rarely faint salmon coloured tints, often a greenish-grey or turquoise tint emerges within the tubes particularly in the pileate part, sometimes in scattered blotches; context and subiculum coriaceous, white; context sometimes faintly zonate in longitudinal section; tube layer up to 2 mm thick; pores (7–)8–9(–11) per mm.

Hyphal structure: skeletal hyphae in context / subiculum (1.0–)2.0–3.3(–4.3) µm wide, in trama (1.0–)2.0–3.9(–5.0) µm wide, generative hyphae in trama 1.0–2.1(–3.0) µm wide.

Basidiospores (2.3–)2.8–3.1(–3.3)×0.4–0.6(–0.7) µm, L=2.97 µm, W=0.55 µm, Q'=(4.1–)4.7–7.0(–7.5), Q=5.43, n=450/15.

Distribution and ecology. Temperate holarctic, extending to south-boreal zone at least in Fennoscandia; on various angiosperm species, often on thin fallen branches but sometimes on coarse wood as well.

Specimens examined. FINLAND. Uusimaa: Helsinki, indet. angiosperm (fallen branch), 9 Oct 2011 Miettinen 14917.4 (H); Kirkkonummi, *Prunus padus* (fallen

tree), 24 Oct 2012 Miettinen 15835 (H). Etelä-Häme: Hämeenlinna, Lammi, *Corylus avellana* (fallen branch), 11 Sep 2002 Miettinen 6694 (H); Pohjois-Häme: Jyväskylä, Vuoritsalo, *Juniperus communis* (fallen trunk), 15 Jul 2017 Miettinen 21003 (H). NORWAY. Møre og Romsdal: Nesset, *Ulmus glabra*, 22 Sep 2006 Ryvarden 47279 (O 361851); Sogn og Fjordane: Luster, *C. avellana*, 25 Aug 2007 Gaarder 5136 & Dybwad (O 293503). POLAND. Podlaskie Voivodeship: Hajnówka, *C. avellana*, 18 Sep 2012 Korhonen 76 (H). RUSSIA. Khabarovsk Reg.: Khabarovsk Dist., Ilga, *Actinidia kolomikta*, 10 Aug 2012 Spirin 5142 (H); Nizhny Novgorod Reg.: Lukoyanov Dist., Sanki, *C. avellana*, 7 Aug 2005 Spirin 2326 (H). UNITED KINGDOM. Scotland: South Lanarkshire, *P. padus* (fallen tree), 6 Jul 2010 Miettinen 14114 (H). U.S.A. Massachusetts: Holden, *Betula* sp. (fallen branch), 6 Sep 2013 Miettinen 16823 (H); Minnesota: Waseca, *Tilia americana* (fallen branch), 18 Aug 2013 Miettinen 16693.1 (H); New York: (lectotype, see above); (epitype, see above); indet. angiosperm wood, 18 Aug 2012 Miettinen 15715 (H); *Betula* sp., 22 Sep 2013 Miettinen 17135 (H); *Fagus grandifolia* (fallen tree crown), 20 Sep 2013 Miettinen 17074 (H).

Discussion. *S. semipileata* seems to be the most widespread species in the *S. nivea* complex and overlaps with many of the other angiosperm-dwelling species: in Europe with *S. futilis* and *S. nemoralis*; in the Far East with *S. lepida* and *S. nivea*; and in North America with *S.* aff. *futilis* and possibly with *S. calida*. Apart from *S.* (aff.) *futilis,* these species are almost impossible to distinguish from each other morphologically.

Skeletocutis unguina **Miettinen & A. Korhonen, sp. nov.**
MycoBank No. MB822251
Figure 4F

Holotype. China. Yunnan: Xishuangbanna, Xishuangbanna Biosphere Reserve, alt. 700 m, indet. angiosperm wood, 5 Aug 2005 Miettinen 10002 (H 7008668, isotype BJFC).

Description. Basidiocarps annual; half-resupinate; small, up to 1 cm wide and 1 mm thick; hard when dry but easy to break apart; pilei thin, protruding up to 4 mm; margin incurved; upper surface minutely rough, matted, white to cream coloured when young, turning ochraceous; context up to 0.7 mm thick, azonate; tube layer up to 0.3 mm thick; pores 7–9 per mm.

Hyphal structure: skeletal hyphae in context 1.0–2.9(–3.5) µm wide, in subiculum (1.0–)2.0–2.9(–3.2) µm wide, in trama 2.0–4.0(–4.8) µm wide, generative hyphae in trama 1.0–1.9(–2.0) µm wide.

Basidiospores 2.9–3.2(–3.3)×(0.4–)0.5–0.6(–0.7) µm, L=3.04 µm, W=0.55 µm, Q'=(4.6–)4.8–6.4(–7.5), Q=5.49, n=30.

Distribution and ecology. The species is known only from the type specimen, collected from Yunnan, China, where it was growing as small individual pilei on thin twigs of unidentified woody angiosperm.

Etymology. Derived from unguis (Lat.), claw, nail; refers to nail-like basidiome caps.

Specimen examined. CHINA. Yunnan: (holotype, see above).

***Skeletocutis yuchengii* Miettinen & A. Korhonen, sp. nov.**
MycoBank No. MB822252

Holotype. China. Yunnan: Xishuangbanna, Menglun, alt. 640 m, indet. angiosperm wood, 4 Aug 2005 Miettinen 9950 (H 7008660, isotype BJFC, strain FBCC 1132).

Description. Basidiocarps annual; resupinate to half-resupinate; small, up to 2.5 cm wide and 3 mm thick; hard when dry but easy to break apart; pilei nodulous, protruding up to 3 mm; margin blunt; upper surface minutely rough, matted, white to cream coloured when young, turning ochraceous; pore surface cream coloured with yellowish to ochraceous tints; context up to 2.7 mm thick faintly zonate in longitudinal section with fuzzy, ochraceous lines separating layers of growth; tube layer up to 0.3 mm thick; pores 8–10(–11) per mm.

Hyphal structure: skeletal hyphae in context / subiculum 1.0–2.9(–3.8) µm wide, in trama (2.0–)3.0–4.0(–5.1) µm wide, generative hyphae in trama 1.0–2.0(–2.2) µm wide.

Basidiospores (2.7–)2.8–3.1(–3.2)×(0.4–)0.5–0.7 µm, L=2.96 µm. W=0.59 µm, Q'=(4.0–)4.1–6.0(–7.2), Q=4.99, n=90/3.

Distribution and ecology. The species is known from three specimens from Yunnan, China, collected from twigs of unidentified woody angiosperm.

Etymology. In honour of the Chinese polypore researcher, Prof. Yu-Cheng Dai.

Specimens examined. CHINA. Yunnan: (holotype, see above); Xishuangbanna Biosphere Reserve, alt. 700 m, indet. angiosperm wood (dead standing tree), 9 Aug 2005 Miettinen 10150.2 (H); Xishuang Banna Primeval Forest Park, indet. angiosperm wood (fallen branch), 16 Aug 2005 Miettinen 10366.1 (H).

Rejected names

***Poria hymeniicola* Murrill, Mycologia 12(6): 305 (1920).**

Holotype. U.S.A. Maine: Piscataquis Co., Medford, Camp Sunday, on dead *Populus*, 28 Aug 1905 Murrill (NY, studied).

Specimen examined. U.S.A. Maine: (holotype, see above)

Discussion. *P. hymeniicola* is a poorly known species from North America which has sometimes been associated with the *S. nivea* complex (*P. semipileatus* by Lowe (1947, 1966)). Niemelä (1998) studied the type specimen and concluded that the dimitic trama with solid skeletal hyphae does not match with the *S. nivea* complex. Even though we have observed some specimens of *S. nivea* with such hyphal structure, they were not observed in North American material. Furthermore, the basidiocarp of the type specimen grew on a dead basidiocarp of another polypore species, unlike any of our studied material of the *S. nivea* complex. The species would appear to be related to *S. stellae* and related species (*Incrustoporia*).

Polyporus alboniger **Lloyd ex G. Cunn., Proceedings of the Linnean Society of New South Wales 75: 227 (1950).**

Type. Australia. Tasmania: Hobart, Rodway (BPI 301712).

Discussion. Cunningham (1950) mentions the name *P. alboniger* as the label of a herbarium specimen he determined to be *P. atromaculus* (see below). We consider the name to be invalid as it lacks proper description (ICBN Melbourne Art. 38.1 & 39.1).

Polyporus atromaculus **Lloyd, Bulletin of the Lloyd Library 35: 98 (1936).**

Type. Australia. Tasmania: Hobart, Rodway (BPI 302037).

Discussion. Cunningham (1965) considered *P. atromaculus* to be a synonym of *S. nivea* (or *Tyromyces chioneus*, as he called it). The name refers to Tasmanian collections of L. Rodway. Lloyd (1922) used the name *P. atromaculatus* in reporting his determinations to Rodway. Referencing Lloyd (1922), Stevenson and Cash (1936) published *Polyporus atromaculus* Lloyd in herb. accompanied by a description and specification of a type specimen in a list of fungus names proposed by Lloyd. It is doubtful whether their intention was to validate the name but the description remains invalid (ICBN Melbourne Art. 39.1) and we reject the name. Ryvarden (1990) appears to share this view as he does not include *P. atromaculus* in his type studies of *Polyporus* species described by Lloyd.

Acknowledgements

Many researchers have contributed valuable material for this study; the following deserve a special mention: Genevieve Gates (Tasmania), Peter Buchanan (Landcare Research), Leif Ryvarden (Oslo) and Viacheslav Spirin (Helsinki). Yu-Cheng Dai (Beijing Forestry University) and his students organised a joint collecting trip in China resulting in important records, Nicholas J. Brazee (University of Massachusetts) provided locality data for North American voucher specimens. This research was supported by the National Science Foundation grant DEB0933081 by David Hibbett (Clark University), the European Commission Marie Curie grant PIOF-GA-2011-302349, Societas Biologica Fennica Vanamo and Lammin biologisen aseman Ympäristötutkimuksen Säätiö.

References

Banik MT, Lindner DL, Ota Y, Hattori T (2010) Relationships among north American and Japanese *Laetiporus* isolates inferred from molecular phylogenetics and single-spore incompatibility reactions. Mycologia 102(4): 911–917. https://doi.org/10.3852/09-044

Brazee NJ, Lindner DL (2013) Unravelling the *Phellinus pini* s.l. complex in North America: a multilocus phylogeny and differentiation analysis of *Porodaedalea*. Forest Pathology 43(2): 132–143. https://doi.org/10.1111/efp.12008

Buchanan PK, Ryvarden L (1988) Type studies in the Polyporaceae 18. Species described by G.H. Cunningham. Mycotaxon 31(1): 1–38.

Carlson A, Justo A, Hibbett DS (2014) Species delimitation in *Trametes*: a comparison of ITS, RPB1, RPB2 and *tef1* gene phylogenies. Mycologia 106(4): 735–745. https://doi.org/10.3852/13-275

Chen J-J, Korhonen K, Li W, Dai Y-C (2014) Two new species of the *Heterobasidion insulare* complex based on morphology and molecular data. Mycoscience 55(4): 289–298. https://doi.org/10.1016/j.myc.2013.11.002

Cunningham GH (1947) New Zealand Polyporaceae 1. The genus *Poria*. Bulletin of the New Zealand Department of Industrial Research 72: 1–43.

Cunningham GH (1950) Australian Polyporaceae in herbaria of Royal Botanic Gardens, Kew, and British Museum of Natural History. Proceedings of the Linnean Society of New South Wales 75: 214–249.

Cunningham GH (1965) Polyporaceae of New Zealand. Bulletin of the New Zealand Department of Industrial Research 164: 1–304.

Dai Y-C, Korhonen K (2009) *Heterobasidion australe*, a new polypore derived from the *Heterobasidion insulare* complex. Mycoscience 50(5): 353–356. https://doi.org/10.1007/s10267-009-0491-3

Darriba D, Taboada GL, Doallo R, Posada D (2012) jModelTest 2: more models, new heuristics and parallel computing. Nature Methods 9: 772. https://doi.org/10.1038/nmeth.2109

David A (1982) Étude monographique du genre *Skeletocutis* (Polyporaceae). Naturaliste Canadien 109: 235–272.

Guindon S, Gascuel O (2003) A simple, fast and accurate method to estimate large phylogenies by maximum-likelihood. Systematic Biology 52(5): 696–704. https://doi.org/10.1080/10635150390235520

Hallenberg N, Nilsson RH, Antonelli A, Wu SH, Maekawa N, Nordén B (2007) The *Peniophorella praetermissa* species complex (Basidiomycota). Mycological Research 111(12): 1366–1376. https://doi.org/10.1016/j.mycres.2007.10.001

Han M-L, Chen Y-Y, Shen L-L, Song J, Vlasák J, Dai Y-C, Cui B-K (2016) Taxonomy and phylogeny of the brown-rot fungi: *Fomitopsis* and its related genera. Fungal Diversity 80(1): 343–373. https://doi.org/10.1007/s13225-016-0364-y

Haynes KA, Westerneng TJ, Fell JW, Moens W (1995) Rapid detection and identification of pathogenic fungi by polymerase chain reaction amplification of large subunit ribosomal DNA. Journal of medical and veterinary mycology: bi-monthly publication of the International Society for Human and Animal Mycology 33(5): 319–25. https://doi.org/10.1080/02681219580000641

Hughes KW, Segovia AR, Petersen RH (2014) Transatlantic disjunction in fleshy fungi. I. The *Sparassis crispa* complex. Mycological Progress 13(2): 407–427. https://doi.org/10.1007/s11557-013-0927-1

Junghuhn FW (1838) Praemissa in floram cryptogamicam Javae insulae: 48.

Justo A, Miettinen O, Floudas D, Ortiz-Santana B, Sjökvist E, Lindner DL, Nakasone K, Niemelä T, Larsson KH, Ryvarden L, Hibbett DS (2017) A revised family-level classification of the Polyporales (Basidiomycota). Fungal Biology 121(9): 798–824. https://doi.org/10.1016/j.funbio.2017.05.010

Kauserud H, Svegarden IB, Decock C, Hallenberg N (2007) Hybridization among cryptic species of the cellar fungus *Coniophora puteana* (Basidiomycota). Molecular Ecology 16(2): 389–399. https://doi.org/10.1111/j.1365-294X.2006.03129.x

Kumar S, Stecher G, Tamura K (2016) MEGA7: Molecular Evolutionary Genetics Analysis version 7.0 for bigger datasets. Molecular Biology and Evolution 33(7): 1870–1874. https://doi.org/10.1093/molbev/msw054

Lindner DL, Banik MT (2011) Intragenomic variation in the ITS rDNA region obscures phylogenetic relationships and inflates estimates of operational taxonomic units in genus *Laetiporus*. Mycologia 103(4): 731–740. https://doi.org/10.3852/10-331

Lindner DL, Carlsen T, Nilsson RH, Davey M, Schumacher T, Kauserud H (2013) Employing 454 amplicon pyrosequencing to reveal intragenomic divergence in the internal transcribed spacer rDNA region in fungi. Ecology and Evolution 2013; 3(6): 1751–1764. https://doi.org/10.1002/ece3.586

Lloyd CG (1922) Mycological Notes 67. Mycological Writings 7(66): 1137–1168.

Lowe JL (1947) Studies in the genus *Poria* 2. White and brightly-colored type material. Lloydia 10: 45–59.

Lowe JL (1966) Polyporaceae of North America. The genus *Poria*. Technical Publications. New York State University College of Forestry 90: 1–183.

Löytynoja A, Goldman N (2010) webPRANK: a phylogenyaware multiple sequence aligner with interactive alignment browser. BMC Bioinformatics 11: 579. https://doi.org/10.1186/1471-2105-11-579

Matheny PB, Wang Z, Binder M, Curtis JM, Lim YW, Nilsson RH, Hughes KW, Hofstetter V, Ammirati JF, Schoch CL, Langer E, Langer G, McLaughlin DJ, Wilson AW, Frøslev T, Ge ZW, Kerrigan RW, Slot JC, Yang ZL, Baroni TJ, Fischer M, Hosaka K, Matsuura K, Seidl MT, Vauras J, Hibbett DS (2007) Contributions of rpb2 and tef1 to the phylogeny of mushrooms and allies (Basidiomycota, Fungi). Molecular Phylogenetics and Evolution 43(2): 430–51. https://doi.org/10.1016/j.ympev.2006.08.024

Miettinen O, Niemelä T (2018) Two new temperate polypore species of *Skeletocutis* (Polyporales, Basidiomycota). Annales Botanici Fennici 55: 195–206.

Miettinen O, Niemelä T, Spirin W (2006) Northern *Antrodiella* species: the identity of *A. semisupina* and type studies of related taxa. Mycotaxon 96: 211–239.

Miettinen O, Spirin V, Niemelä T (2012) Notes on the genus *Aporpium* (Auriculariales, Basidiomycota), with a new species from temperate Europe. Annales Botanici Fennici 49: 359–368. https://doi.org/10.5735/085.049.0607

Miettinen O, Vlasák J, Rivoire B, Spirin V (2018) *Postia caesia* complex (Polyporales, Basidiomycota) in temperate Northern Hemisphere. Fungal Systematics and Evolution 1: 101–129. https://doi.org/10.3114/fuse.2018.01.05

Miller MA, Pfeiffer W, Schwartz T (2010) Creating the CIPRES Science Gateway for inference of large phylogenetic trees. Proceedings of the Gateway Computing Environments Workshop (GCE), New Orleans, 1–8. https://doi.org/10.1109/GCE.2010.5676129

Niemelä T (1985) Mycoflora of Poste-de-la-Baleine, Northern Quebec. Polypores and the Hymenochaetales. Naturaliste Canadien 112(4): 445–472.

Norros VM, Karhu E, Nordén J, Vähätalo AV, Ovaskainen O (2015) Spore sensitivity to sunlight and freezing can restrict dispersal in wood-decay fungi. Ecology and Evolution 5(16): 3312–3326. https://doi.org/10.1002/ece3.1589

Otrosina WJ, Garbelotto M (2010) *Heterobasidion occidentale* sp. nov. and *Heterobasidion irregulare* nom. nov.: A disposition of North American *Heterobasidion* biological species. Fungal Biology 114(1): 16–25. https://doi.org/10.1016/j.mycres.2009.09.001

Overholts LO (1953) The Polyporaceae of the United States, Alaska and Canada, University of Michigan Press, Ann Arbor.

Rajchenberg M (1995) Notes on New Zealand polypores (Basidiomycetes) 2. Cultural and morphological studies of selected species. New Zealand Journal of Botany 33(1): 99–109. https://doi.org/10.1080/0028825X.1995.10412947

Rehner S (2001) Primers for Elongation Factor 1-α (EF1-α). http://ocid.NACSE.ORG/research/deephyphae/EF1primer.pdf

Riess K, Oberwinkler F, Bauer R, Garnica S (2013) High genetic diversity at the regional scale and possible speciation in *Sebacina epigaea* and *S. incrustans*. BMC Evolutionary Biology 13: 102. https://doi.org/10.1186/1471-2148-13-102

Ronquist F, Teslenko M, van der Mark P, Ayres DL, Darling A, Hohna S, Larget B, Liu L, Suchard MA, Huelsenbeck JP (2012) MrBayes 3.2: Efficient Bayesian Phylogenetic Inference and model choice across a large model space. Systematic Biology 61(3): 539–542. https://doi.org/10.1093/sysbio/sys029

Ryvarden L (1990) Type studies in the Polyporaceae 22. Species described by C.G. Lloyd in *Polyporus*. Mycotaxon 38: 83–102.

Ryvarden L (2018) Studies in African Aphyllophorales 25. New species from East and Central Africa. Synopsis Fungorum 38: 25–32.

Song J, Cui B-K (2017) Phylogeny, divergence time and historical biogeography of *Laetiporus* (Basidiomycota, Polyporales). BMC Evolutionary Biology 17: 102. https://doi.org/10.1186/s12862-017-0948-5

Spirin V, Runnel K, Vlasák J, Miettinen O, Põldmaa K (2015) Species diversity in the *Antrodia crassa* group (Polyporales, Basidiomycota). Fungal Biology 119(12): 1291–1310. https://doi.org/10.1016/j.funbio.2015.09.008

Spirin V, Vlasák J, Miettinen O (2017) Studies in the *Antrodia serialis* group (Polyporales, Basidiomycota). Mycologia 109(2): 217–230. https://doi.org/10.1080/00275514.2017.1300087

Stamatakis A (2014) RAxML Version 8: A tool for Phylogenetic Analysis and Post-Analysis of Large Phylogenies. Bioinformatics 30(9): 1312–1313. https://doi.org/10.1093/bioinformatics/btu033

Stevenson JA, Cash EK (1936) The new fungus names proposed by C.G. Lloyd. Bulletin of the Lloyd Library 35: 1–209.

Söderström L (1988) Sequence of bryophytes and lichens in relation to substrate variables of decaying coniferous wood in northern Sweden. Nordic Journal of Botany 8: 89–97. https://doi.org/10.1111/j.1756-1051.1988.tb01709.x

Tamura K, Kumar S (2002) Evolutionary distance estimation under heterogeneous substitution pattern among lineages. Molecular Biology and Evolution 19(10): 1727–1736. https://doi.org/10.1093/oxfordjournals.molbev.a003995

Tamura K, Nei M, Kumar S (2004) Prospects for inferring very large phylogenies by using the neighbor-joining method. Proceedings of the National Academy of Sciences of the United States of America 101(30): 11030–11035. https://doi.org/10.1073/pnas.0404206101

Thiers B (2017) Index Herbariorum: A global directory of public herbaria and associated staff. New York Botanical Garden's Virtual Herbarium. http://sweetgum.nybg.org/science/ih/

Tomovský M, Vampola P, Sedlák P, Byrtusová Z, Jankovský L (2010) Delimitation of central and northern European species of the *Phellinus igniarius* group (Basidiomycota, Hymenochaetales) based on analysis of ITS and translation elongation factor 1 alpha DNA sequences. Mycological Progress 9(3): 431–445. https://doi.org/10.1007/s11557-009-0653-x

Vasaitis R, Menkis A, Lim YW, Seok S, Tomsovsky M, Jankovsky L, Lygis V, Slippers B, Stenlid J (2009) Genetic variation and relationships in *Laetiporus sulphureus* s. lat., as determined by ITS rDNA sequences and in vitro growth rate. Mycological Research 113(3): 326–336. https://doi.org/10.1016/j.mycres.2008.11.009

Vilgalys R, Hester M (1990) Rapid genetic identification and mapping of enzymatically amplified ribosomal DNA from several *Cryptococcus* species. Journal of Bacteriology 172(8): 4239–4246. https://doi.org/10.1128/jb.172.8.4238-4246.1990

Vlasák J, Kout J, Vlasák J, Ryvarden L (2011) New records of polypores from southern Florida. Mycotaxon 118: 159–176. https://doi.org/10.5248/118.159

Wilkinson DM, Koumoutsaris S, Mitchell EAD, Bey I (2012) Modelling the effect of size on the aerial dispersal of microorganisms. Journal of Biogeography 39(1): 89–97. https://doi.org/10.1111/j.1365-2699.2011.02569.x

Zhou LW, Vlasák J, Qin WM, Dai Y-C (2016) Global diversity and phylogeny of the *Phellinus igniarius* complex (Hymenochaetales, Basidiomycota) with the description of five new species. Mycologia 108(1): 192–204. https://doi.org/10.3852/15–099

Supplementary material 1

Specimens and INSDC accession numbers of DNA sequences used in this study

Authors: Aku Korhonen, Jaya Seelan Sathiya Seelan, Otto Miettinen

Data type: molecular data

Explanation note: Sequences retrieved from INSDC are denoted with*.

Link: https://doi.org/10.3897/mycokeys.36.27002.suppl1

Supplementary material 2

Estimates of average genetic divergence over sequence pairs within species

Authors: Aku Korhonen, Jaya Seelan Sathiya Seelan, Otto Miettinen

Data type: molecular data

Explanation note: The number of base substitutions per site ×100 (%) obtained from averaging over all sequence pairs within each species are shown in first column, followed by standard error (SE) estimates (500 bootstrap replicates) and the number (N) of compared sequences are shown.

Link: https://doi.org/10.3897/mycokeys.36.27002.suppl2

Supplementary material 3

Estimates of genetic divergence over ITS sequence pairs between species

Authors: Aku Korhonen, Jaya Seelan Sathiya Seelan, Otto Miettinen

Data type: molecular data

Explanation note: The number of base substitutions per site ×100 (%) obtained from averaging over all sequence pairs between species (1–14) are shown below the diagonal and standard error (SE) estimates (500 bootstrap replicates) above the diagonal.

Link: https://doi.org/10.3897/mycokeys.36.27002.suppl3

Supplementary material 4

Estimates of evolutionary divergence over tef1 sequence pairs between species

Authors: Aku Korhonen, Jaya Seelan Sathiya Seelan, Otto Miettinen

Data type: molecular data

Explanation note: The number of base substitutions per site ×100 (%) obtained from averaging over all sequence pairs between species (1–13) are shown below the diagonal and standard error (SE) estimates (500 bootstrap replicates) above the diagonal.

Link: https://doi.org/10.3897/mycokeys.36.27002.suppl4

Supplementary material 5

Distribution maps

Authors: Aku Korhonen, Jaya Seelan Sathiya Seelan, Otto Miettinen

Data type: occurence

Explanation note: Collection localities of specimens included in this study, indicating the approximate species distributions of the *Skeletocutis nivea* complex (A) in Europe and Western Asia, (B) in East Asia, Indomalaya and Australasia and (C) in North America.

Link: https://doi.org/10.3897/mycokeys.36.27002.suppl5

MycoKeys 36: 83–105 (2018)
doi: 10.3897/mycokeys.36.27051
http://mycokeys.pensoft.net

RESEARCH ARTICLE

A peer-reviewed open-access journal
MycoKeys
Launched to accelerate biodiversity research

New species in *Dictyosporium*, new combinations in *Dictyocheirospora* and an updated backbone tree for Dictyosporiaceae

Jing Yang[1,2], Jian-Kui Liu[1], Kevin D. Hyde[2,3,4], E.B. Gareth Jones[5], Zuo-Yi Liu[1]

1 *Guizhou Key Laboratory of Agricultural Biotechnology, Guizhou Academy of Agricultural Sciences, Guiyang 550006, Guizhou, China* **2** *Center of Excellence in Fungal Research, Mae Fah Luang University, Chiang Rai 57100, Thailand* **3** *Key Laboratory for Plant Diversity and Biogeography of East Asia, Kunming Institute of Botany, Chinese Academy of Science, Kunming 650201, Yunnan, China* **4** *World Agroforestry Centre, East and Central Asia, 132 Lanhei Road, Kunming, 650201, Yunnan, China* **5** *Department of Entomology and Plant Pathology, Faculty of Agriculture, Chiang Mai University, Huay Keaw Road, Suthep, Muang District, Chiang Mai 50200, Thailand*

Corresponding author: *Zuo-Yi Liu* (gzliuzuoyi@163.com)

Academic editor: *Paul Kirk* | Received 29 May 2018 | Accepted 1 July 2018 | Published 18 July 2018

Citation: Yang J, Liu JK, Hyde KD, Jones EBG, Liu ZY (2018) New species in *Dictyosporium*, new combinations in *Dictyocheirospora* and an updated backbone tree for Dictyosporiaceae. MycoKeys 36: 83–105. https://doi.org/10.3897/mycokeys.36.27051

Abstract

A survey of freshwater fungi on submerged wood in China and Thailand resulted in the collection of three species in *Dictyocheirospora* and four species in *Dictyosporium* including two new species in the latter genus. Morphological characters and phylogenetic analyses based on ITS, LSU and TEF1α sequence data support their placement in *Dictyocheirospora* and *Dictyosporium* (Dictyosporiaceae). An updated backbone tree is provided for the family Dictyosporiaceae. Descriptions and illustrations of the new taxa and re-collections are provided. Four new combinations are proposed for *Dictyocheirospora*.

Keywords

2 new taxa, asexual morph, Dothideomycetes, phylogeny, taxonomy

Introduction

The family Dictyosporiaceae was introduced by Boonmee et al. (2016) to accommodate mostly aquatic lignicolous species with cheiroid, digitate, palmate and/or dictyosporous conidia and their sexual morphs that form a monophyletic clade in the class Dothideomycetes.

Dictyosporium, the type genus of the family, has been reported worldwide from dead wood and plant litter in terrestrial and aquatic habitats (Hyde and Goh 1998, Ho et al. 2002, Pinnoi et al. 2006, Pinruan et al. 2007). Corda (1836) established the genus with *D. elegans* Corda as the type species. The holomorph genus is characterised by dark brown, subglobose superficial ascomata, bitunicate cylindrical asci and hyaline, fusiform uniseptate ascospores with or without a sheath; sporodochial colonies, micronematous to macronematous conidiophores and cheiroid, digitate complanate conidia with several parallel rows of cells. Goh et al. (1999) reviewed the genus accepting 22 species and the remaining 16 species were doubtful or excluded. Tsui et al. (2006) first considered that the genus is closely related to Massarinaceae (Pleosporales) based on phylogenetic analysis using SSU and LSU sequence data. Tanaka et al. (2015) and Boonmee et al. (2016) confirmed the phylogenetic placement of *Dictyosporium* in Dictyosporiaceae (Massarineae, Pleosporales). Recent comparisons of *Dictyosporium* species were provided by Whitton et al. (2012), Prasher and Verma (2015) and Silva et al. (2015) with up to 48 accepted species. Since Silva et al. (2015), *D. araucariae* S.S. Silva, R.F. Castañeda & Gusmão, *D. hydei* I.B. Prasher & R.K. Verma, *D. indicum* I.B. Prasher & R.K. Verma, *D. olivaceosporum* Kaz. Tanaka, K. Hiray., Boonmee & K.D. Hyde, *D. palmae* Abdel-Aziz, *D. pseudomusae* Kaz. Tanaka, G. Sato & K. Hiray., *D. sexualis* Boonmee & K.D. Hyde, *D. splendidum* Alves-Barb., Malosso & R.F. Castañeda and *D. wuyiense* Y. Zhang & G.Z. Zhao were newly introduced to the genus (Prasher and Verma 2015, Tanaka et al. 2015, Abdel-Aziz 2016, Boonmee et al. 2016, da Silva et al. 2016, Alves-Barbosa et al. 2017, Zhang et al. 2017) and nine species were re-assigned to *Dictyocheirospora*, *Jalapriya* and *Vikalpa* (Boonmee et al. 2016). Wijayawardene et al. (2017a) provided information on the availability of cultures and references to accessible sequence data.

Dictyocheirospora was introduced by Boonmee et al. (2016) with *Di. rotunda* D'souza, Bhat & K.D. Hyde as the type species. *Dictyocheirospora* is morphologically similar to *Dictyosporium* except in having cheiroid, non-complanate or cylindrical conidia, mostly with conidial arms closely gathered together at the apex. Ten species are accepted in the genus including four species transferred from *Dictyosporium* (Boonmee et al. 2016, Wang et al. 2016, Hyde et al. 2017, Li et al. 2017).

During a survey of freshwater fungi on submerged wood along a north/south gradient in the Asian/Australasian region (Hyde et al. 2016), two new freshwater species and five previously described species were collected and identified based on phylogenetic analyses and morphological characters. We therefore introduce *Dictyosporium tubulatum* and *Dictyosporium tratense* as new species, with an illustrated account and

phylogenetic evidence for the new taxa. An updated backbone tree based on the combined ITS, LSU and TEF1α sequence data is provided for Dictyosporiaceae. Four new combinations are proposed in *Dictyocheirospora*.

Materials and methods

Collection and examination of specimens

Specimens of submerged, decaying wood were collected from streams in Chiang Rai, Prachuap Khiri Khan, Phang Nga and Trat Provinces, Thailand, in December 2014, 2015, April 2016 and Guizhou Province, China, in October 2016. Specimens were brought to the laboratory in plastic bags and incubated in plastic boxes lined with moistened tissue paper at room temperature for one week. Morphological observations were made using a Motic SMZ 168 Series dissecting microscope for fungal structures on natural substrate. The fungal structures were collected using a syringe needle and transferred to a small drop of distilled water on a clean slide and covered with a cover glass. The fungi were examined using a Nikon ECLIPSE 80i compound microscope and photographed with a Canon 550D, 600D or 70D digital camera fitted to the microscope. Measurements were made with the TAROSOFT (R) IMAGE FRAME WORK programme and images used for figures were processed with ADOBE PHOTOSHOP CS6 software. Single spore isolations were made on to potato dextrose agar (PDA) or water agar (WA) and later transferred on to malt extract agar (MEA) or PDA following the method of Chomnunti et al. (2014). Specimens (dry wood with fungal material) are deposited in the herbarium of Mae Fah Luang University (MFLU), Chiang Rai, Thailand and Kunming Institute of Botany, Academia Sinica (HKAS), China. Axenic cultures are deposited in Mae Fah Luang University Culture Collection (MFLUCC). Facesoffungi and Index Fungorum numbers are registered as outlined in Jayasiri et al. (2015) and Index Fungorum (2018).

DNA extraction, PCR amplification and sequencing

Isolates were grown on PDA and/or MEA medium at 25 °C for one month. Fungal mycelium was scraped off and transferred to a 1.5-ml microcentrifuge tube using a sterilised lancet for genomic DNA extraction. Ezup Column Fungi Genomic DNA Purification Kit (Sangon Biotech, China) was used to extract DNA following the manufacturer's instructions. ITS, LSU and TEF1α gene regions were amplified using the primer pairs ITS5 or ITS1 with ITS4 (Vilgalys and Hester 1990), LROR with LR5 or LR7 (White et al. 1990) and EF1-983F with EF1-2218R (Rehner 2001). The amplifications were performed in a 25 µl reaction volume containing 9.5 µl ddH_2O, 12.5 µl 2 × Taq PCR Master Mix with blue dye (Sangon Biotech, China), 1 µl of DNA template and 1 µl of each primer (10 µM). The amplification condition for ITS, LSU and TEF1α consisted of initial denaturation at 94 °C for 3 min; followed by 40 cycles of 45 s at 94 °C, 50 s at

56 °C and 1 min at 72 °C and a final extension period of 10 min at 72 °C. Purification and sequencing of PCR products were carried out using the above-mentioned PCR primers at Sangon Biotech (Shanghai) Co. Ltd. in China.

Phylogenetic analyses

The taxa included in the phylogenetic analyses were selected and obtained from previous studies and GenBank (Boonmee et al. 2016, Wang et al. 2016, Li et al. 2017). Three gene regions (ITS, LSU and TEF1α) were used for the combined sequence data analyses. SEQMAN v. 7.0.0 (DNASTAR, Madison, WI) was used to assemble consensus sequences. The sequences were aligned using the online multiple alignment programme MAFFT v.7 (http://mafft.cbrc.jp/alignment/server/) (Katoh and Standley 2013). The alignments were checked visually and improved manually where necessary.

Phylogenetic analysis of the sequence data consisted of maximum likelihood (ML) using RAxML-HPC v.8 (Stamatakis 2006, Stamatakis et al. 2008) on the XSEDE Teragrid of the CIPRES science Gateway (https://www.phylo.org) (Miller et al. 2010) with rapid bootstrap analysis, followed by 1000 bootstrap replicates. The final tree was selected amongst suboptimal trees from each run by comparing likelihood scores under the GTRGAMMA substitution model.

Maximum parsimony (MP) analyses were performed with PAUP v. 4.0b10 (Swofford 2003) using the heuristic search option with 1000 random taxa addition and tree bisection and reconnection (TBR) as the branch swapping algorithm. All characters were unordered and of equal weight and gaps were treated as missing data. Maxtrees were unlimited, branches of zero length were collapsed and all multiple, equally parsimonious trees were saved. Clade stability was assessed using a bootstrap (BT) analysis with 1000 replicates, each with 10 replicates of random stepwise addition of taxa (Hillis and Bull 1993).

The programme MRMODELTEST2 v. 2.3 (Nylander 2008) was used to infer the appropriate substitution model that would best fit the model of DNA evolution for the combined datasets for Bayesian inference analysis with GTR+G+I substitution model selected. Posterior probabilities (PP) (Rannala and Yang 1996, Zhaxybayeva and Gogarten 2002) were determined by Markov Chain Monte Carlo sampling (MCMC) in MRBAYES v. 3.0b4 (Huelsenbeck and Ronquist 2001). Six simultaneous Markov chains were run for 1 million generations, with trees sampled every 100 generations (resulting in 10000 trees). The first 2000 trees, representing the burn-in phase of the analyses were discarded and the remaining 8000 trees were used for calculating posterior probabilities (PP) in the majority rule consensus tree (Larget and Simon 1999).

The resulting trees were printed with FIGTREE v. 1.4.0 (http://tree.bio.ed.ac.uk/software/figtree/) and the layout was created in MICROSOFT POWERPOINT for Mac v. 15.19.1. The alignment of phylogenetic analyses and resultant tree were deposited in TreeBASE (www.treebase.org, submission number 22802). Sequences generated in this study were submitted to GenBank (Table 1).

Table 1. Isolates and sequences used in this study (newly generated sequences are indicated in bold, ex-type strains are indicated with T after strain number).

Species	Source	GenBank accession number		
		ITS	LSU	TEF1α
Aquadictyospora lignicola	MFLUCC 17-1318^{T}	MF948621	MF948629	MF953164
Aquaticheirospora lignicola	HKUCC 10304^{T}	AY864770	AY736378	–
Cheirosporium triseriale	HMAS 180703^{T}	EU413953	EU413954	–
Dendryphiella eucalyptorum	CBS 137987^{T}	KJ869139	KJ869196	–
Dendryphiella fasciculata	MFLUCC 17-1074^{T}	MF399213	MF399214	–
Dendryphiella paravinosa	CBS 141286^{T}	KX228257	KX228309	–
Dictyocheirospora aquatica	KUMCC 15-0305^{T}	KY320508	KY320513	–
Dictyocheirospora bannica	KH 332^{T}	LC014543	AB807513	AB808489
Dictyocheirospora bannica	**MFLUCC 16-0874**	**MH381765**	**MH381774**	–
Dictyocheirospora garethjonesii	MFLUCC 16-0909^{T}	KY320509	KY320514	–
Dictyocheirospora garethjonesii	DLUCC 0848	MF948623	MF948631	MF953166
Dictyocheirospora gigantica	BCC 11346	DQ018095	–	–
Dictyocheirospora heptaspora	CBS 396.59	DQ018090	–	–
Dictyocheirospora indica	**MFLUCC 15-0056**	**MH381763**	**MH381772**	**MH388817**
Dictyocheirospora pseudomusae	yone 234^{T}	LC014550	AB807520	AB808496
Dictyocheirospora rotunda	MFLUCC 14-02^{9}3T	KU179099	KU179100	–
Dictyocheirospora rotunda	**MFLUCC 17-0222**	**MH381764**	**MH381773**	**MH388818**
Dictyocheirospora rotunda	MFLUCC 17-1313	MF948625	MF948633	MF953168
Dictyocheirospora subramanianii	BCC 3503	DQ018094	–	–
Dictyocheirospora vinaya	MFLUCC 14-0294^{T}	KU179102	KU179103	–
Dictyosporium alatum	ATCC 34953^{T}	NR_077171	DQ018101	–
Dictyosporium aquaticum	MF 1318^{T}	KM610236	–	–
Dictyosporium bulbosum	yone 221	LC014544	AB807511	AB808487
Dictyosporium digitatum	KH 401	LC014545	AB807515	AB808491
Dictyosporium digitatum	yone 280	LC014547	AB807512	AB808488
Dictyosporium elegans	NBRC 32502^{T}	DQ018087	DQ018100	–
Dictyosporium hughesii	KT 1847	LC014548	AB807517	AB808493
Dictyosporium meiosporum	MFLUCC 10-0131^{T}	KP710944	KP710945	–
Dictyosporium nigroapice	BCC 3555	DQ018085	–	–
Dictyosporium nigroapice	**MFLUCC 17-2053**	**MH381768**	**MH381777**	**MH388821**
Dictyosporium olivaceosporum	KH 375^{T}	LC014542	AB807514	AB808490
Dictyosporium sexualis	MFLUCC 10-0127^{T}	KU179105	KU179106	–
***Dictyosporium* sp.**	**MFLUCC 15-0629**	**MH381766**	**MH381775**	**MH388819**
Dictyosporium stellatum	CCFC 241241^{T}	NR_154608	JF951177	–
Dictyosporium strelitziae	CBS 123359^{T}	NR_156216	FJ839653	–
Dictyosporium tetrasporum	KT 2865	LC014551	AB807519	AB808495
Dictyosporium thailandicum	MFLUCC 13-0773^{T}	KP716706	KP716707	–
Dictyosporium tratense	**MFLUCC 17-2052^{T}**	**MH381767**	**MH381776**	**MH388820**
Dictyosporium tubulatum	**MFLUCC 15-0631^{T}**	**MH381769**	**MH381778**	**MH388822**
Dictyosporium tubulatum	**MFLUCC 17-2056**	**MH381770**	**MH381779**	–
Dictyosporium wuyiense	CGMCC 3.18703^{T}	KY072977	–	–
Dictyosporium zhejiangense	MW-2009a^{T}	FJ456893	–	–
Digitodesmium bambusicola	CBS 110279^{T}	DQ018091	DQ018103	–

Species	Source	GenBank accession number		
		ITS	LSU	TEF1α
Gregarithecium curvisporum	KT 922[T]	AB809644	AB807547	–
Jalapriya inflata	NTOU 3855	JQ267362	JQ267363	–
Jalapriya pulchra	MFLUCC 15-0348[T]	KU179108	KU179109	–
Jalapriya pulchra	MFLUCC 17-1683	MF948628	MF948636	MF953171
Jalapriya toruloides	CBS 209.65	DQ018093	DQ018104	–
Periconia igniaria	CBS 379.86	LC014585	AB807566	AB808542
Periconia igniaria	CBS 845.96	LC014586	AB807567	AB808543
Pseudocoleophoma calamagrostidis	KT 3284[T]	LC014592	LC014609	LC014614
Pseudocoleophoma polygonicola	KT 731[T]	AB809634	AB807546	AB808522
Pseudocoleophoma typhicola	MFLUCC 16-0123[T]	KX576655	KX576656	–
Pseudodictyosporium elegans	CBS 688.93[T]	DQ018099	DQ018106	–
Pseudodictyosporium indicum	CBS 471.95	DQ018097	–	–
Pseudodictyosporium thailandica	MFLUCC 16-0029[T]	KX259520	KX259522	KX259526
Pseudodictyosporium wauense	NBRC 30078	DQ018098	DQ018105	–
Pseudodictyosporium wauense	DLUCC 0801	MF948622	MF948630	MF953165
Vikalpa australiensis	HKUCC 8797[T]	DQ018092	–	–

Phylogenetic results

The analysed dataset consisted of combined ITS (557 bp), LSU (803 bp) and TEF1α (918 bp) sequence data (a total of 2278 characters including gaps) for 59 taxa in Dictyosporiaceae with *Periconia igniaria* E.W. Mason & M.B. Ellis (CBS 379.86, CBS 845.96) as the outgroup taxon. The best scoring RAxML tree is shown in Figure 1.

Phylogenetic analyses indicated the placement of three isolates (MFLUCC 15-0056, MFLLUCC 16-0874 and MFLUCC 17-0222) within the genus *Dictyocheirospora*. Five isolates (MFLUCC 15-0629, MFLUCC 17-2052, MFLUCC 17-2056, MFLUCC 15-0631 and MFLUCC 17-2053) nested in *Dictyosporium*. Phylogenetic results showed that *Dictyocheirospora indica* (MFLUCC 15-0056) clustered with *Dictyocheirospora subramanianii* (B. Sutton) D'souza, Boonmee & K.D. Hyde (BCC 3503) with good support. *Dictyocheirospora bannica* (MFLUCC 16-0874) was placed as sister taxon to the ex-type strain *Dictyocheirospora bannica* (KH 332). *Dictyocheirospora rotunda* (MFLUCC 17-0222) grouped together with *Dictyocheirospora rotunda* (MFLUCC 17-1313) and the ex-type strain *Dictyocheirospora rotunda* (MFLUCC 14-0293) with strong support. The strain *Dictyosporium* sp. (MFLUCC 15-0629) clustered as sister taxon to *Dictyosporium digitatum* J.L. Chen, C.H. Hwang & Tzean (KH 401), *Dictyosporium aquaticum* Abdel-Aziz (MF 1318) and *Dictyosporium stellatum* G.P. White & Seifert (CCFC 241241). The new taxon *Dictyosporium tratense* (MFLUCC 17-2052) formed a single clade within *Dictyosporium* which is distinct from other species in the genus. The new collection *Dictyosporium nigroapice* (MFLUCC 17-2053) was placed as sister taxon to a previous isolate *Dictyosporium nigroapice* (BCC 3555). Two isolates of the new taxon *Dictyosporium tubulatum* (MFLUCC 15-0631 and MFLUCC 17-2056) nested in *Dictyosporium* as sister clade to *Dictyosporium nigroapice* (MFLUCC 17-2053 and BCC 3555).

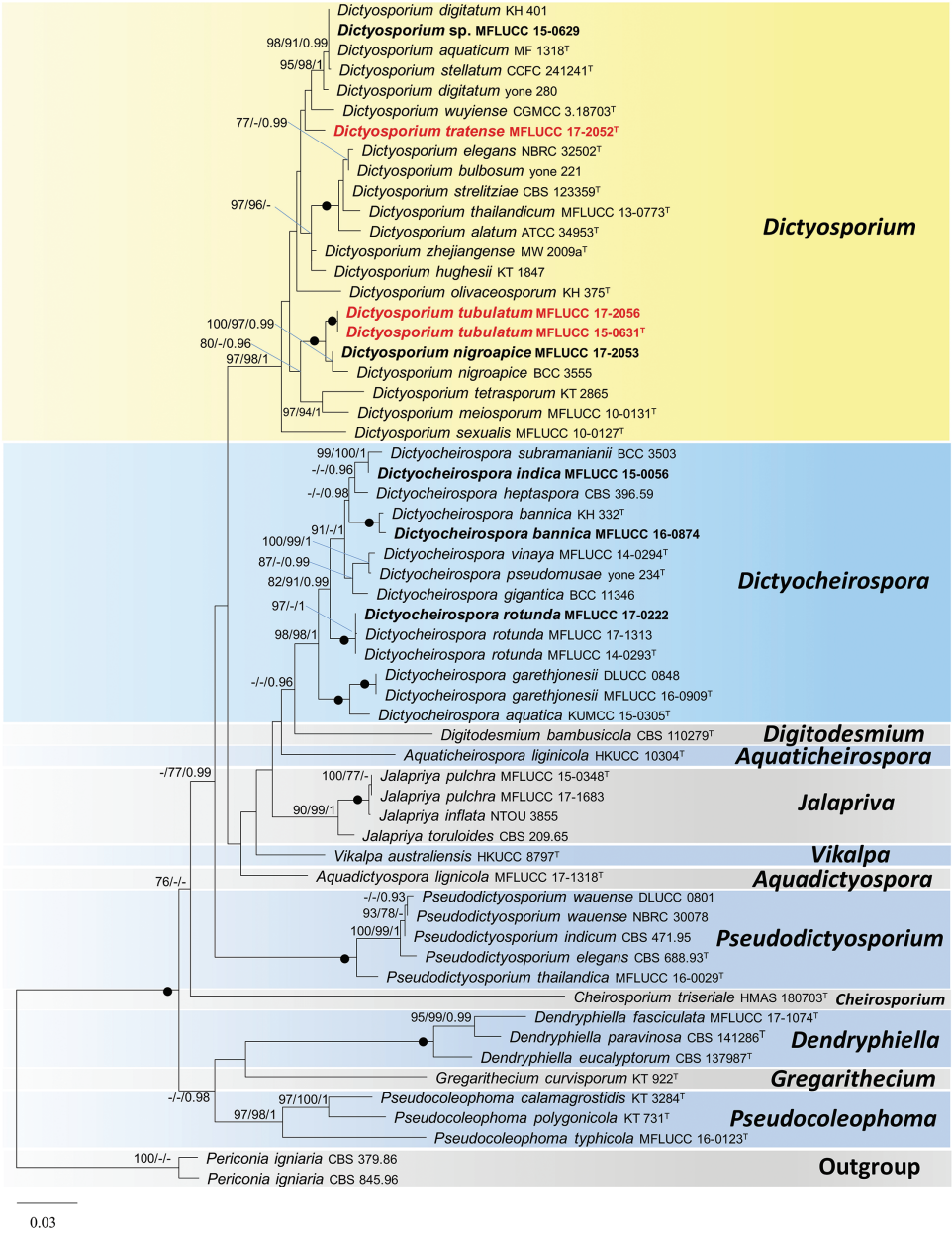

Figure 1. Maximum likelihood majority rule consensus tree for the analysed Dictyosporiaceae isolates based on a dataset of combined ITS, LSU and TEF1α sequence data. Bootstrap support values for maximum likelihood (ML) and maximum parsimony (MP) greater than 75% and Bayesian posterior probabilities greater than 0.95 are indicated above the nodes as MLBS/MPBS/PP. The scale bar represents the expected number of changes per site. The tree is rooted with *Periconia igniaria* (CBS 379.86, CBS 845.96). The strain numbers are noted after the species names with ex-type strains indicated with T. The new collections are in bold with new taxa in red. Branches with 100% ML BS, 100% MP BS and 1.0 PP are shown as black nodes. Genera are indicated as coloured blocks.

Taxonomy

Dictyocheirospora species

Dictyocheirospora bannica **Kaz. Tanaka, K. Hiray., Boonmee & K.D. Hyde, Fungal Diversity 80: 467 (2016)**
Index Fungorum number: IF551997
Facesoffungi number: FoF02014
Figure 2

Material examined. THAILAND. Phang Nga Province, Bann Tom Thong Khang, on decaying wood submerged in a freshwater stream, 17 Dec 2015, J. Yang, Site 7-70-1 (MFLU 18-1040, HKAS 102131), living culture MFLUCC 16-0874 (Additional SSU sequence GenBank MH381759).

Notes. The phylogenetic result showed the strain MFLUCC 16-0874 clustered with the ex-type (KH 332) of *Dictyocheirospora bannica*. The morphological examination of this collection matched well with the holotype of *Dictyocheirospora bannica* (Boonmee et al. 2016). *Dictyocheirospora bannica* was previously collected in Japan, while this is a new record for Thailand.

Dictyocheirospora hydei **(I.B. Prasher & R.K. Verma) J. Yang & K.D. Hyde, comb. nov.**
Index Fungorum number: IF554773
Facesoffungi number: FoF04679

Basionym. *Dictyosporium hydei* I.B. Prasher & R.K. Verma, Phytotaxa 204 (3): 196 (2015).

Holotype. INDIA. Himachal Pradesh, Bilaspur, on bark of *Tecoma stans*, 17 September 2013, I.B. Prasher and R.K. Verma (PAN 30364).

Notes. Considering the latest generic concept of *Dictyocheirospora* and *Dictyosporium*, we suggest that *Dictyosporium hydei* should be referred to *Dictyocheirospora* with the key character of non-complanate or cylindrical conidia with conidial arms closely gathered together at the apex. We have not examined the holotype of *Dictyocheirospora hydei*. The details provided by Prasher and Verma (2015) are adequate being illustrative and descriptive.

Dictyocheirospora indica **(I.B. Prasher & R.K. Verma) J. Yang & K.D. Hyde, comb. nov.**
Index Fungorum number: IF554774
Facesoffungi number: FoF04680
Figure 3

Basionym. *Dictyosporium indicum* I.B. Prasher & R.K. Verma, Phytotaxa 204 (3): 194 (2015).

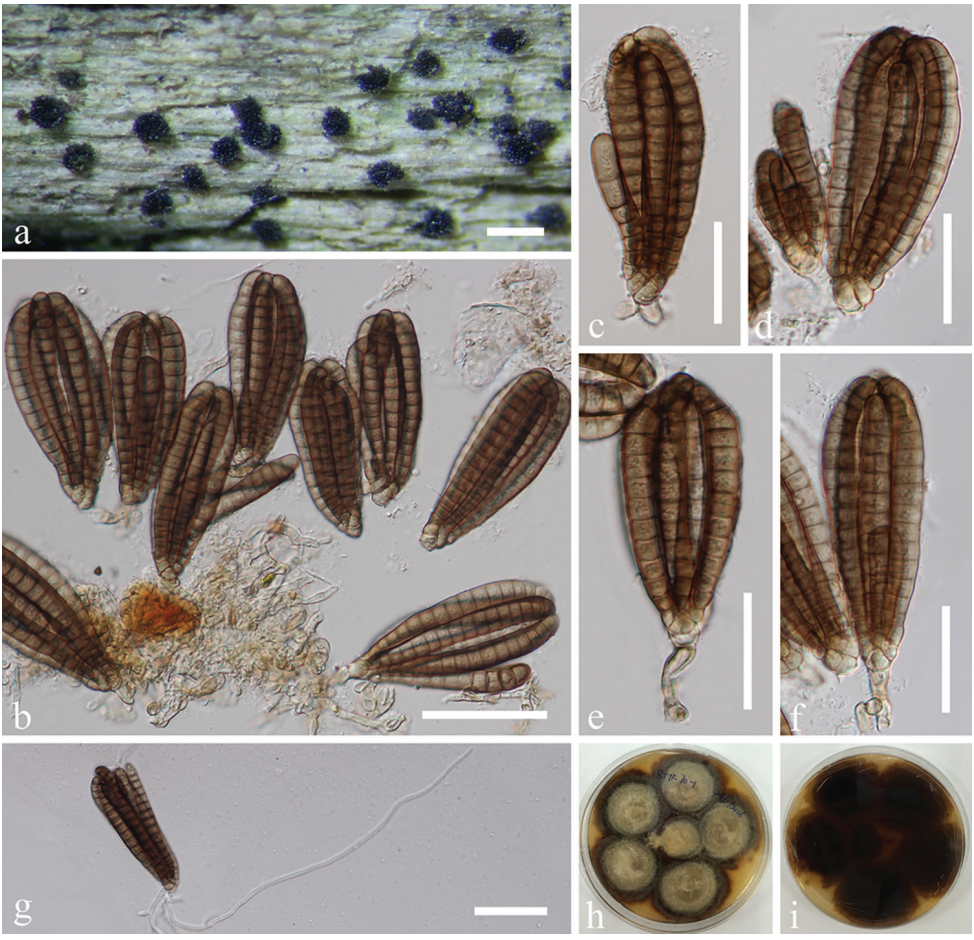

Figure 2. *Dictyocheirospora bannica* (MFLU 18-1040) **a** Colonies on submerged wood **b** Conidia and conidiophores **c–f** Conidia **g** Germinated conidium **h, i** Culture, h from above, i from reverse. Scale bars: **a** = 200 μm, **b, g** = 50 μm, **c–f** = 30 μm.

Holotype. INDIA. Himachal Pradesh, Mandi, on petiole of *Phoenix rupicola*, 19 November 2012, I.B. Prasher and R.K. Verma (PAN 30313).

Material examined. THAILAND. Chiang Rai, stream flowing in Tham Luang Nang Non Cave, on decaying submerged wood, 25 November 2014, J. Yang, YJ-3 (MFLU 15-1169 **reference specimen designated here**, HKAS 102135), living culture MFLUCC 15-0056 (Additional SSU sequence GenBank MH381757).

Notes. Collection MFLU 15-1169 was identified as *Dictyocheirospora indica* (*Dictyosporium indicum*) based on morphological examination. Phylogenetic analyses indicated the placement of this taxon within *Dictyocheirospora* and sister to *Di. subramanianii* (BCC 3503). *Dictyocheirospora subramanianii* differs from *Di. indica* in lacking appendages. *Dictyocheirospora indica* resembles *Di. musae* in having non-complanate, cylindrical conidia with globose to subglobose appendages. However, conidial append-

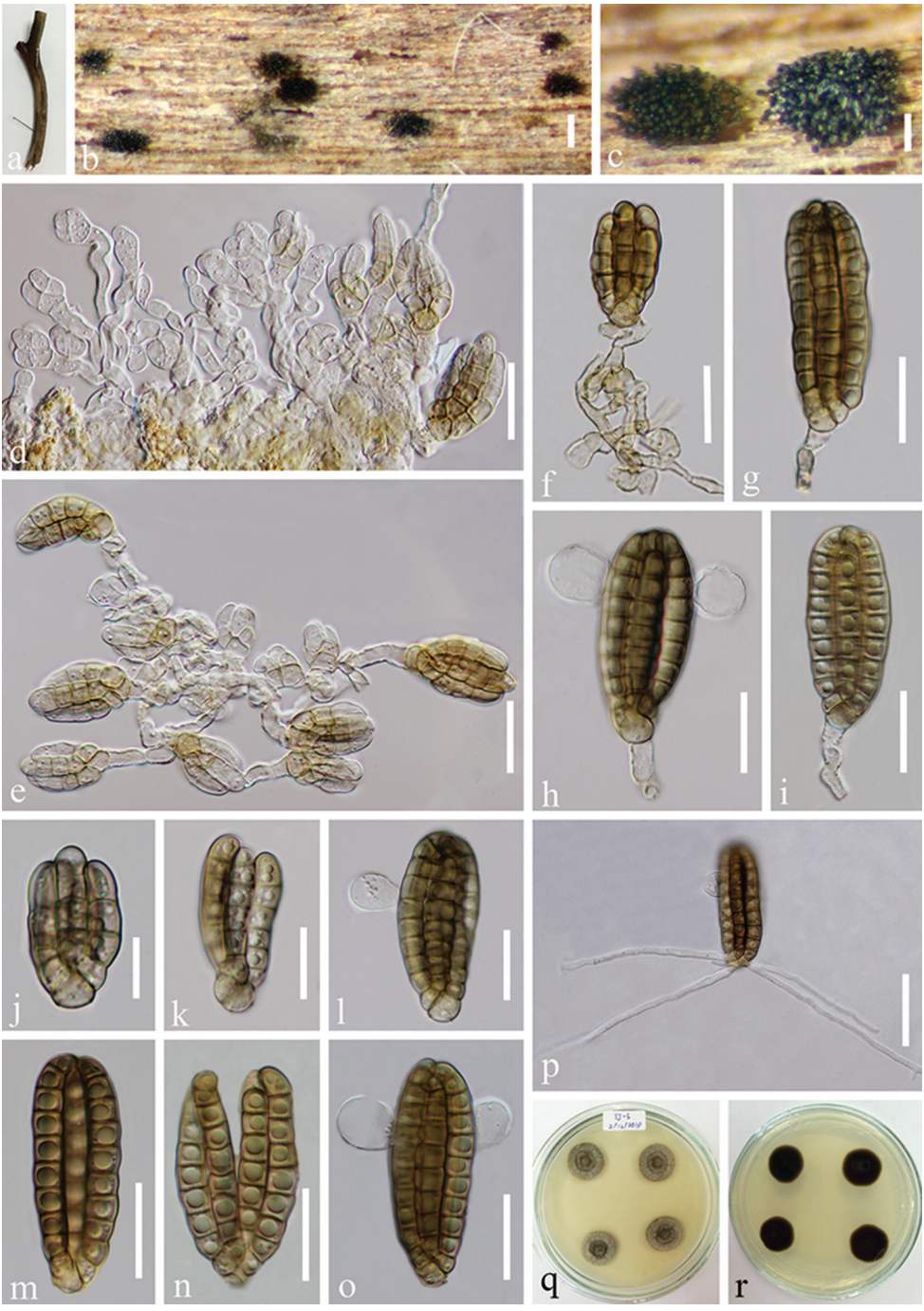

Figure 3. *Dictyocheirospora indica* (MFLU 15-1169, reference specimen). **a** Substrate **b, c** Colonies on woody substrate **d, e** Conidial formation **f–i** Conidia with partial conidiophores **j–o** Conidia **p** Germinated conidium **q–r** Culture, q from above, r from reverse. Scale bars: **b** = 200 μm, **c** = 100 μm, **d–i, l–o** = 20 μm, **j** = 10 μm, **k** = 15 μm, **p** = 30 μm.

ages of *Di. indica* are attached at the subapical cells, while appendages of *Di. musae* are attached at the central cells of the outer cell-row. The conidial size of *Di. indica* (33–48 × 13–18 µm) is smaller than that of *Di. musae* (45–65 × 20–27 µm) (Photita et al. 2002, Prasher and Verma 2015). In this study, sequence data of our collection *Dictyocheirospora indica* (MFLUCC 15-0056) was generated and, as there is no sequence data available for the previous collection (*Dictyosporium indicum*), we therefore designated our collection as the reference specimen (*sensu* Ariyawansa et al. 2014) for *Dictyocheirospora indica*.

Dictyocheirospora musae **(Photita) J. Yang, K.D. Hyde & Z.Y. Liu, comb. nov.**
Index Fungorum number: IF554775
Facesoffungi number: FoF04681

Basionym. *Dictyosporium musae* Photita, Mycotaxon 82: 416 (2002)

Holotype. THAILAND. Mae Hong Son Province, Sob Mei, Huay Thicha Village, on decaying petioles of *Musa acuminata*, 23 November 2000, W. Photita (PDD 74135).

Notes. *Dictyocheirospora musae* is morphologically similar to *Di. hydei* in having non-complanate, cylindrical conidia with globose to subglobose appendages. However, *Dictyocheirospora musae* differs in having appendages in the middle cells while *Di. hydei* has appendages on the basal cells (Photita et al. 2002, Prasher and Verma 2015).

Dictyocheirospora rotunda **D'souza, Bhat & K.D. Hyde, Fungal Diversity 80: 465 (2016)**
Index Fungorum number: IF551581
Facesoffungi number: FoF01262
Figure 4

Material examined. CHINA. Guizhou Province, Anshun city, Gaodang village, 26°4.267'N, 105°41.883'E, on decaying wood submerged in Suoluo river, 19 October 2016, J. Yang, GD 2-3 (MFLU 18-1041, HKAS 102132), living culture MFLUCC 17-0222 (Additional SSU sequence GenBank MH381758).

Notes. This species is known in China and Thailand from freshwater habitats (Boonmee et al. 2016, Wang et al. 2016).

Dictyocheirospora tetraploides **(L. Cai & K.D. Hyde) J. Yang & K.D. Hyde, comb. nov.**
Index Fungorum number: IF554776
Facesoffungi number: FoF04682

Basionym. *Dictyosporium tetraploides* L. Cai & K.D. Hyde, Sydowia 55 (2): 132 (2003)

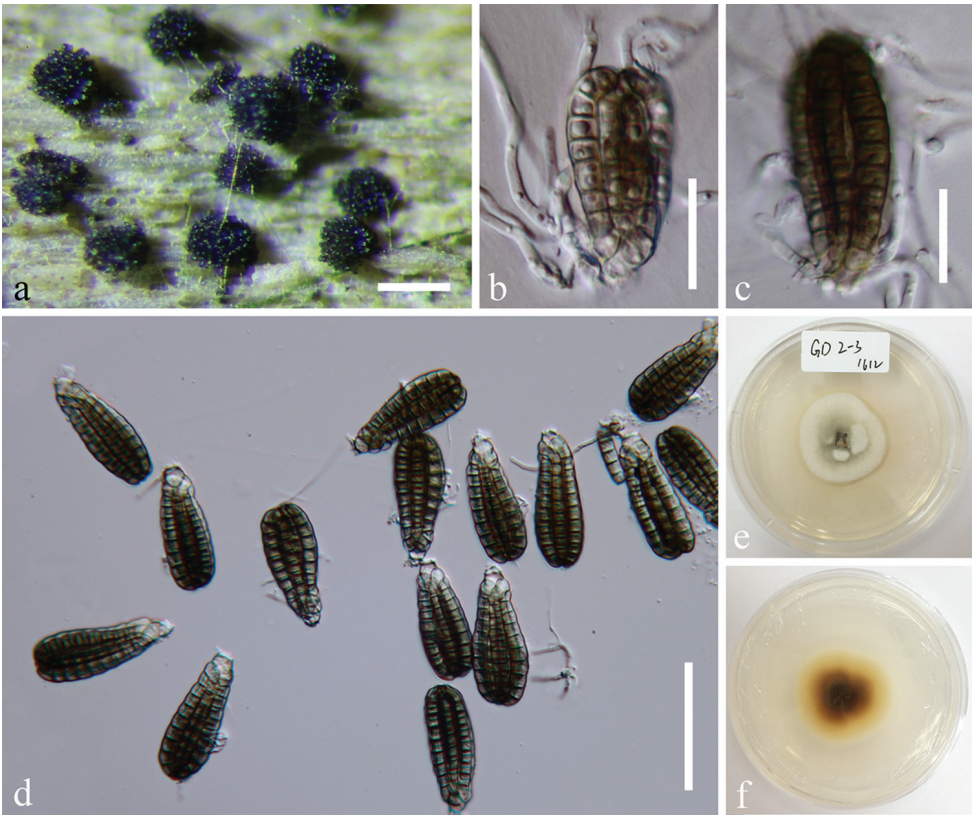

Figure 4. *Dictyocheirospora rotunda* (MFLU 18-1041). **a** Colonies on submerged wood **b, c** Germinated conidia **d** Conidia **e, f** Culture, e from above, f from reverse. Scale bars: **a** = 200 μm, **b, c** = 20 μm, **d** = 50 μm.

Holotype. CHINA. Yunnan, Xishuangbanna, Menglun, a small stream, on submerged wood, 21 June 2002, L. Cai (HKUM 17146).

Notes. *Dictyocheirospora tetraploides* is morphologically similar to *Di. musae* in conidial shape, size, colour and appendages. However, conidia of *Di. tetraploides* have 5-rowed cells, while those of *Di. musae* are 7-rowed cells (Photita et al. 2002, Cai et al. 2003).

Dictyosporium species

***Dictyosporium tubulatum* J. Yang, K.D. Hyde & Z.Y. Liu, sp. nov.**
Index Fungorum number: IF554771
Facesoffungi number: FoF04677
Figure 5

Etymology. Referring to the tubular conidial appendages.

Figure 5. *Dictyosporium tubulatum* (MFLU 15-1166, holotype). **a, b** Colonies on woody substrate **c** Squash mount of a sporodochium **d–g** Conidia **h–i** Conidia with conidiophores **j–l** Conidia with appendages **m** lateral view of a conidium **n** Germinated conidium **o, p** Culture, o from above **p** from reverse. Scale bars: **a** = 1000 µm, **b** = 200 µm, **c, n** = 30 µm, **d, e** = 10 µm, **f–m** = 15 µm.

Description. *Saprobic* on decaying plant substrates. **Asexual morph**: *Colonies* punctiform, sporodochial, scattered, dark brown to black, glistening. *Mycelium* mostly immersed, composed of smooth, septate, branched, hyaline to pale brown hyphae. *Conidiophores* micronematous, mononematous, septate, cylindrical, hyaline to pale brown, smooth-walled, 6.5–15 × 3.5–6 µm, sometimes reduced to conidiogenous cells. *Conidiogenous cells* monoblastic, integrated, terminal, determinate, hyaline to pale brown. *Conidia* acrogenous, solitary, cheiroid, smooth-walled, complanate, yellowish-brown to medium brown, mostly consisting of four arms closely compact with side arms lower than middle arms, rarely with five arms, 5–7-euseptate in each arm, guttulate, (22–)29–35(–38) × (14–)17–19(–22) µm ($\bar{x}$ = 32.5 × 18 µm, n = 40), with hyaline, tubular, elongated appendages which are 19–24 × 3.5–7 µm and mostly attached at the apical part of two outer arms. **Sexual morph**: Undetermined.

Cultural characteristics. Conidia germinating on PDA within 24 h and germ tubes produced from the basal cell. Colonies on MEA reaching 5–10 mm diam. in a week at 25 °C, in natural light, circular, with fluffy, dense, white mycelium on the surface with entire margin; in reverse yellow in the middle and white at the margin.

Material examined. THAILAND. Prachuap Khiri Khan Province, near 12°30.19'N, 99°31.35'E, on decaying wood submerged in a freshwater stream, 25 December 2014, J. van Strien, Site 5-11-1 (MFLU 15-1166 **holotype**, HKAS 102136 **isotype**), ex-type living culture MFLUCC 15-0631; *ibid.* Trat Province, Amphoe Ko Chang, 12°08'N, 102°38'E, on decaying wood submerged in a freshwater stream, 27 April 2017, Y.Z. Lu, YJT 22-2 (MFLU 18-1044, HKAS 102137 **paratype**), living culture MFLUCC 17-2056.

Notes. Phylogenetic analyses showed that *Dictyosporium tubulatum* nested in *Dictyosporium* and sister to *D. nigroapice*. *Dictyosporium tubulatum* morphologically resembles *D. alatum* Emden, *D. canisporum* L. Cai & K.D. Hyde and *D. thailandicum* D' souza, D.J. Bhat & K.D. Hyde in conidial ontogeny and conidial shape, colour and appendages. *Dictyosporium tubulatum* differs from the three species in the number of conidial cell rows. There are mostly four conidial columns in *D. tubulatum* while mostly five columns in the others. *Dictyosporium tubulatum* has smaller conidia (25–38 × 14–22 µm) than those in *D. canisporum* (32.5–47.5 × 20–25 µm) but has similar conidial size with *D. alatum* (26–32 × 15–24 µm) and *D. thailandicum* (15.4–34.5 × 14.5–20.6 µm) (Cai et al. 2003, Liu et al. 2015). Based on the molecular phylogeny, *D. tubulatum* is distinct from *D. thailandicum* and *D. alatum*. Unfortunately, molecular data are unavailable for *D. canisporum*.

***Dictyosporium tratense* J. Yang & K.D. Hyde, sp. nov.**
Index Fungorum number: IF554772
Facesoffungi number: FoF04678
Figure 6

Etymology. Referring to the collecting site in Trat province, Thailand.

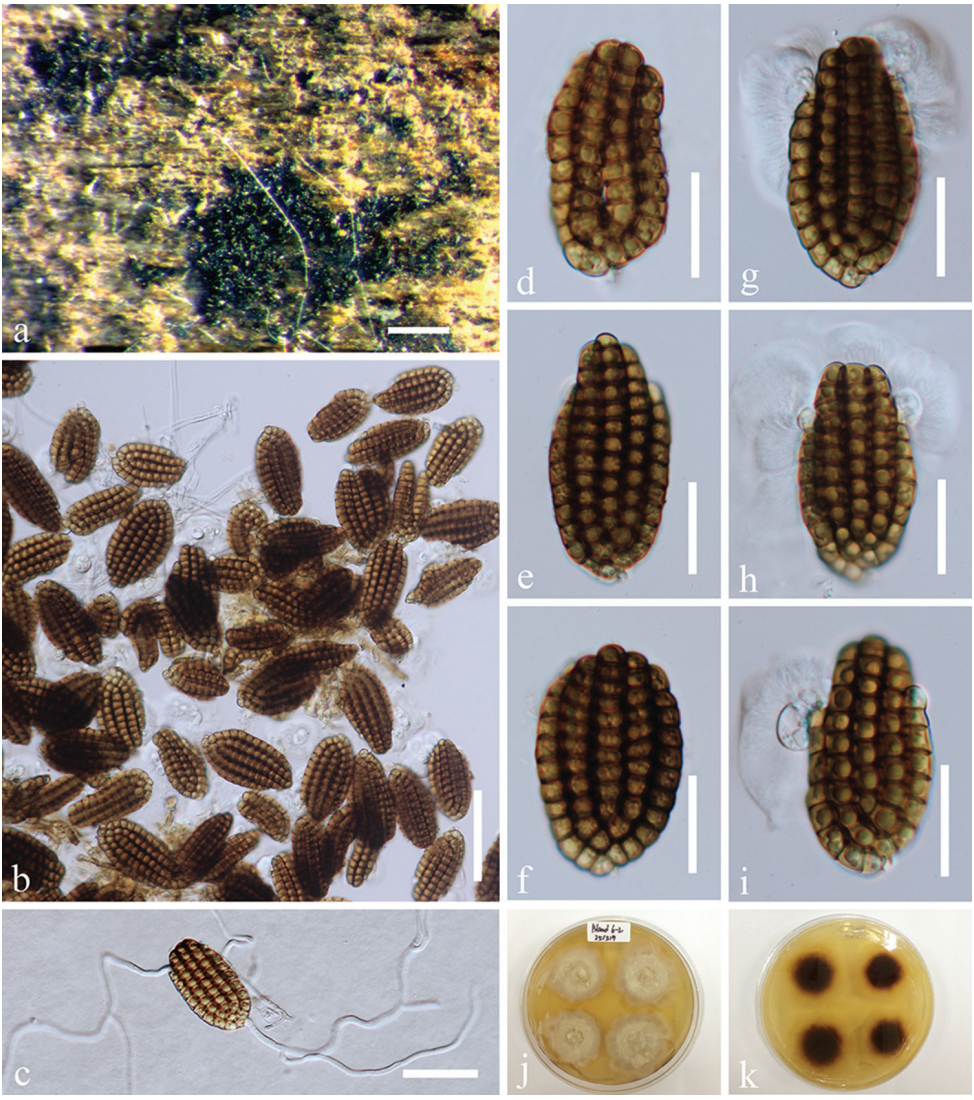

Figure 6. *Dictyosporium tratense* (MFLU 18-1042, holotype). **a** Colonies on submerged wood **b** Squash mount of a sporodochium **c** Germinated conidium **d–i** Conidia **j, k** Culture **j** from above **k** from reverse. Scale bars: **a** = 200 µm, **b** = 50 µm, **c** = 30 µm, **d–i** = 20 µm.

Description. *Saprobic* on decaying plant substrates. **Asexual morph**: *Colonies* punctiform, sporodochial, scattered, black, glistening. *Mycelium* mostly immersed, composed of smooth, septate, branched, hyaline to pale brown hyphae. *Conidiophores* micronematous, mononematous, septate, cylindrical, hyaline to pale brown, smooth-walled, sometimes reduced to conidiogenous cells. *Conidiogenous cells* monoblastic, integrated, terminal, determinate, hyaline to pale brown. *Conidia* (40–)43–54(–57) × (20–)23–32(–36) µm ($\bar{x}$ = 49.5 × 26 µm, n = 40), acrogenous,

solitary, cheiroid, smooth-walled, complanate, yellowish-brown to light brown, consisting of 39–68 cells arranged in 4–6 (mostly 5) closely compact columns, 9–11-euseptate in each column, guttulate; the inner columns nested within the outer columns, the outer columns derived from the basal cell of the conidium; the intermediate columns are derived from the first or second cell of the outer columns; the inner columns derived from the first or second cell of the intermediate columns; usually with 2–3 central columns longest and of equal length, 2–3 peripheral columns shorter and of equal length; sometimes with hyaline globose appendages at the apical cells of outer columns with hyaline cloud-shaped mucilaginous sheath. **Sexual morph**: Undetermined.

Cultural characteristics. Conidia germinating on PDA within 24 h and germ tubes produced from basal cell. Colonies on MEA reaching 5–10 mm diam. in a week at 25 °C, in natural light, circular, with fluffy, dense, pale yellow mycelium in the middle and sparse mycelium in the outer ring on the surface with irregular margin; in reverse, dark yellow to brown in the middle and pale yellow at the margin.

Material examined. THAILAND. Trat Province, Amphoe Ko Chang, 12°08'N, 102°38'E, on decaying wood submerged in a freshwater stream, 27 April 2017, Y.Z. Lu, YJT 6-2 (MFLU 18-1042 **holotype**, HKAS 102133 **isotype**), ex-type living culture MFLUCC 17-2052 (Additional SSU sequence GenBank MH381761).

Notes. Phylogenetic analyses indicated *Dictyosporium tratense* nested within *Dictyosporium* and close to *D. wuyiense*. It is distinguished from the other species in the genus in having a mucilaginous sheath. Morphologically, *D. tratense* is most comparable to *D. elegans* in conidial colour and shape, but conidia of the new taxon (40-57 × 20-36 μm) are smaller than those of *D. elegans* (40-80 × 24-36 μm) (Goh et al. 1999).

***Dictyosporium* sp.**
Figure 7

Material examined. THAILAND. Prachuap Khiri Khan Province, near 12°30.19'N, 99°31.35'E, on decaying wood submerged in a freshwater stream, 25 December 2014, J. van Strien, Site 5-5-1 (MFLU 15-1164), living culture MFLUCC 15-0629 (Additional SSU sequence GenBank MH381760).

Notes. Phylogenetic analyses indicated the isolate *Dictyosporium* sp. (MFLUCC 15-0629) was placed as sister taxon to *D. digitatum* (KH 401), *D. aquaticum* (MF 1318) and *D. stellatum* (CCFC 241241) with good support. The strain *D. digitatum* (KH 401), *D. aquaticum* (MF 1318) and our strain MFLUCC 15-0629, showed the same nucleotide (490 bp) between them for ITS gene regions, while there is only one nucleotide difference between our strain and *D. stellatum* (CCFC 241241). However, the strain *Dictyosporium* sp. (MFLUCC 15-0629) showed seven nucleotides different from *D. digitatum* (yone 280) for ITS gene regions. Morphologically, *D. digitatum* and *D. aquaticum* share the character in having appendages borne at the terminal cells of each conidial arm (Chen et al. 1991, Liu et al. 2015). *Dictyosporium stellatum* dif-

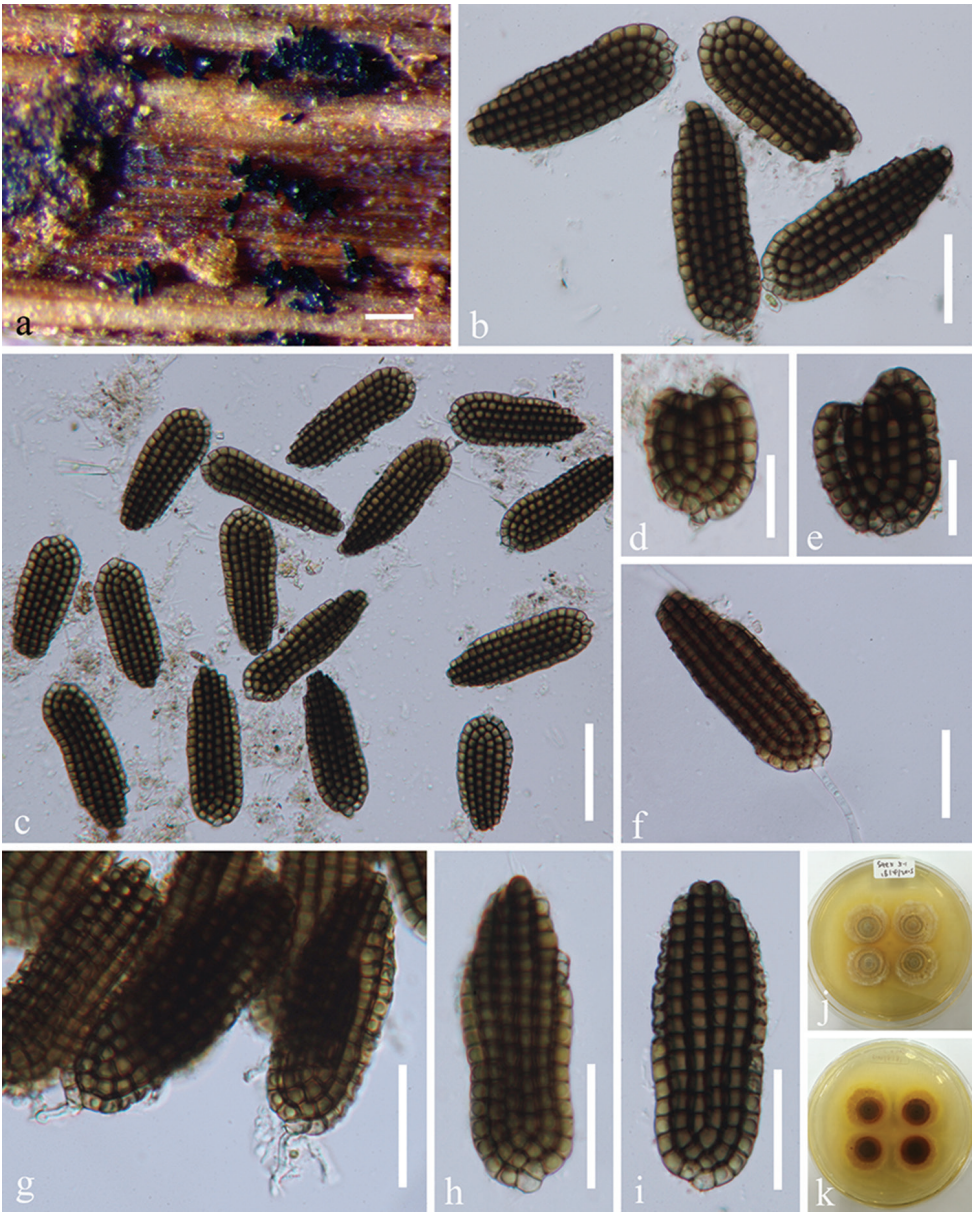

Figure 7. *Dictyosporium* sp. (MFLU 15-1164). **a** Colonies on submerged wood **b** Squash mount of a sporodochium; **c** Germinated conidium **b–e, h, i** Conidia **f** Germinated conidium **g** Conidia with conidiophores **j, k** Culture, j from above, k from reverse. Scale bars: **a** = 200 µm, **b, f–i** = 30 µm, **c** = 50 µm **d, e** = 20 µm.

fers from *D. digitatum* and *D. aquaticum* in lacking conidial appendages (Crous et al. 2011). In this case, it is difficult to identify our collection based on the recommendations advocated by Jeewon and Hyde (2016) for differentiating species or establishing

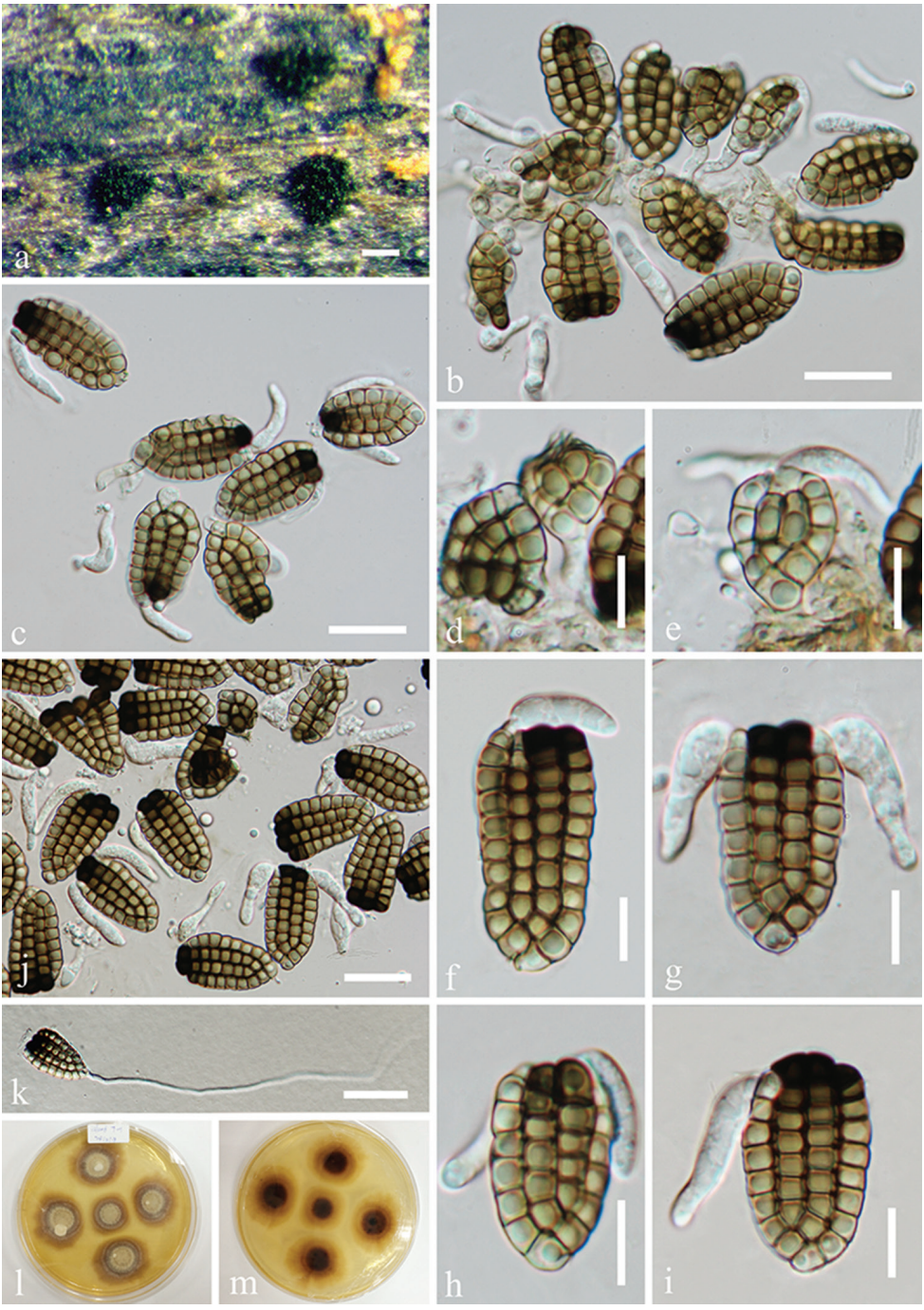

Figure 8. *Dictyosporium nigroapice* (MFLU18-1043). **a** Colonies on submerged wood **b, c** Conidia and conidiophores **d–j** Conidia **k** Germinated conidium **l, m** Culture, l from above, m from reverse. Scale bars: **a** = 100 μm, **b, c, j** = 20 μm, **d–i** = 10 μm, **k** = 30 μm.

new species. Thus, we recommend designating this collection as unknown species until enough evidence is available for its identification.

Dictyosporium nigroapice **Goh, W.H. Ho & K.D. Hyde, Fungal Diversity 2: 83 (1999)**
Index Fungorum number: IF450470
Facesoffungi number: FoF04683
Figure 8

Material examined. THAILAND. Trat Province, Amphoe Ko Chang, 12°08'N, 102°38'E, on decaying wood submerged in a freshwater stream, 27 April 2017, Y.Z. Lu, YJT 7-1 (MFLU 18-1043, HKAS 102134), living culture MFLUCC 17-2053 (Additional SSU sequence GenBank MH381762).

Notes. Conidia in *Dictyosporium nigroapice* are characterised by conspicuously darker apical cells of the two inner arms, rarely darker at the apex of the outer arms. Morphological characters of this collection well agree with the original diagnosis of the holotype of *D. nigroapice* (Goh et al. 1999).

Discussion

Dictyosporiaceae accommodates a holomorphic group of Dothideomycetes, including 12 genera with nine being dictyosporous (Wijayawardene et al. 2017b, Wijayawardene et al. 2018). *Dictyocheirospora* and *Dictyosporium* are the two largest genera in the family. *Dictyosporium* has cheiroid, digitate and complanate conidia without separating arms, while *Dictyocheirospora* is characterised by non-complanate conidia with arms arising from the basal cell and closely gathered at the apex and compact. Thus, *Dictyosporium hydei*, *D. indicum*, *D. musae* and *D. tetraploides* are transferred to *Dictyocheirospora* based on the clear morphological characters. Phylogenetic analyses revealed the placement of *Dictyocheirospora indica* (MFLUCC 15-0056 reference specimen) within *Dictyocheirospora*. We believe that the other three species belong to *Dictyocheirospora* in having similar conidia and appendages to *Dictyocheirospora indica*, although molecular data are unavailable for them.

Acknowledgement

We would like to thank The Research of Featured Microbial Resources and Diversity Investigation in the Southwest Karst area (project no. 2014FY120100) for its financial support. Kevin D. Hyde would like to thank the Thailand Research grants entitled "The future of specialist fungi in a changing climate: baseline data for generalist and

specialist fungi associated with ants, *Rhododendron* species and *Dracaena* species" (grant no: DBG6080013) and "Impact of climate change on fungal diversity and biogeography in the Greater Mekong Subregion" (grant no: RDG6130001) for supporting this study. Jing Yang thanks Shaun Pennycook for the corrections to the Latin names. Zong-Long Luo is acknowledged for the help with phylogenetic analyses.

References

Abdel-Aziz FA (2016) Two new cheirosporous asexual taxa (Dictyosporiaceae, Pleosporales, Dothideomycetes) from freshwater habitats in Egypt. Mycosphere 7(4): 448–457. https://doi.org/10.5943/mycosphere/7/4/5

Alves-Barbosa M, Costa PMO, Malosso E, Castañeda-Ruiz RF (2017) Two new species of *Dictyosporium* and *Helminthosporium* (Ascomycota) from the Brazilian Atlantic Forest. Nova Hedwigia 105: 65–73. https://doi.org/10.1127/nova_hedwigia/2017/0401

Ariyawansa HA, Hawksworth DL, Hyde KD, Jones EBG, et al. (2014) Epitypification and neotypification: guidelines with appropriate and inappropriate examples. Fungal Diversity 69: 57–91. https://doi.org/10.1007/s13225-014-0315-4

Boonmee S, D'souza MJ, Luo ZL, Pinruan U, Tanaka K, Su H, Bhat DJ, McKenzie EHC, Jones EBG, Taylor JE, Phillips AJL, Hirayama K, Eungwanichayapant PD, Hyde KD (2016) Dictyosporiaceae fam. nov. Fungal Diversity 80: 457–482. https://doi.org/10.1007/s13225-016-0363-z

Cai L, Zhang KQ, McKenzie EHC, Hyde KD (2003) New species of *Dictyosporium* and *Digitodesmium* from submerged wood in Yunnan, China. Sydowia 55: 129–135.

Chen JL, Hwang CH, Tzean SS (1991) *Dictyosporium digitatum*, a new hyphomycete from Taiwan. Mycological Research 95: 1145–1149. https://doi.org/10.1016/S0953-7562(09)80565-0

Chomnunti P, Hongsanan S, Aguirre-Hudson B, Tian Q, Peršoh D, Dhami MK, Alias AS, Xu J, Liu X, Stadler M, Hyde KD (2014) The sooty moulds. Fungal Diversity 66: 1–36. https://doi.org/10.1007/s13225-014-0278-5

Corda AC (1836) Mykologische Beobachtungen. Weitenweber's Beitrage zur gesammtem Natur-und Heilwissenschaften Prague.

Crous PW, Groenewald JZ, Shivas RG, Edwards J, et al. (2011) Fungal Planet Description Sheets: 69–91. Persoonia 26: 108–156. https://doi.org/10.3767/003158511x581723

da Silva SS, Castañeda-Ruiz RF, Gusmão LFP (2016) New species and records of *Dictyosporium* on *Araucaria angustifolia* (Brazilian pine) from Brazil. Nova Hedwigia 102: 523–530. https://doi.org/10.1127/nova_hedwigia/2015/0325

Goh TK, Hyde KD, Ho WH, Yanna (1999) A revision of the genus *Dictyosporium*, with descriptions of three new species. Fungal Diversity 2: 65–100.

Hillis DM, Bull JJ (1993) An empirical test of bootstrapping as a method for assessing confidence in phylogenetic analysis. Systematic Biology 42(2): 182. https://doi.org/10.2307/2992540

Ho WH, Yanna, Hyde KD, Hodgkiss IJ (2002) Seasonality and sequential occurrence of fungi on wood submerged in Tai Po Kau Forest Stream, Hong Kong. Fungal Diversity 10: 21–43.

Huelsenbeck JP, Ronquist F (2001) MRBAYES: Bayesian inference of phylogenetic trees. Bioinformatics 17(8): 754–755. https://doi.org/10.1093/bioinformatics/17.8.754

Hyde KD, Fryar S, Tian Q, Bahkali AH, Xu JC (2016) Lignicolous freshwater fungi along a north-south latitudinal gradient in the Asian/Australian region; can we predict the impact of global warming on biodiversity and function? Fungal Ecology 19: 190–200. https://doi.org/10.1016/j.funeco.2015.07.002

Hyde KD, Goh TK (1998) Fungi on submerged wood in Lake Barrine, north Queensland, Australia. Mycological Research 102: 739–749. https://doi.org/10.1017/s0953756297005868

Hyde KD, Norphanphoun C, Abreu VP, Bazzicalupo A, et al. (2017) Fungal diversity notes 603–708: taxonomic and phylogenetic notes on genera and species. Fungal Diversity 87: 1–235. https://doi.org/10.1007/s13225-017-0391-3

Index Fungorum (2018) http://www.indexfungorum.org

Jayasiri SC, Hyde KD, Ariyawansa HA, Bhat DJ, et al. (2015) The faces of fungi database: fungal names linked with morphology, phylogeny and human impacts. Fungal Diversity 74(1): 3–18. https://doi.org/10.1007/s13225-015-0351-8

Jeewon R, Hyde KD (2016) Establishing species boundaries and new taxa among fungi: recommendations to resolve taxonomic ambiguities. Mycosphere 7(11): 1669–1677. https://doi.org/10.5943/mycosphere/7/11/4

Katoh K, Standley DM (2013) Multiple sequence alignment software version 7: improvements in performance and usability. Molecular Biology and Evolution 30: 772–780. https://doi.org/10.1093/molbev/mst010

Larget B, Simon DL (1999) Markov Chain Monte Carlo algorithms for the Bayesian analysis of phylogenetic trees. Molecular Biology and Evolution 16: 750–759. https://doi.org/10.1093/oxfordjournals.molbev.a026160

Li WL, Luo ZL, Liu JK, Bhat DJ, Bao DF, Su HY, Hyde KD (2017) Lignicolous freshwater fungi from China I: *Aquadictyospora lignicola* gen. et sp. nov. and new record of *Pseudodictyosporium wauense* from northwestern Yunnan Province. Mycosphere 8(10): 1587–1597. https://doi.org/10.5943/mycosphere/8/10/1

Liu JK, Hyde KD, Jones EBG, Ariyawansa HA, et al. (2015) Fungal diversity notes 1–110: taxonomic and phylogenetic contributions to fungal species. Fungal Diversity 72: 1–197. https://doi.org/10.1007/s13225-015-0324-y

Miller MA, Pfeiffer W, Schwartz T (2010) Creating the CIPRES Science Gateway for inference of large phylogenetic trees. Proceedings of the Gateway Computing Environments Workshop (GCE), 14 Nov 2010. New Orleans, LA, 1–8. https://doi.org/10.1109/GCE.2010.5676129

Nylander J (2008) MrModeltest2 v. 2.3 (Program for selecting DNA substitution models using PAUP*). Evolutionary Biology Centre, Uppsala, Sweden.

Photita W, Lumyong P, McKenzie EHC, Hyde KD, Lumyong S (2002) A new *Dictyosporium* species from *Musa acuminata* in Thailand. Mycotaxon 82: 415–419.

Pinnoi A, Lumyong S, Hyde KD, Jones EBG (2006) Biodiversity of fungi on the palm *Eleiodoxa conferta* in Sirindhorn peat swamp forest, Narathiwat, Thailand. Fungal Diversity 22: 205–218.

Pinruan U, Hyde KD, Lumyong S, McKenzie EHC, Jones EBG (2007) Occurrence of fungi on tissues of the peat swamp palm *Licuala longicalycata*. Fungal Diversity 25: 157–173.

Prasher IB, Verma RK (2015) Two new species of *Dictyosporium* from India. Phytotaxa 204: 193–202. https://doi.org/10.11646/phytotaxa.204.3.2

Rannala B, Yang Z (1996) Probability distribution of molecular evolutionary trees: a new method of phylogenetic inference. Journal of Molecular Evolution 43: 304–311. https://doi.org/10.1007/pl00006090

Rehner S (2001) Primers for Elongation Factor 1-α (EF1-α). http://ocid.NACSE.ORG/research/deephyphae/EF1primer.pdf

Silva CR, Gusmão LFP, Castañeda-Ruiz RF (2015) *Dictyosporium amoenum* sp. nov from Chapada, Diamantina, Bahia, Brazil. Mycotaxon 130: 1125–1133. https://doi.org/10.5248/130.1125

Stamatakis A (2006) RAxML-VI-HPC: maximum likelihood-based phylogenetic analyses with thousands of taxa and mixed models. Bioinformatics 22: 2688–2690. https://doi.org/10.1093/bioinformatics/btl446

Stamatakis A, Hoover P, Rougemont J (2008) A rapid bootstrap algorithm for the RAxML web servers. Syst Biol 57: 758–771. https://doi.org/10.1080/10635150802429642

Swofford DL (2003) PAUP*: Phylogenetic analysis using parsimony (*and other methods). Version 4. Sinauer, Sunderland

Tanaka K, Hirayama K, Yonezawa H, Sato G, Toriyabe A, Kudo H, Hashimoto A, Matsumura M, Harada Y, Kurihara Y, Shirouzu T, Hosoya T (2015) Revision of the Massarineae (Pleosporales, Dothideomycetes). Studies in Mycology 82: 75–136. https://doi.org/10.1016/j.simyco.2015.10.002

Tsui CKM, Berbee ML, Jeewon R, Hyde KD (2006) Molecular phylogeny of *Dictyosporium* and allied genera inferred from ribosomal DNA. Fungal Diversity 21: 157–166.

Vilgalys R, Hester M (1990) Rapid genetic identification and mapping of enzymatically amplified ribosomal DNA from several *Cryptococcus* species. Journal of Bacteriology 172(8): 4238–4246. https://doi.org/10.1128/jb.172.8.4238-4246.1990

Wang RX, Luo ZL, Hyde KD, Bhat DJ, Su XJ, Su HY (2016) New species and records of *Dictyocheirospora* from submerged wood in north-western Yunnan, China. Mycosphere 7(9): 1357–1367. https://doi.org/10.5943/mycosphere/7/9/9

White TJ, Bruns T, Lee SJ, Taylor JW (1990) Amplification and direct sequencing of fungal ribosomal RNA genes for phylogenetics. PCR protocols: a guide to methods and applications 18(1): 315–322. https://doi.org/10.1016/B978-0-12-372180-8.50042-1

Whitton SR, McKenzie EHC, Hyde KD (2012) Anamorphic fungi associated with Pandanaceae. Springer Netherlands 21: 125–353. https://doi.org/10.1007/978-94-007-4447-9_4

Wijayawardene NN, Hyde KD, Lumbsch HT, Liu JK, et al. (2018) Outline of Ascomycota: 2017. Fungal Diversity 88: 167 –263. https://doi.org/10.1007/s13225-018-0394-8

Wijayawardene NN, Hyde KD, Rajeshkumar KC, et al. (2017a) Notes for genera: Ascomycota. Fungal Diversity 86(1): 1–594. https://doi.org/10.1007/s13225-017-0386-0

Wijayawardene NN, Hyde KD, Tibpromma S, Wanasinghe DN, Thambugala KM, Tian Q, Wang Y (2017b) Towards incorporating asexual fungi in a natural classification: check-

list and notes 2012–2016. Mycosphere 8(9): 1457–1555. https://doi.org/10.5943/mycosphere/8/9/10

Zhang Y, Cai CS, Zhao GZ (2017) *Dictyosporium wuyiense* sp. nov. from Wuyi Mountain China. Phytotaxa 314(2): 251–258. https://doi.org/10.11646/phytotaxa.314.2.6

Zhaxybayeva O, Gogarten JP (2002) Bootstrap, Bayesian probability and maximum likelihood mapping: exploring new tools for comparative genome analyses. BMC Genomics 3: 4. https://doi.org/10.1186/1471-2164-3-4